ROLL-TO-ROLL VACUUM DEPOSITION OF ORGANIC THIN FILMS FOLLOWED BY IN-LINE CURING

Carmen Alonso Herr

Kellogg College

University of Oxford

Supervised by:

Professor Hazel Assender

Submitted: Michaelmas Term, 2020

This thesis is submitted to the Department of Materials Science, University of Oxford, in partial fulfilment of the requirements for the degree of Master of Science by Research

Declaration

I declare that this thesis is entirely my own work, and except where otherwise stated, describes my own research.

Carmen Alonso Herr,

Kellogg College

ABSTRACT

The process that is being investigated is a roll-to-roll vacuum deposition of a polymer film by evaporation of a liquid monomer followed by in-line curing. In the process, a continuous stream of an acrylate is introduced in a hot tank in order to be flash evaporated. Afterwards, the monomer vapor passes through a nozzle and is directed to a cooled, moving substrate where it re-condenses as a liquid monomer film. The deposition takes place in a vacuum chamber at approximately 10^{-4}mbar. The moving substrate carrying the liquid film moves away from the evaporation source towards an ionizating radiation source, plasma or electron beam, inducing the curing and crosslinking of the liquid films, solidifying them to become a network polymer.

The research project is based on making a robust comparison of an acrylate-based coating cured with one of two power sources, plasma and electron-beam, with an investigation of the influence of process parameters on the materials properties. For the purpose of this line of research, the chemical used is a difunctional acrylate, TGPDA. The comparison will include a deep study on the chemical and physical properties obtained by different power sources, at different powers and radiation time. The aim of this part of the project is being able to link the parameters of the curing source with the polymer properties, i.e cross-linking density, curing degree, mechanical properties, topography and thickness. Furthermore, it would help in the better understanding of the cure control, particularly when investigating more advanced processes, such as the mixed materials and selective curing.

Acknowledgements

This thesis would not be possible without the help of all the professors and students that I had collaborated with. I would also like to appreciate to the OMCS staff members for their help and support.

I am especially thankful to Clara Barker and especially to my supervisor Professor Hazel Assender for helping me gaining so many different skills as a researcher and for their time and energy. I also would like to highlight the importance Richard Turner had in my research project. He helped me with everything that I needed and made my research work much easier in a daily basis.

By last, I want to thank my family all their effort, sacrifice and love throughout my live. In the same way, I would like to express my gratitude and admiration to Kiron Neale, for his continuous love and support.

TABLE OF CONTENTS

LIST OF FIGURES, EQUATIONS AND TABLES

CHAPTER 1. INTRODUCTION

This project seeks to explore the roll-to-roll vacuum deposition of polymer layers, in particular the effect of process parameters on the properties of the resulting films, made up of a difunctional acrylate monomer.

The process that will be investigated is a roll-to-roll vacuum deposition by evaporation of a liquid monomer followed by in-line curing. In the process, a continuous stream of an acrylate monomer is introduced into a hot tank in order to be flash evaporated. Afterwards, the monomer vapor passes through a nozzle and is directed to a cooled, moving substrate where it re-condenses as a liquid monomer film. The deposition takes place in a vacuum chamber at approximately 10^{-4}mbar. The moving substrate carrying the liquid film moves away from the evaporation source towards an ionizating radiation source, plasma or electron beam, inducing the curing to crosslink the liquid film, solidifying it to become a network polymer.

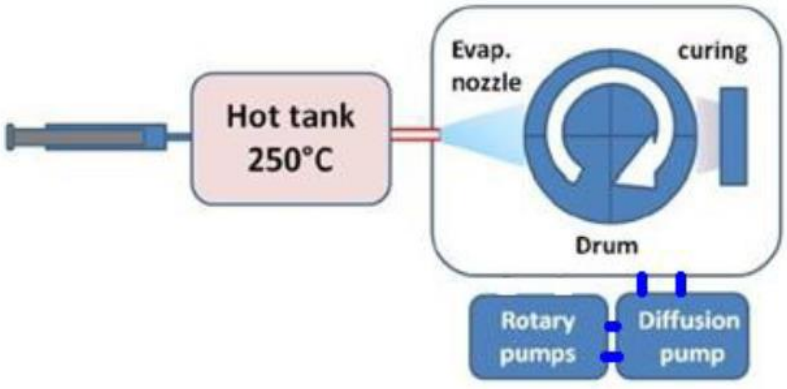

Figure 1.1: Schematic of the process

The research project is based in making a comparison between two curing sources (plasma and electron beam) when vacuum depositing organic thin films. In addition, it consists in an understanding on how the different process variables affect the polymer's properties. Previous to this work, it was observed within my research group, that the dielectric and barrier properties of transistors and barrier coatings, respectively, differed when modifying the process parameters when vacuum depositing acrylate coatings. This finding was thought to be as a result of many factors such as degree of cure, topography, mechanical properties. The main hypothesis for the transistor properties in which the acrylate layer was used as a gate dielectric (1) was that, when the acrylate coatings are not completely cured, the uncured part of the layers will be able to conduct electricity to some degree, and this manifest itself a high leakage current in the transistor (the undesirable current between gate and drain electrodes) that leads to a low on/off current ratio, or at worst, short circuiting. A second factor that was observed, also thought to be due to poor cure, which would lead to high polarizability of the polymer under an applied field, is a high hysteresis in the voltage/current characteristic as the transistor is switched off and on, which is undesirable for circuit design. . In addition, acrylate coatings were used in the barrier coatings as smoothing layers, prior to deposition of inorganic layers that have high barrier properties, in order to reduce permeation. The acrylate smoothing layer acts to reduce the defects in the oxide, reducing the permeation too (2) (3) (4). So, in order to improve the barrier performance they are deposited on top of a smooth, well cured, organic layer with appropriate mechanical properties to minimize the formation of localized defects in the rather fragile inorganic gas barrier layer, and to ensure a good interface between the substrate and the inorganic coating. In conclusion, the control of curing, and hence also dependent properties such as polarizability, topography and

mechanical properties, is important as it one of the key factors when it comes to applications, as exemplified in the work on for organic electronics and barrier coatings.

Therefore, the project was born because it was felt a need of controlling the degree of cure and hence the polymer´s properties. The project seeks to develop a curing model out of the process variables, by exploring the degree of cure under a range process conditions.

The thickness of the resulting film will also be dependent on many process factors. In vacuum deposition, the acrylate is put down from a vapor state, which cools down on the substrate. Therefore, the condensation and re-evaporation rates, and indeed etching by the curing source, play a key role in determining the thickness of the resulting layer. Again, this study is novel, especially when trying to link these parameters out of the process parameters or the degree of cure.

The nature of the curing source seemed to have an influence on the coatings as well. Previous studies had been performed comparing UV and EB on one hand (5) (6), and UV and plasma on the other hand (7) (8). However, any studies had been performed comparing EB and plasma, which is where the novelty of this research project leads. So, a complete study of plasma and electron beam would be performed, being the ultimate goal, the comparison of the two curing sources. In plasma, ions, electrons or photons interact with the material, however in E-beam only electrons are present. Because of that, given the different nature of the two curing sources, the properties of the resulting coatings maybe different, and it is exactly any such difference that should be studied.

Lastly, not only the degree of cure and thickness is studied but also the topography and crosslinking density (hence mechanical properties). The challenge would be trying to explain how the curing source influences these properties.

So, in summary the main research lines are:

The study of the degree of cure and thickness for all the process parameters (injection rates, gas flow, power, curing source…).

The comparison of the results between plasma and electron beam.

The influence of the degree of cure or the process conditions on the topography and crosslinking density.

The machine used is based on a roll-to-roll technique, hence the thin films would be subjected to the curing source only once in normal conditions. However, in order to better understand the effect of subjecting the material to a variable time to the curing source, a single short length of substrate attached directly to a rotating drum was used in the research project. By doing it so, multiple layers will be built on top of each other on the surface of the drum, so that the inner layers would pass under the curing source more times, as opposed to the "fresh layers". All the parameters that played a role in the research project are explained:

- Injection rate: it refers to the rate (volume per unit time) the monomer is introduced into the flash evaporation system, and hence controls to the amount of material that is introduced on top of the drum at each pass. It is controlled by the speed at which a syringe moves to inject material into the system. Therefore, the speed at which the material is introduced in the vacuum chamber will cause differences on the thickness of each layer given that as the speed is increased, more material will be deposited on top of the drum at each pass, but fewer layers will be deposited for a given volume of material. As for example, when decreasing

the injection rate by half, from case A to case B in Figure 1.2 the thickness of each layer would be reduced by half as well, but the number of layers will be twice as many. The information that would be obtained out of it, is a better understanding of the amount of material the reactive species of the curing source are able to interact with at each pass of the drum.

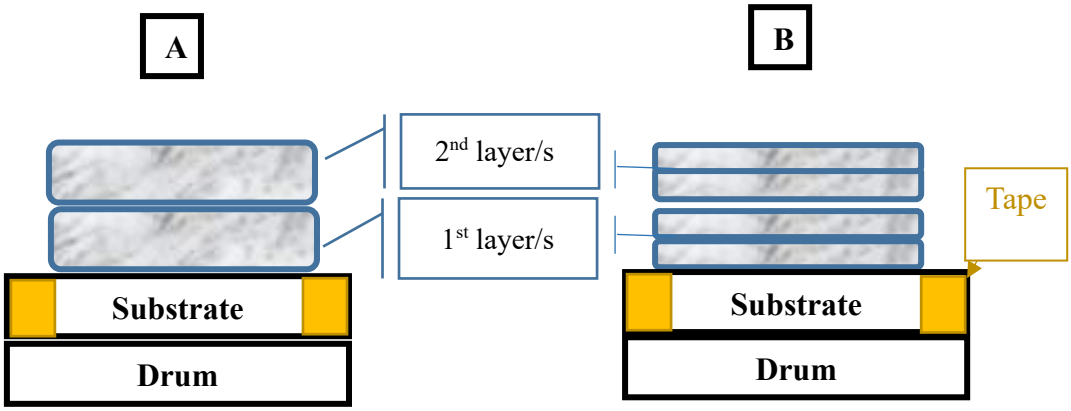

Figure 1.2: Schema of the deposition of two thin films when modifying the injection rate (A has a v1 ml/min and B has a speed of v2= v1/2)

- Volume: the total volume of monomer material injected into the flash evaporation chamber. Thicker films will be obtained where there is more material interacting with the plasma or E-Beam species. Doubling the volume of material from case C to case D (Figure 1.3), for the same injection rate and drum speed increases the number of rotations under the curing source the sample makes during the experiment. So, by changing the volume, it provides information about any "post-curing" effect, as the first layers deposited during the injection will pass the curing source multiple times. This means, understanding on whether or not the reactive species are able to

interact with the underlayers, breaking the C=C bonds to further polymerize the material.

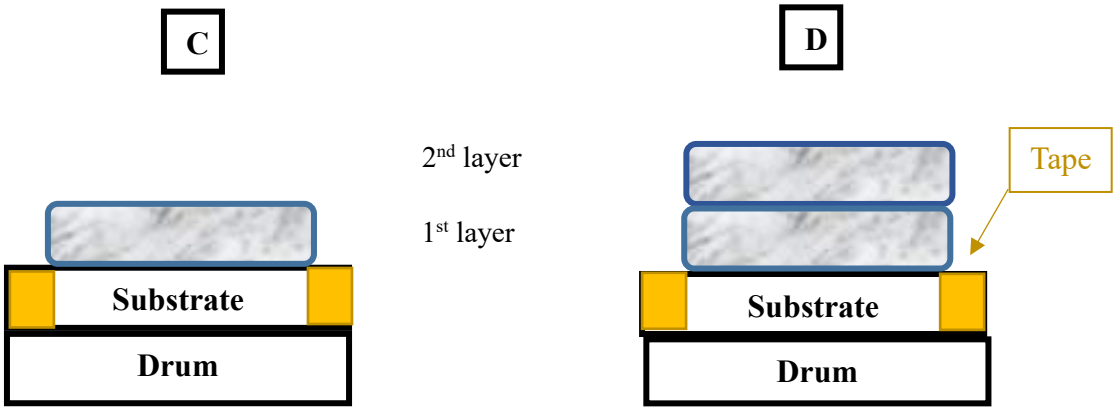

*Figure 1.3: Schema of the deposition of two thin films when modifying the volume (C has a volume V1 ml and D has a volume of V2= 2*V1)*

- Volume and injection rate: When combining the volume and injection rates effects onto the curing degree, different overall thickness, thickness per layer and number of passes under the curing source are obtained, as it can be observed in the following table (Table 1.1)

Volume (ml) / Injection rate (ml/min)	LOW	HIGH
LOW	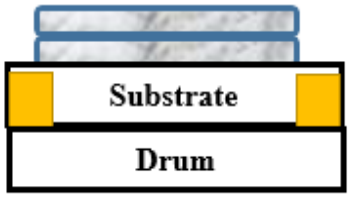	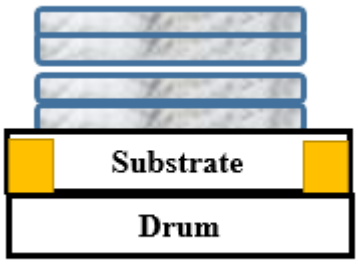
HIGH	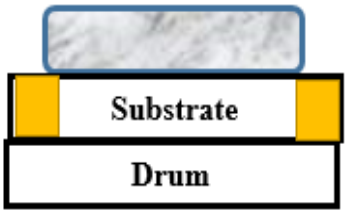	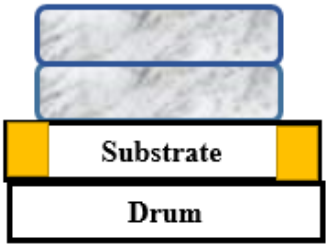

Table 1.1: Combination of volume (ml) and injection rate(ml/min) on the thickness per layer, number of layers(= number of passes under the curing source) and overall thickness of the coatings.

- Power: As the power of the curing source is increased, more reactive species will interact with the material. As for how the power is controlled, when using plasma the current is modified whereas the voltage will stay unchanged. This will cause a power modification. Regarding the E-Beam, since all the variables are linked together in this specific case, as changing the current, not only the voltage will change, but also the gas flow.
- Gas flow: The gas flow was also modified when using plasma. As the gas flow is increased, in theory, more reactive sites will be created, as there is more gas subjected to the ionization. In E-Beam as mentioned before, the gas flow can't be modified without altering the voltage and the current. So, in this case, it is not possible to distinguish the influence of each variable on the curing source. Finally, the gas flow was changed. Since in both curing sources, the reactive species are created from Ar, one can think that the more the gas flow, the more the reactive species and therefore, the degree of cure.

CHAPTER 2. LITERATURE REVIEW

2.1. COATING TECHNIQUES

2.1.2. Vacuum deposition

Once the most widely used non radiation curing techniques had been described, the process under study will be explained. Vacuum polymer deposition (VPD) or polymer multilayer (PML) is a method in which ultrasmooth and pin-hole free films are deposited at very high rates. The evaporative process can deposit films up to 10 microns thick (9) , with the upper thickness limit largely imposed by the penetration depth of the crosslinking radiation employed. Physical vapor deposition often takes place in a “good vacuum” in order to provide a long free mean path between collisions. It requires a pressure below 10-4 Torr, in order to avoid the reactive species from the curing source to interact with air molecules, reducing the curing efficiency.

One of the many advantages of vacuum processing in radiation curing is that it prevents the oxygen consuming the free radicals formed in the polymerization process. (2)Also, it is especially useful for reducing the vapor and gas contaminants within the coating material during the processing. In addition, it is more cost-effective given that the polymers are deposited 10-100 times more quickly, as it permits ultrafast deposition of polymer films in the same vacuum environment as conventional physical vapor deposition (sputtered or evaporated) thin films. It is especially useful for multilayer coatings, as it permits the deposition of multiple layers in a single pass through a vacuum coater, involving other vacuum-deposited layers such as metals and ceramics without issues of solvent compatibility (9). Thus, it is commonly used for polymer/metal layers

for gas barrier coating or dielectric films, as it is compatible with other vacuum processes such as sputtering or plasma enhanced chemical vapor deposition (PECVD). (10).

Vacuum deposition techniques allow formation of thin films that actually smooth the substrate on large areas. Polymer films can be deposited at speeds up 300m/min with an excellent thickness uniformity (~2%) (9) When comparing it to other printing techniques, the thermal source is less affected by the polymer viscosity, hence, as long as the vapor pressure is maintained the coating uniformity will be good (11). Since vacuum deposition is a solvent-free process, no solvent has to be removed after deposition. That is especially useful in organic-inorganic multilayer applications, given that there is no problem of swelling of the lower layer when depositing the top material. (12) .

Disadvantages include that it requires complicated equipment to maintain the vacuum environment, and high temperatures are required in order to evaporate the monomer. Furthermore, vacuum processes can cause the development of high internal stress in the resulting film due to the high deposition/curing rate. (11)

Coating technology's newest trend is looking for environmentally-friendly or more economic processes. Among them, vacuum deposition is being seriously considered as it does not involve solvents. (13)

2.1.3.Curing techniques

The monomers need some curing after being deposited onto the web, the different curing techniques include: Plasma, which induce electronic excitation and ionization, and UV, or E-Beam, which only have electronic excitation. But polymer can also be thermal cured by using some techniques such as infrared radiation, microwave or radiofrequency (11). Before giving a full detailed explanation of all these curing techniques, a classification

depending on the physical science beneath the different techniques is listed in the following table (Table 2.1):

Thermal curing	**Radiation heating**
	Convection/Conduction heating
	Induction heating
	Ultrasonic heating
	Resistance heating
	Thermal additives based heating
Radiation curing	EB
	Plasma
	UV
	X-Ray/Gamma

Table 2.1: List of curing techniques

2.1.3.1.Thermal curing

Nowadays, thermal curing is by far the most popular curing method for polymers. However, it has some drawbacks. In order to keep the temperature profile in range without degrading the material, long curing cycles are required. So, because of the low heat conductivity of polymers, the curing efficiency or in other words, the amount of time a polymer needs to be fully cured is greater than in radiation curing. In addition, it is a non-homogeneous process in which large thermal stress is induced in the material due to the thermal gradients. Also, it is still challenged by the size limitation, especially in the autoclave curing process. (11). For that reason, low-cost and highly efficient curing methods are being investigated. (14)

Thermal curing can be categorized, by the mechanism of heat applied, into radiation heating, convection and conduction heating, induction heating, ultrasonic heating, resistance heating and thermal additive-based heating.

None of these techniques produce ionization in the material due to the low energy of the infrared and microwave radiation. Also, due to the low thermal conductivity of polymers, they are challenged by the speed of heating, leading to long cure cycles, making it difficult to achieve reliable uniform heating of the films. (14)

2.1.3.2.Radiation curing

Radiation curing is a technique in which the polymerization is initiated by the use of high-energy ionizing (EB, plasma) or electromagnetic (UV) radiation. The use of ionization of radiation-sensitive polymers not only induces curing but also crosslinking, when working with multifunctional monomers. It has been found to be widely applicable in not only curing but also modifying the properties of polymers, as well as to tailor the performance of either the bulk or the surfaces. (14) (15) (16) Since the first patent in radiation curing in the early 1960s many applications have been developed, including gas barrier coatings (3) (6) (2), optical coatings (17), microstructuring (7) (18), gate dielectric (1) (19) (20), adhesives (21) (22) (23) floor covering (24) , printing inks (25) or antistatic layers (26).

Radiation curing provides some unique technological superiority compared to thermal curing, including improved resin stability, handling flexibility, fast curing speed, energy efficiency, high productivity, high solids and elimination of solvents, low cost and energy consumption, possible multiple operations, high degrees of cross-linking, and improved chemical, abrasion and stain resistance. (27) . In addition, it is a more convenient

technology in terms of the size of the equipment needed (11) and it offers a better control on the degree of cure (14).

2.1.3.2.1.Chemical reactions

Ionizing radiation may initiate various chemical changes in polymers. The energy of the source is absorbed by the polymer, and free radicals are produced, resulting in the following processes (28):

1) **Polymerization:** where monomers are joined together. This process consists of three steps:

1.1) Initiation: It occurs when introducing a material that interacts with the radiation generating suitable radicals.

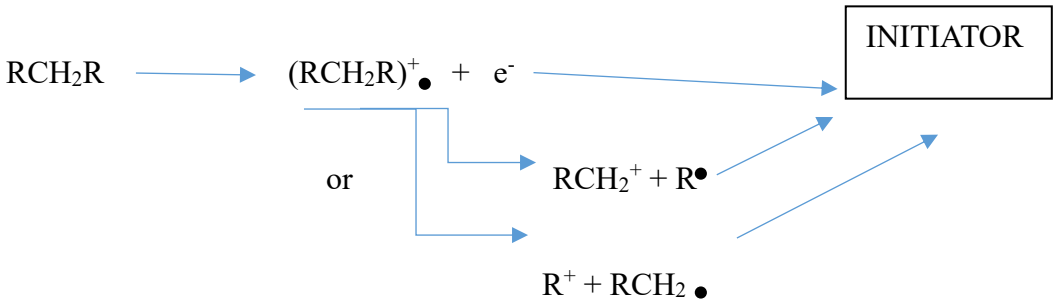

Figure 2.1: Initiation mechanism in radiation curing

1.2) Propagation: The reaction between the derived radicals with the polymerisable species.

Figure 2.2: Propagation mechanism in radiation curing

2.1.3.2.2.UV

The principles of UV curing differ from the other techniques aforementioned, as it is a non-ionising radiation and it usually requires the presence of a photoinitiator. This is because monomers don´t absorb UV light in an efficient way, hence why they won´t initiate the radical polymerization fast enough. There are essentially two types of compounds used in UV curing in order to absorb the light: The photoiniatior is a compound which under light excitation, is capable of generating large amounts of free radicals, leading to photo-polymerization and crosslinking processes (29) (14) (30) and a photosensitizer which is a light sensitive material capable of converting the UV radiation onto a more useful form of energy, or in other words, a compound capable of activating the photoinitiators even under visible light creating a synergetic effect with the photoinitiators . So, the process would be as follows: Photoiniators generate free radicals through unimolecular photocleavage or bimolecular hydrogen abstraction. Firstly, they absorb the incoming radiation and then they split up to form free radicals causing the polymerization of the formulation. (27) (31) Then, the chain propagation takes place and the monomer is consumed. By last, the combination of polymer radicals occur leading to the chain termination (32).

Light absorption PI $\longrightarrow$ PI*

Energy transfer to photoinitiator S* +PI $\longrightarrow$ S+PI*

Radical generation PI* $\longrightarrow$ R'

Initiaton R' +M $\longrightarrow$ RM'

Propagation $RM_n^+ + M \longrightarrow RM_{n+1}^+$

Termination $RM_n^+ + RM_m^+ \longrightarrow$ Polymer

Photoinitiators have to be selected depending on the wavelength of the radiation, so the maximum absorption has to match the emission of the light source, so it must have a high absorption at the exposure wavelength. The choice of the photoinitiator plays an important role as it will govern the curing rate. The photoinitiatior must display a high quantum yield of formation of initiating species, and a high reactivity of the radical towards the monomer. In addition, a photosensitizer is commonly added in the formulation in order to transfer the light energy to the other compounds. (33)

UV curing is a fast and room temperature process. It is cost efficient, energy-saving, environment and user friendly, which requires little space for the equipment and has low energy consumption. However, under air atmosphere it still has to overcome the oxygen inhibition effect. (33) (14) (27) (31) . UV cannot provide efficient curing in non-UV-transparent coatings due to the very limited penetration of the radiation. (14)

2.1.3.2.3.Plasma

Plasma cured polymers are deposited when the monomer is placed into the discharge zone of a plasma. The plasma is generated by the excitation of a carrier gas by means of electrical energy, creating reactive species such as ions, electrons, photons and excited molecules. The plasma-derived species reach the monomers inducing the polymerization. Additionally, the polymer obtained by plasma processes is subjected to further attacks by the reactive plasma species which may cause modifications to the surface properties and morphology. The mechanism of the plasma-induced polymerization is believed to be a combination of the UV radiation (indirect transfer) and the active species bombardment

(direct transfer) (18) (7) (34) (35) . However, the interaction between the plasma species and the organic precursors is not yet well understood.

2.1.3.2.4.Electron Beam

Electron beam curing is based on highly-energetic electrons that provide enough energy to initiate the curing reactions. Although it is well-known for almost 70 years now that accelerated electrons can be used to enhance the physical properties of polymers, industrial applications dates from the early 1980´s. (5) The energy used nowadays is typically 10 times greater than in thermal curing, which makes it an appealing technique for polymer processing. In addition, the electrons generated in EB curing can penetrate the full depth of (suitable thickness) coatings (14) vs thermal curing in which the heat energy diffuses through the material from the surface. (11) (27). Another advantage is that the rate of curing is really fast and it is more associated with the absorbed radiation instead of with the temperature achieved in the thermal curing process. As mentioned in the previous section, thermal curing induces residual stress, and this is completely erased by radiation curing because of the lack of thermal expansion/contraction (27).

E-beam curing has a high-dose rate and short processing times. One of the main advantages compared to other ionization sources such as plasma or gamma, is that the samples absorb all the energy of the source. However, they have a quick energy loss, and that's why it's use is limited to thin films. However, the greater the energy of the electrons the greater the penetration will be. (28) In addition, another important drawback of EB-curing is that any oxygen present combines with the primary radicals, terminating the chains and hence limiting the cure. However, since the curing takes place under vacuum

conditions, the oxygen inhibition does not represent an issue in the curing process, when using VPD, since even though the oxygen is not erased, at least is greatly reduced. (11)

When compared to UV, no photoinitiator is required, so they won't interfere with the curing reaction. However, the capital cost in the EB equipment is much greater. (27)

As for how the E-beam is created, a high current is passed through a filament, heating it up when using a low voltage and a high current. At that temperature, a stream of electrons are emitted from the surface, and are directed and accelerated to hit the source material. The filament is surrounded with a negatively charged cathode except for a gap (anode). Because of that the electrons can be directed in a specific direction in the beam. The process normally takes place at low pressure to prevent the losses due to gas collisions (9).

2.1.3.3. Conclusions Thermal curing vs Radiation curing

Due to the energy absorption mechanism in radiation curing, it provides unique technological superiority compared to thermal curing, including fast curing speed, energy efficiency, and improved resin stability. In addition, it offers a better control of the cure. However, it requires a radiation sensitive material, and more complex equipment is required. (14)

2.1.4. Summary

Now the main coating and curing techniques have been reviewed and compared, the technology that will be used in the project will be discussed with vacuum deposition as the coating technique and plasma and electron beam as curing sources to polymerize a diacrylate (Tripropylene glycol diacrylate).

Vacuum processing is a cost-effective and solventless process, which offers a great quality of the films, pinholes and defects free. Regarding the curing sources, to the best of my knowledge no studies have previously been performed on comparing plasma and e-beam as curing sources for polymers. However, some research has been done on each of plasma and e-beam treatment. While the chemistry of plasma samples seems to be unchanged before and after plasma treatment, e-beam samples present scission and branching throughout the film. This correlates with small changes on the glass transition of the polymers. (8) It would be interesting to know if those differences occur in these coatings, and if so, what changes about the properties of the polymers does the curing source cause. In this regard, the research project will be based on correlating the different process variables with the polymer´s properties.

2.2.CONTROLLING THE THIN FILMS PROPERTIES

The project is focussed on analysing the effect of the different process parameters on the polymer´s properties. The aim is to be able to control the curing degree and the crosslinking density, as it will further have an effect on other polymer´s properties such as mechanical properties, adhesion, wear resistance etc. Such properties will be of interest for applications of such layers such as packaging, or OTFTs. In addition, since evaporated acrylate is usually used in multilayer applications, the surface properties such as topography will also be investigated.

2.2.1.Curing degree

Curing refers to the polymerization and crosslinking processes in oligomers and monomers. The curing degree can be measured, by comparing the IR absorption of the C=C double bond (810cm-1), which is present in the unreacted functional group on the monomer, using the C=O (1730cm-1) as a standard baseline in order to normalise for the sample thickness, as the concentration of C=O groups does not change during curing. Figure 11 shows the 810cm-1 peak clearly in a sample of completely unreacted monomer, with this peak absent in well cured material. The conversion degree (i.e. the proportion of double bonds in the acrylate groups that have been reacted with) is then obtained by the following equation (7):

$$Conversion = \frac{\left[\frac{A_{810}}{A_{1730}}\right]_0 - \left[\frac{A_{810}}{A_{1730}}\right]_t}{\left[\frac{A_{810}}{A_{1730}}\right]_0}$$

Equation 2.1: Double bond conversion

Where:

$\left[\frac{A_{810}}{A_{1730}}\right]_0$ *is the monomer concentration of C=C bond with respect to the C=O bonds (before curing)*

$\left[\frac{A_{810}}{A_{1730}}\right]_t$ *is the polymer concentration of C=C bond with respect to the C=O bonds (at time t after curing started)*

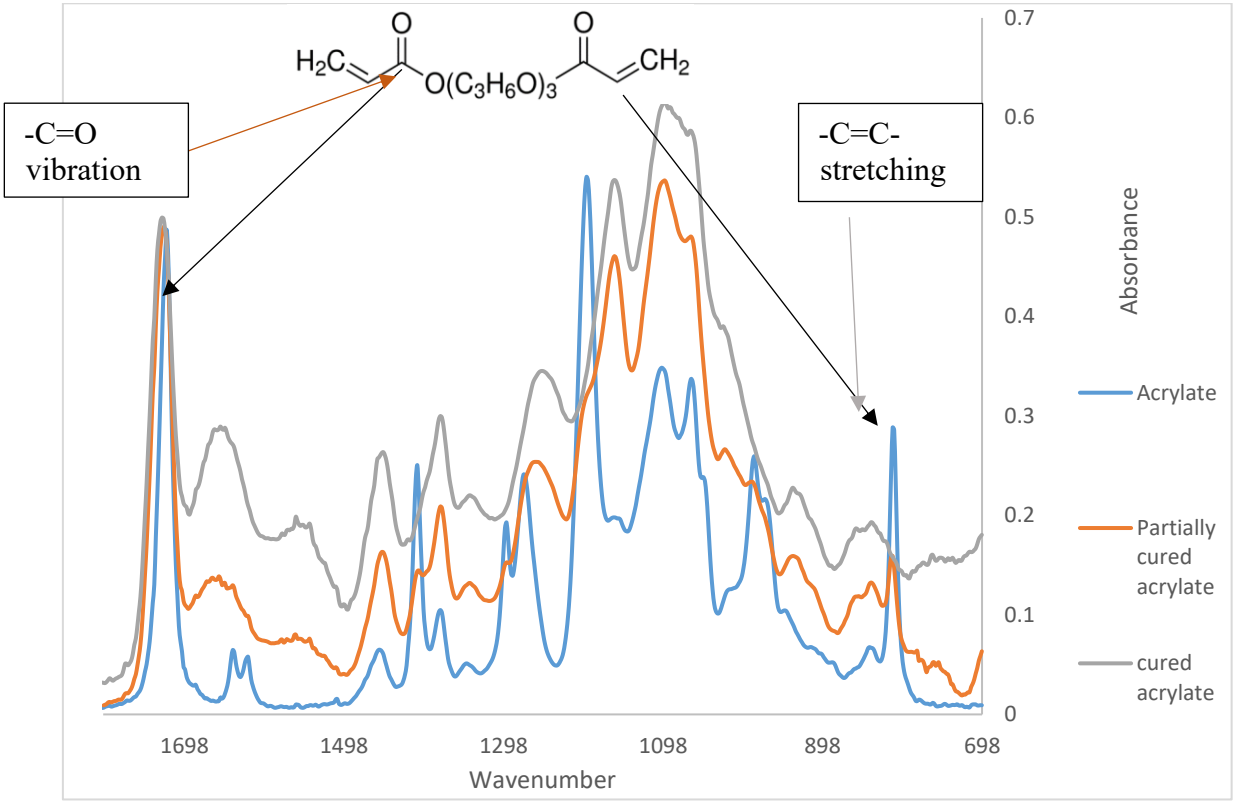

Figure 2.3: FTIR-spectrum of TGPDA in the monomeric and plasma cured

As it can be observed in equation 2.1, the degree of cure is based on the ratio of the absorbances. What is measured in this work is the peak heights (above the background intensity) of both: the –C=C- and the –C=O bond peaks, as opposed to the area. The peak areas are linked to the concentration of a specific bond within the material followed by the Beer-Lambert law (See section 3.2.2.2). Measuring peak areas, however, requires peak fitting rather than a simple measurement as it will be the peak height case. Since it is thought that the peak widths will not vary significantly with degree of cure, given that the peak width describes the intermolecular interactions mainly due to the hydrogen bonding, then measuring the peak height is a good approximation for estimating the relative concentrations of the functional groups. In addition, since both peaks are conveniently isolated from neighbouring peaks, peak fitting to deconvolute overlapping peaks is not necessary. This technique is by far the most widely used technique to estimate degree of cure (32) (9) (11) (36)

2.2.1.1.Chemistry

Acrylate-based coatings are by far the most widely used resins in UV, EB or plasma curing applications because of their high reactivity and fast curing speed, together with the large choice of functionalized acrylates. Since the early 1970s, acrylate coatings have experienced a steady growth in market in both volume and the range of applications. Therefore, many formulations have been developed in order to increase the curing speed or to enhance the polymer´s properties. In the following graphic the double-bond conversions of different chemistries are shown (30):

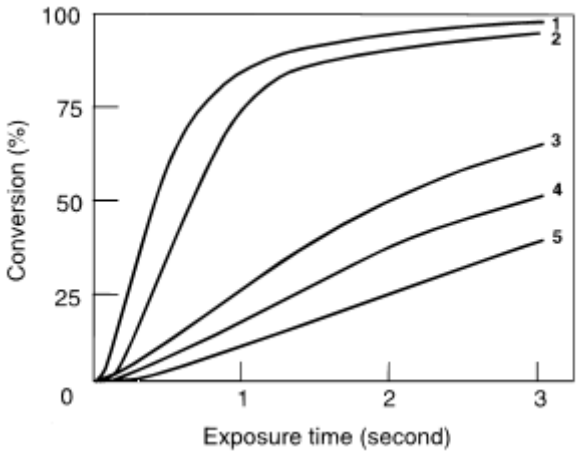

Figure 2.4: Polymerization profiles of different types of UV-curable systems: 1. Acrylate, 2. Vinyl ether, 3. Cycloepoxide, 4. Methacrylate, 5. Glycidyl ether (30)

The monomer functionality plays an important role in the final double-bond conversion and in the polymerization rate (36). As the functionality increases, the polymerization rate at the initial stage increases as well. This is due to the higher initial concentration of acrylate groups and viscosity, which accelerates the initial degree of cure.

However, it is expected to result in a lower final degree of conversion due to the fast increase of the crosslinking density (36). When a monomer reacts quickly, there are many unreacted monomers in the polymer network because the monomers form a network before achieving complete conversion. So, the chains won't have enough time to find other chains to crosslink with (11) . So, the fast increase on the gel fraction would limit the extent of final conversion, given that the likelihood of reactive species to reach a C=C would be reduced. (which is called, "the gel effect")

On the other hand, when a monomer reacts slowly, monomers achieve complete conversion without leaving unreacted monomers (21). In the following figure (figure 2.6)

the curing kinetics of acrylates with different functionalities is shown: It can be observed that indeed the monoacrylate may eventually cure to a greater extent than the diacrylate but will take a much longer time to cure.

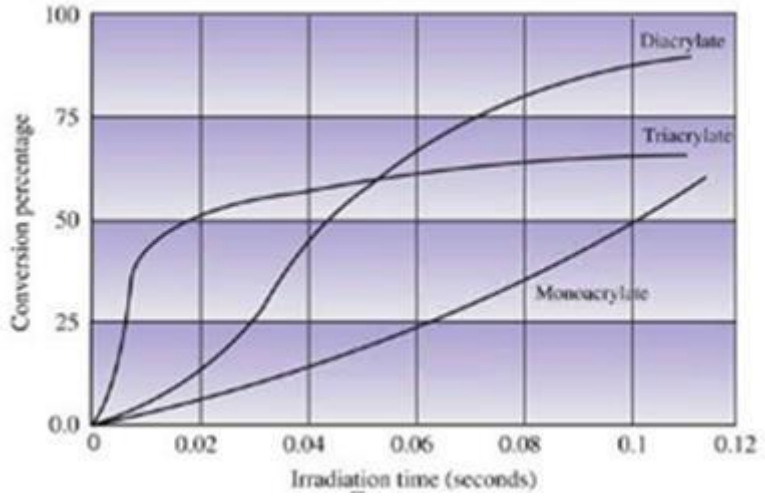

Figure 2.5: Curing performance of different acrylates at different irradiation time (11)

In one report, C. Elsner et al. found that greater functionality of the monomer, led to both reduced curing and slower polymerization (7) . The difunctional acrylates showed a double bond conversion of 100% after 5 minutes, while a pentafunctional acrylate achieved only 50% for the same curing time. In contradiction to the theory, it was found that increasing the functionality was detrimental for both the initial curing rate and the final double bond conversion. They suggested that this may be due to the differences in viscosities between the monomers, limiting the diffusion of the reactive species within the thin film. (37) In addition it is expected that the greater the functionality, the greater crosslinking density and hence the stronger and stiffer the material. In addition, by increasing the functionality, the solvent resistance, hardness and glass transition

temperature are increased. (38) However, it has found that the chemistry of the end groups also plays an important role in the mechanical properties such as pendulum hardness. It was found that when investigating the gel fraction (fraction of bonds connected to a three dimensional network) on different chemistries the results obtained differed between EB and UV. Depending on the chemistry, gel fractions where greater with one curing source or another, although it is still not well understood the real reasons of such contrasting phenomena. However, it still shows the importance of choosing the right chemistry for the right curing source. (37)

All in all, TGPDA has been shown to be one of the best curing acrylates by far, not only in curing rate but also in final double bond conversion, leading to a highly cross-linked polymer film, (7) and thus it forms the baseline polymer for this study.

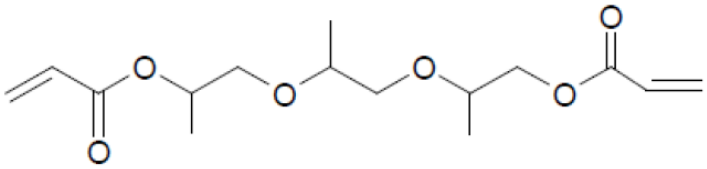

Figure 2.6: TGPDA formula

2.2.1.2.Importance of the degree of cure

As mentioned above, acrylate thin films can be used in many applications (Section 1.2.2) , but in this specific case, the project was born when two applications were studied within my research group, using acrylate thin films for barrier layers or as dielectric layers. In both research projects, it was concluded that the curing degree is one of the crucial parameters that must be controlled in order to use the acrylate thin films for those specific applications. (6) (1) (3)

Polymer/oxide/polymer coatings have exceptional barrier properties. When introducing polymer layers on either side of the oxide, the barrier performance is improved a factor of 15 or more. The acrylate layers smooth the substrate and protect the oxide layer from being scratched and against fracture at the high points of the substrate, which reduces the permeation rates. Affinito mentioned that even small amounts of monomer remaining the polymer layers would lead to poor barrier performance. Indeed, when depositing an uncured acrylate, the barrier performance was worse than the oxide layer alone. The reason of this experimental result is not obvious to the authors (6) (1) , although it is suspected to be a consequence of the increase of defects in the partially cured layers, which would ultimately allow the oxygen and vapor to go through the thin films. Therefore, one must be certain that the Polymer Multilayers or PML are fully cured, in order to prevent the fracture of the coating at the sharp, high points during wind up, given the surface roughness. The uncured layers showed a rougher topography, this will lead to an uneven load distribution, causing the oxygen and water diffusion throughout the PML layers.

The electrical characteristics of all-vacuum-processed pentacene (dinaphtho-thienothiophene (DNTT)) organic thin film transistors(OTFTs) using a polymerised tripropyleneglycol diacrylate (TPGDA) insulator layer were studied (3) (39). In the process, The acrylate layers were vacuum-deposited on top of PEN substrates patterned with Al gate electrodes as the bottom-gate dielectric using a radiation curing source to polymerise the TPGDA, then the semiconductor (DNTT) was evaporated directly onto the TPGDA surface, using evaporated gold source drain electrodes. The source–drain current was studied and it was observed that the total device current was small. It was hypothesized that the low mobility could have been caused by the highly polar nature of

the TPGDA surface. In addition, a comparison between devices using different curing sources (plasma, EB and UV) was performed. It was noticed that some of the devices failed due to the high the 'leakage current' (i.e. current passing between gate and drain). By studying the cause of the failure, it was found that it could have been a consequence of the poorly cured dielectric layer. There was noticed an increase on the leakage current values and break-down strength, as the degree of cure of the TGPDA layers decrease, when measuring the degree of cure qualitatively by the FTIR, studying whether or not the disappearance of the –C=C- was observed. (3) So, the most cured samples were obtained by plasma, whereas the least cured was the UV sample. So, it was concluded that the higher leakage current of EB or UV cured sample devices was probably caused due to defects e.g. pinholes or areas of poorly cured material.

These two examples show the importance of working with very well cured materials. There are other instances on the contrary in which partially cured films are necessary i.e manufacturing of 3D-micro- and nanostructures for micromechanical or microoptical devices. In this case, the replication of 3D-structures by moulding with UV-curing of liquid acrylates require two UV curing duplication cycle. First, a VUV-irradiation pre-treatment prior the moulding, followed by a complete UV curing cycle (25). In any case, it seems clear that being able to control the degree of cure seems to be an important goal to achieve. So, one of the main aims of the research project is not only comparing two curing sources, but also trying to link all the process parameters such as substrate speed, gas flow, deposition rates, and curing power with the curing degree of the thin films.

2.2.2.Crosslinking density

Crosslinking refers to the formation of a three-dimensional network structure from a linear polymer. (40) As opposed to the degree of cure, which measures the average C=C concentration, in crosslinking density the distribution of the linkages between the polymeric chains is determined. Hence, it is feasible that two thin films with the same degree of cure present different crosslinking densities. (24)

Almost 20 years ago, some studies on polyethylene revealed that even though it was thought to be an unreactive polymer, it did react under irradiation. Therefore, crosslinking didn´t require the addition of chemicals such as sulphur or the presence of double bonds. Radiation technology was capable of generating covalent bonds between the polymer chains even when they lack reactive functional groups. Since then, crosslinking by radiation on different polymers has been extensively studied. Therefore, radiation curing not only induces polymerization but also crosslinking processes. Since the monomer used here is a difunctional acrylate, each molecule has two sites that are highly reactive and hence, it enables the impartation of crosslinking or branching sites to polymer architectures. As an example, in a study of a pressure sensitive adhesive of acrylate, a correlation between the e-beam dose and the thin film´s shrinkage was found. A shrinkage of as much as 1.5% was possible with higher doses, but at the lowest doses there is no change in thickness, suggesting that that dose is enough only to cure but not to crosslink the polymer film. (22)

Crosslinking density determines the properties of the thin films as, for instance, the crosslinking at the surface has an influence in the film hardness, while other mechanical properties such as mechanical strength, storage modulus or stress at rupture are influenced

by the curing degree and the overall crosslinking density. (37) (41) In addition, improvements in the crosslinking density enhance not only the mechanical properties but also the chemical resistance. (40)

To determine the crosslinking density of polymeric materials, some indirect measurements can indicate an increase in the crosslinking density, such as the relationship between the applied force and the penetration depth when pressure is applied to the material with an AFM tip. Another method is, according to the kinetic theories of rubber elasticity, the stress-strain-crosslink density relationship by performing tensile tests can be established using the Mooney-Rivlin equation (40) (42):

$$F = 2A_0\,(\varepsilon - \varepsilon^{-2})(C_1 + C_2/\varepsilon)$$

$$2C_1 = \rho RT/M_c$$

Equation 2.2: Mooney-Rivlin equation

where:

F:Load [N]

A_0:initial cross-sectional area [m^2]

ε: extension ratio[m]

ρ: sample density[g/m^3]

*R: gas constant [m^3*Pa/K*mol]*

T: absolute temperature [K]

M_c: Average molecular weight of rubber segment between crosslinks [g/mol]

C_1 & C_2: Mooney-Rivlin elastic constant [Pa], with C_1 expressing the ideal elastic behavior and C_2 the deviations from that behavior

Other important characterization techniques are:

1. Crosslinking can be determined by modulus measurements in the rubbery plateau via Dynamic mechanical analysis (DMA). When the deformation when stretching only depends on the conformational changes of sections of chain between the crosslinks, instead of in bending or in the breakage of the bond, the relationship between the mechanical properties and the crosslinking density can be determined from rubber elasticity theory which gives the relationship: (41) (43)

$$v_e = \frac{G'}{RT} = \frac{E'}{3RT}$$

Equation 2.3: Relationship between rubbery plateau modulus and crosslink density

Where:

v_e: the crosslink density [mol/m^3]

G' is the shear storage modulus [Pa]

E' is the tensile storage modulus [Pa]

T is temperature [K]

*R is the gas constant. [m^3*Pa/K*mol]*

2. If the sample is not completely cured, further curing would occur when heating the samples during the DMA measurements, leading to changes in the crosslinking density. (43) In that case, swelling experiments is a more appropriate

method: (40) once the sample has reached the swelling equilibrium in an appropriate solvent, the swollen samples are weighed, and the apparent crosslinking density is measured using the Flory-Rehner equation (44). This requires the polymer-solvent interaction (χ), which can be obtained from the solubility parameters of both the polymer and the solvent. These parameters can be determined using various methods such as inverse gas chromatography, limiting viscosity measurements or turbidimetric determination. (45)

$$v = -\frac{\left(ln(1 - V_1) + V_1 + \chi {V_1}^2\right)}{V_0\left({V_1}^{\frac{1}{3}} - \frac{V_1}{2}\right)}$$

Equation 2.4: Flory-Rehner equation

Where:

V_1: the volume fraction of rubber in the swollen gel

v: the crosslink density [mol/ cm^3]

V_0 : the molar volume of solvent [cm^3/mol]

In swelling experiments is desired the greatest weight gain possible, which is achieved when the solvent has the closest polar contribution of the solubility parameter to that of the polymer. In previous works (46) , it was demonstrated that the solvent which has the closest solubility parameters to TGPDA is ethyl acetate (EtAc), so it was the solvent used, and the crosslinking was determined using the experimental parameters from the same research paper (46) .

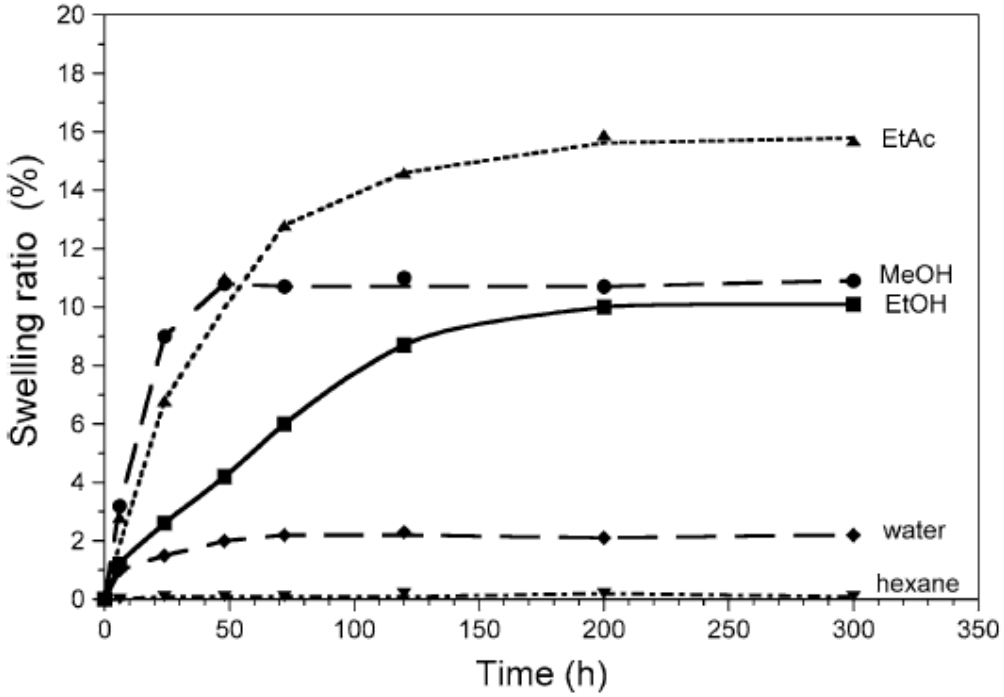

Figure 2.7: Swelling ratio of TGPDA for different solvents (46)

2.2.3.Mechanical properties

As mentioned above (Section 2.2), mechanical properties can be an interesting tool to better understand the structure of a polymeric thin film. They are not only interesting to measure by itself, but also to determine the crosslinking at the surface and in the bulk of the thin film. (37)

Some studies performed on TGPDA showed a strong correlation between the radiation dose and both the Young modulus and stress at rupture. The greater is the radiation dose, the higher is the crosslinking density and thus the better mechanical properties, such as Young modulus. (47) (48) However this relationship isn´t proportional: at very low powers, increases in the absorbed radiation dose of ionizing radiation leads to large increases in the gel fraction and crosslinking density, resulting in the formation of a

compact network. However, above a certain dose, when the crosslinking density reaches a critical extent, the mobility of the molecules is restricted and the gel fraction increases only slowly. It is called the crosslinking saturation effect. (49). Another study on UV cured samples, indicates that the greater the degree of cure, the higher the mechanical properties such as flexural strength and modulus. However, the relationship between degree of cure and power density was linear, whereas the flexural modulus showed a parabolic relationship. That might be a consequence of the different curing conditions, leading not only to differences in the curing degree but also in differences in the crosslinking density. (48)

Apart from the influence of the degree of cure and crosslinking density on the mechanical properties, some research has been done on comparing the mechanical properties of thin films cured by different sources. When comparing the mechanical properties such as microhardness and modulus between plasma and UV it was found that they were identical, indicative of the same radical polymerization process. (7)

On the other hand, comparative studies between E-beam and UV had been performed on urethane acrylate films. The tensile strength was much greater on the UV cured films. It is believed that the EB, which has a higher energetic radiation, doesn´t allow to the monomers to properly align such that they can attain maximum strength on polymerization. The results were double checked by measuring the overall gel content, which was much higher in the UV-cured systems than the EB-cured process. (37)

However, other studies performed on TGPDA showed the opposite result. In this case, the EB samples exhibit a 20% higher mechanical strength than their UV counterparts, caused mainly by the differences in the crosslinking density when the polymer is cured

with different radiation sources. (Fig. 2.9) It is believed that these differences arise because in UV curing cross-linking reactions tend to occur at the end of the polymer chain, whereas in EB curing crosslinking occurs either via radical-radical combination or radical attack upon an acrylate group, leading to a more regularly structured homogeneous polymer network, with a greater crosslinking density. (47)

All in all, crosslinking density is affected by the radiation dosage, acrylate chemical structure, curing source…

- As the radiation dosage is increased, the crosslinking density is increased as well. However, upon a certain radiation dose the crosslinking density does not increase any further.

- Given the polymerization kinetics difference between curing sources, it is believed that the faster the curing reaction occurs, the lower crosslinking density would be obtained. But also, due to the difference in how the curing reaction occurs when using different curing sources, different crosslinking densities will be achieved. EB and UV cured samples behave differently when it comes to mechanical properties. However, when comparing plasma and UV regarding the coating´s mechanical properties the results obtained were identical.

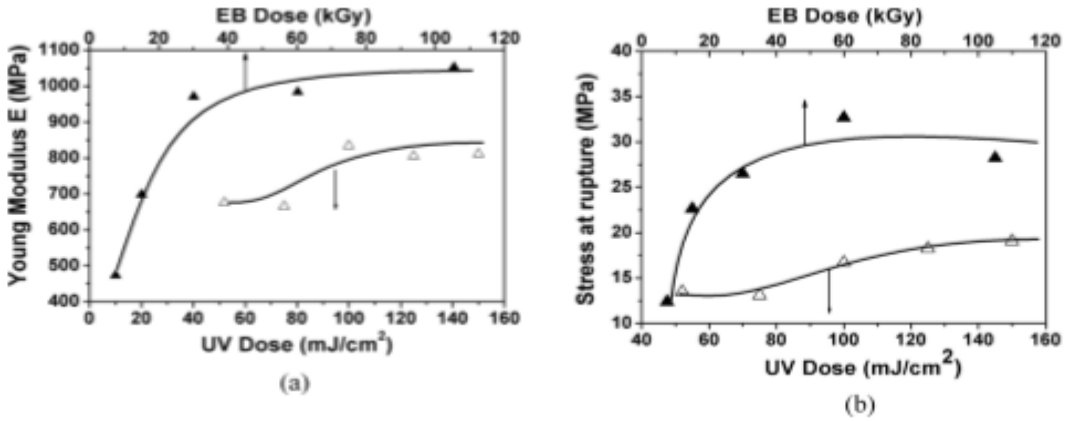

Figure 2.8: Dependence of the Young modulus (a) and stress at rupture (b) on the delivered dose for TGPDA films which were exposed to EB and UV irradiation (47)

2.2.4.Topography

In VPD, unlike in other deposition techniques, the coating doesn't replicate the substrate surface roughness. On the contrary, the monomer vapour condenses on the surface of the substrate as a full-thickness liquid film, resulting in an ultrasmooth pinhole- and defect-free coating. (9)

In gas barrier applications the topography is one of the key factors. It is desirable that the film is smooth in order to minimise the defects, in subsequently-deposited ceramic layers, that allow gas transmission. However, the smoother it gets, the more likely the phenomenon of blocking (when two surfaces stick together when rolled up or stacked during handling) occurs, since the imperfections on the film's surface prevent the total contact of the two film layers (24) . Evaporated deposited acrylate has been studied as a smoothing layer on different substrates. All in all, the results indicate that the smaller the peaks are to cover, the smoother will be the resulting film once the acrylate is deposited. As suspected, the greater the thickness of the acrylate, the smoother the resulting films

(2). This effect can be also useful for optical applications. It was proved that the reflectivity of silver thin films was enhanced when it was grown on top of an evaporated acrylate. When evaporating a monomer, the polymer doesn´t reproduce the defects of the substrate, erasing the defects and decreasing the pin holes in the metal film. (17)

Having explained above why topography is important, there may be a number of origins of topography e.g. etching, or migration of material during the curing process, (either due to surface energy effects or due to repulsion between residual charges).

As for instance, regarding the effect of the curing source on the thin film topography, a study of evaporated polymers EB-cured showed that instead of obtaining smooth layers, the RMS roughness was much greater in EB than in UV-cured samples (Fig.2.10). It was believed to be a consequence of the electrostatic repulsion between the electrons that are left in the thin film. (6)

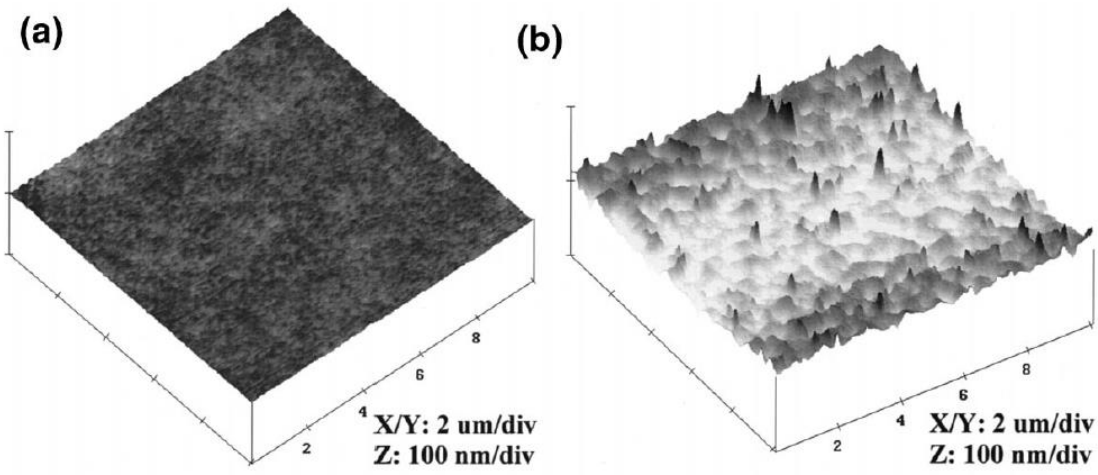

Figure 2.9: AFM scan of: a. UV cured, b. EB cured (6)

Plasma can be used to selectively etch thin films. Plasma etching of polymers is not homogeneous as the reactive species have the tendency to preferentially etch the soft segments of the polymer. Plasma breaks the chemical bonds resulting in the ablation of the resulting low molecular weight compounds. (8)

In addition, some differences are expected between partially and completely cured coatings. M. Fokina reported that when the curing wasn't homogeneous, the monomers flow towards the polymer due to the volume shrinkage of the cured areas (50). Indeed, they accumulate on top of the polymer due to it´s higher surface energy. In other words, if some regions cure first, and then there is time before further reaction takes place, for non-bonded uncured species to migrate to the top of the first cured regions. Thus the films will be rougher due to the accumulation of the uncured species towards the surface of the cured areas. (51) For instance, when comparing partially and completely UV cured samples, both were really smooth, but the surface of the partially cured coating was covered with shallow depressions. (6)

CHAPTER 3. METHODOLOGY

3.1. Process conditions

Now that both vacuum physical deposition and radiation curing had been explained (Chapter 2, Part 1), the specific process used in the research project will be described:

To manufacture acrylic coatings, TPGDA was vacuum-flash evaporated (flash evaporator on Fig.3.1a) onto the substrates, which were taped to the coating drum of the Oxford vacuum web-coater (Aerre Machines) (Fig 3.1b).

Two alternative curing sources were used: plasma and e-beam. For plasma curing, a plasma was generated and confined by a magnetron sputter target., The power supply was an MDX10 K (Fig 3.1c), with a maximum current of 25A for the lowest range of voltage (0-500V) and the lowest impedance. The power range used in the experiments was from 100 to 1500 W. Prior to polymer deposition, by the use of O_2 gas flow, the sputter target was passivated in order to avoid sputtering. And by means of the electrical energy, the ionization of the Ar gas will take place, creating reactive species which will then interact with the uncured material. In the experiments the complete cure is ensured by using the 10% of the maximum power approximately (Hence, at 150W, but only for injection rates below 0.1 ml/min). Therefore, the standard current is set at 6 A, which due to the MDX impedance causes a 230-250V.

From that initial value, the power was reduced in order to obtain partially cured samples, which allowed to understand the breakage of the double bonds caused by interaction between ions and electrons with the matter. Since, not only the power, but also the

injection rate has an influence on the degree of cure, the value at which partially cured films are obtained is not a straightforward value.

This plasma curing was compared with electron beam curing. When using plasma as the curing source, highly energetic ions, electrons and even UV will interact with the material. However, when using E-Beam, only high energetic electrons interact with the monomers. The electron beam was formed by a diode-sputter-cathode which was mounted in an earthed metal box with a slit of about 4 mm width and 400 mm long directly facing the cathode. The electron gun operates at between -2 to -5 kV. These electrons are accelerated by the cathode and exit the box through the slot, forming an electron beam. In this case, the standard input current is set at 100 mA, which means a 6,4-6,8 kV. But the actual e-beam output was, however, much smaller. These parameters again, ensured a complete cure. So from there the power was reduced until there was no polymerization. (Fig 3.1d)

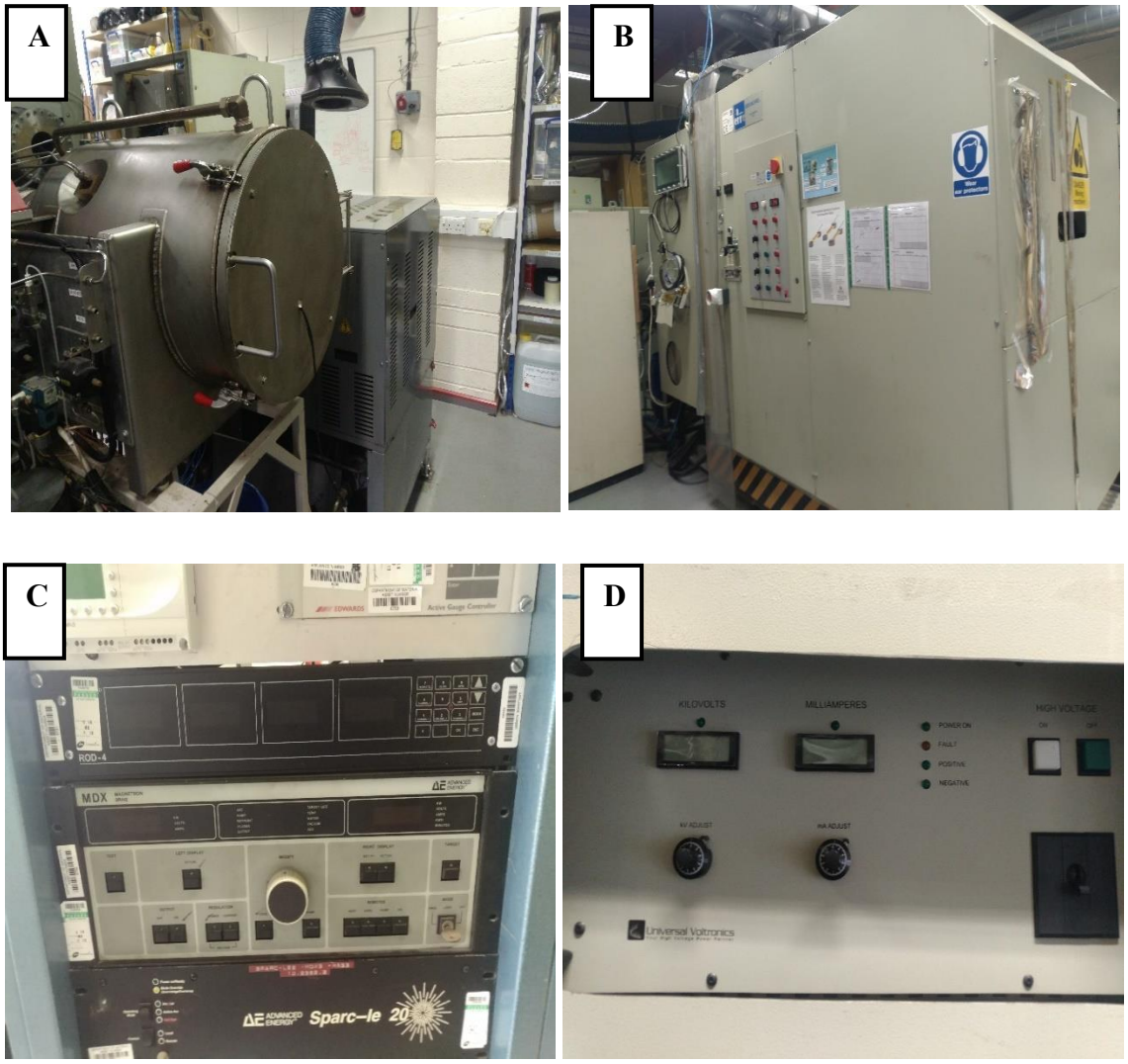

Figure 3.1: Webcoater images. A)Flash evaporator. B)Vacuum chamber. C)Plasma power supply.

D) E-Beam power supply

3.2.Characterization techniques

In this chapter the techniques used in this thesis to characterize the materials are outlined. In order to measure the thin films' properties, the substrates used were either silicon

wafers or gelatin. Characterizing a thin layer of one polymer (acrylate) on top of another (substrate) is challenging, as much of the signal will likely be due to the underlying substrate. In order to avoid "the substrate effect" (which will cause the obtention of a signal from a substrate when measuring the chemical composition of the samples through spectroscopic techniques), not only by the addition of the substrate weight when using Soxhlet extraction but also to avoid the characteristic peaks of the Si or glass substrate when using spectroscopic techniques (FTIR, XPS), mechanical testing (DMA) or gel fraction studies (Soxhlet extraction) the substrate was removed. This was achieved by depositing the acrylate onto gelatin leafs fixed in the coater by sticking the leafs with tape. After coating, the gelatin was dissolved in hot water at 60ºC to obtain free-standing films of the acrylate. The hot water is not expected to have an effect on the properties of the acrylate material (46) . In addition, when measuring the weight loss before and after being subjected to Soxhlet, the weight of the substrate is eliminated, so all the data obtained in the microbalance correspond to the sample´s weight.

3.2.2.FTIR

FTIR is a non-destructive technique in which molecular-level information can be obtained. The identification and measurement of the compounds can be made for samples in various states. The technique enables the simultaneous detection of the whole spectrum at once.

3.2.2.1.Basic Principles

When irradiating a sample with infrared light with an energy hν, it induces a transition between the vibrational modes of the molecules. Since this interaction depends on the displacement of the atoms from their equilibrium state, the absorption due each bond-

type takes place at different frequencies. Therefore, the different functional groups can be identified by their unique characteristic vibration bands. The representation of all these bands results in the absorption spectrum, in which the vibrational movement caused by the electromagnetic radiation depends on the direction of the movement (stretching or wagging for example).

3.2.2.2.Instrumentation

First of all, an IR source is needed. When electricity passes through a conducting ceramic bar (glow bar) causing the resistance to conduction of the current to heat up. This finally results in the emission of light in the IR region.

The radiation is then reflected in equal parts by the use of a beam splitter. By the use of two mirrors, the radiation reflects back causing the radiation to recombine for all the wavelengths, which is called interference. The beam splitter-mirror distance is a multiple of the laser's radiation wavelength. So when the radiation is reflected back to the beam splitter it would arrive "in phase" and a strong signal will be seen at the detector as a result of the recombination of two signals (constructive interference), obtaining then a sinusoidal signal at the detector. So, the resulting radiation goes from the sample towards the detector. This responsive element changes the radiation into an electrical signal (Fig.3.2).

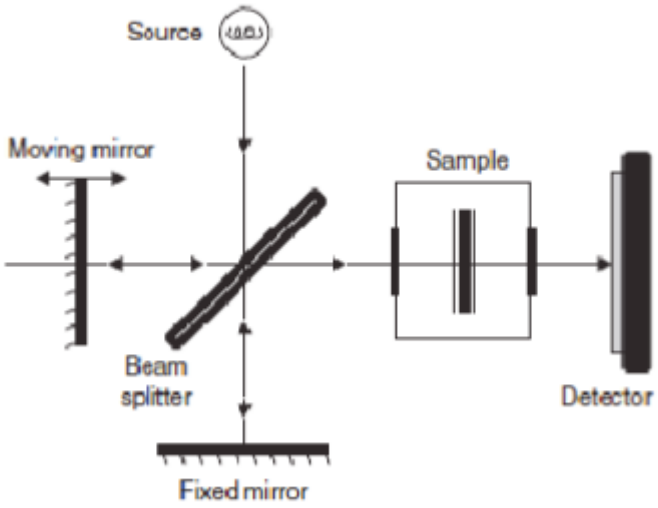

Figure 3.2: FTIR instrumentation (52)

In terms of use, the spectrum obtained combines the bands of the sample and the environment, therefore a background spectrum must be performed. Once the data had been gathered, not only qualitative, but also quantitative information can be made. This is because the FTIR technique is based on the Beer-Lambert law (Equation 3.1). So all the peaks absorbancies are proportional to their concentration in the sample (52) (53).

$$A = \varepsilon lc = -\log_{10}\left(\frac{I}{I_0}\right)$$

Equation 3.1: Beer Lambert law

Where:

A: IR absorbance

ε*: absorptivity of the attenuating species [cm^2/mol]*

b: path-length[cm]

c: concentration of the evaluated group [mol/cm^3]

I: light transmitted through the sample

I_0: incoming intensity of light

However, there is a decay on the intensity of the incoming light as it interacts with the atoms of the material, absorbing the light. And this principle was observed in the electrons and plasma interaction with the thin films (See Chapters 4 and 5)

In the experiments, FTIR measurements were obtained using a Varian Excalibur FTS 3500 FT-IR Spectrometer, working in the mid IR range 7,000 to 350 cm-1, with DTGS detector, in ATR conditions.

3.2.3.Soxhlet extraction

The FTIR data were then double-checked with the weight loss of the polymer films measured before and after being subjected to a Soxhlet extraction in a suitable solvent (toluene) to remove unbound monomer (54). Soxhlet extraction is a solid–liquid extraction in which a solvent is heated up until it evaporates. When the liquid reaches an overflow level, a siphon aspirates the solvent and unloads it back into the distillation flask, carrying the extracted molecules in the bulk liquid. (55) (Fig. 3.3) It is highly important that the molecules that would be extracted are soluble in the solvent. Therefore, the liquid must have a similar polarity with respect to the liquid, defining polarity as the ability of a molecule to enter into interactions of all kinds. Soxhlet extraction is considered a hybrid continuous–discontinuous technique, since on one hand the solvent acts stepwise, but on the other hand the solvent is recirculated through the sample. (56)

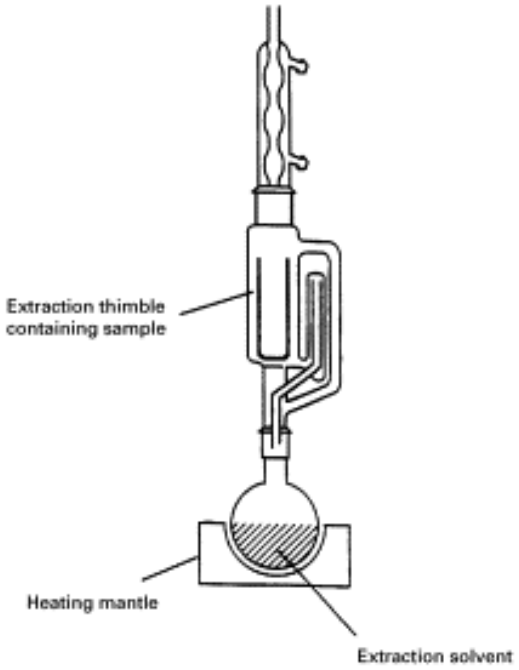

Figure 3.3: Soxhlet extraction set-up (56)

The aim of Soxhlet extraction is to get rid of the uncured material in order to reach the gel point, in which the solvent would undergo gelation, as reflected in a loss in fluidity, whereas the formation of a pure 3D network (gel fraction) would occur in the polymer (spanning the entire system), as there won't be internally unconnected material susceptible to be dissolved left in the polymer.

Regarding the conditions in which the experiments took place, the polymer films were extracted with toluene since it interacts with the uncured material. The films were then held in a vacuum oven at 65ºC for 2 days in order to be sure that it won´t be solvent left in the material. The dried films were weighted and the gel content was calculated following the formula (Equation 3.2):

$$Gel\ content\ \% = \frac{Mass\ of\ sample\ after\ extraction\ (mg)}{Mass\ of\ sample\ before\ extraction\ (mg)}\ x100$$

Equation 3.2: Gel content equation

When comparing the Soxhlet extraction and FTIR results different data were obtained. This is because by means of the FTIR technique the total –C=C- are obtained. This will include the unreacted material and the chain ends. However, by using the Soxhlet method only the unreacted proportion is obtained, given that what is measured by this technique is the loss of weight once the material that is not connected to the polymer network is extracted.

3.2.4.Ellipsometry

The ellipsometry technique real-time monitors the changes in the polarization state of the light wave produced by a solid.

3.2.4.1.Basic Principles

When the light is reflected at a planar surface, the electric field of the polarized wave can be expressed by the contribution of two components: a parallel and perpendicular electric field to the plane of incidence, or in other words, to the sample. The relationship between them to respect to a plane determines the amplitude and the phase, or incident angle.

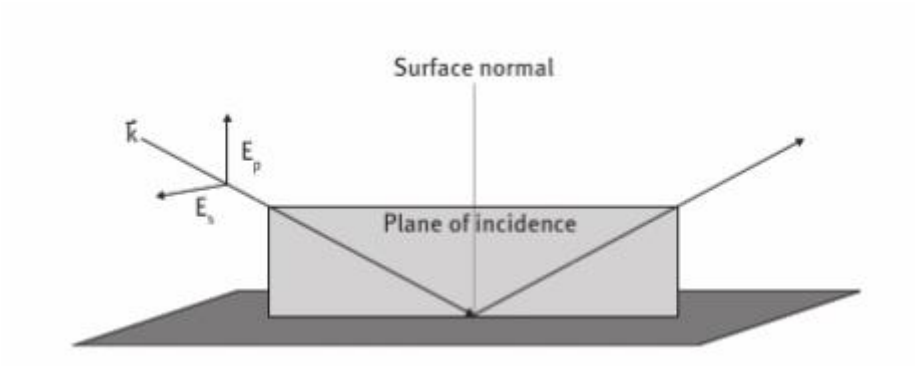

Figure 3.4: Reflection of the light in Ellipsometry (57)

Both components of the electric field have an amplitude and a phase. So, when the light is reflected in this certain plane, both, the phase and intensity change at the point of reflection. The light wave interacts with the thin film, altering the complex index of the electric field. The change in polarization is measured by the ellipsometer, and since it depends on the wavelength of the light, the environment, the angles (incident and refractive), but as well on the thickness of the sample, a relationship between the amplitudes and angles of the electrical field and the thickness of the sample can be obtained. (57)

3.2.4.2.Instrumentation

Light from the source is directed to a polarizing element that fixes the elliptically polarized state of the light, and, after reflection from the sample it is detected by a device capable of gathering the measuring the polarization state of the reflected beam (57) (58).

In the research project case, the coating thickness was studied via Ellipsometry, measuring the coatings deposited onto a Si substrate. A Beaglehole Instruments Picometer Ellipsometer at single wavelenght was used.

3.2.5.AFM

AFM is a technique which allows us to see the surface structure under minimally invasive conditions. It is based on the interatomic interaction forces of between the atoms in a sharp tip and the surface of a sample, allowing one to build up a map of the sample´s surface heights with resolution and accuracy.

The first non-contact profiler was invented in 1971 by Russell Young, who used the dependence between the electron field emission of an electrically conductive sample and the probe-surface distance to re-create the topography. It was improved by Binning and Roher (1981) using the electron tunnelling instead, increasing therefore, the vibration isolation.

The first AFM paper was published in 1986 by Binning, Quate and Gerber, which allowed for the very first time the characterization of not only electrically conductive sample but on insulating samples as well.

3.2.5.1.Basic Principles

In AFM the movements of a tip are controlled by a voltage applied to a piezoactuator. Then the interaction between a sharp tip in proximity to the surface is measured. The cantilever on which the tip is set behaves as a spring, which will locally deform as a

consequence of the forces induced between the hemispherical end of the tip and the sample. The z piezoelectric moves up and down to maintain the tip–sample distance fixed, so the cantilever bends as a result of the sample topography. The amount of bend determines the force on the cantilever. If this force is kept constant, then the height of the tip must be changed to map the profile of the sample. In this way, by monitoring the voltage applied to the z piezo, a map of the surface shape (a height image) is measured. (59)

In the case of study, the imaging mode used is tapping mode, in which the tip is placed close enough to the surface of the sample for short-range forces to become detectable, but avoiding the tip-sample contact (contact mode) which would be undesirable especially for partially cured samples, because the tip could potentially stick to the sample. In addition, by using this technique sample or tip degradation can be avoided. When comparing tapping with non-contact mode, the images resolution are greater as the changes in force will be greater as well when using tapping mode.

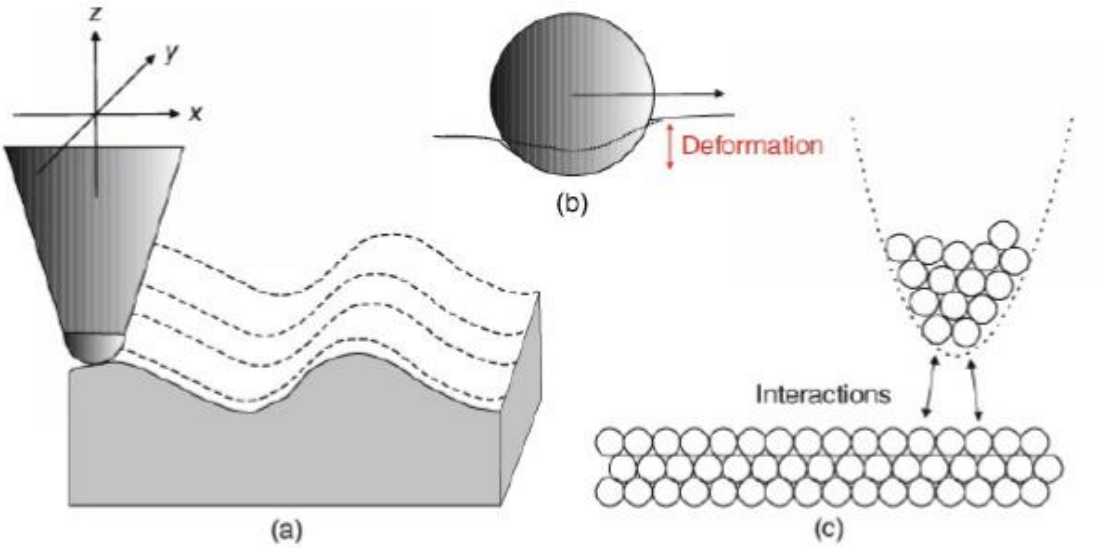

Figure 3.5: Interaction between atoms of the probe and the sample (59)

3.2.5.2.Instrumentation

AFM has two main components:

1) A piezoelectric transducer, that through a voltage applied, moves a tip converting the electrical potential into mechanical motion. By applying a voltage, tiny movements of the free end of the tip can be controlled.

2) The force transducer converts the output force between the sample and the probe into voltage (59) (60) (61).

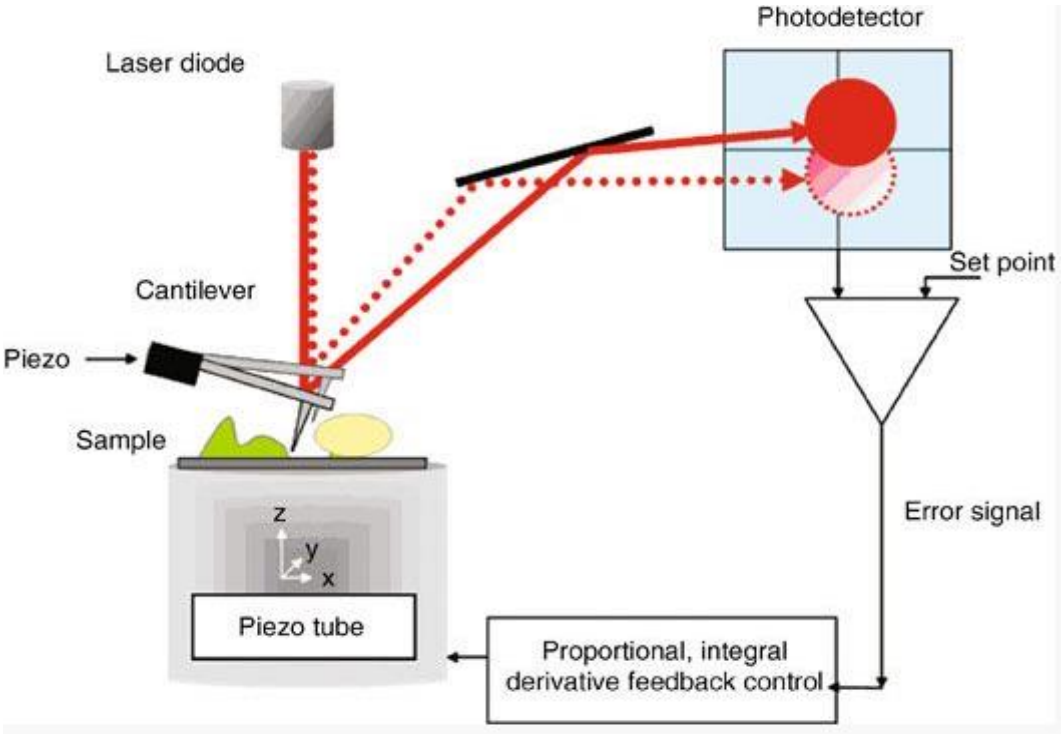

Figure 3.6: AFM instrumentation (61)

3.2.6.DMA

Dynamic mechanical analysis is a technique in which the complex modulus of the mechanical properties of viscoelastic materials is obtained as a function of temperature.

3.2.6.1.Basic Principles

When a load is applied sinuosoidally, it creates a sinusoidal deformation. The resulting strain wave depends on the elastic and viscous contribution of viscoelastic materials.

The behaviour is then in between the elastic and the viscous behaviour. In the elastic limit the behaviour is described by Hooke´s law, in which stress is linearly dependant on the strain. Whereas, in the viscous limit the behaviour is described by Newton´s law, in which the stress is dependant to the strain rate. Then, the intermediate mechanical behaviour is

defined as a complex modulus: storage modulus for the elastic component and loss modulus for the viscous component. In polymers, the mechanical properties-temperature dependence will vary depending on the chain length (distribution), degree of crosslinking, degree of crystallinity and thermal stability. And the motions of the polymer chains can be obtained by this sensitive technique. In polymers, the space that a molecule has for internal movement (free volume) increases as the temperature does. Then, by treating the polymer as n mobile segments, many useful information such as the transition of polymers or the crosslinking density can be estimated.

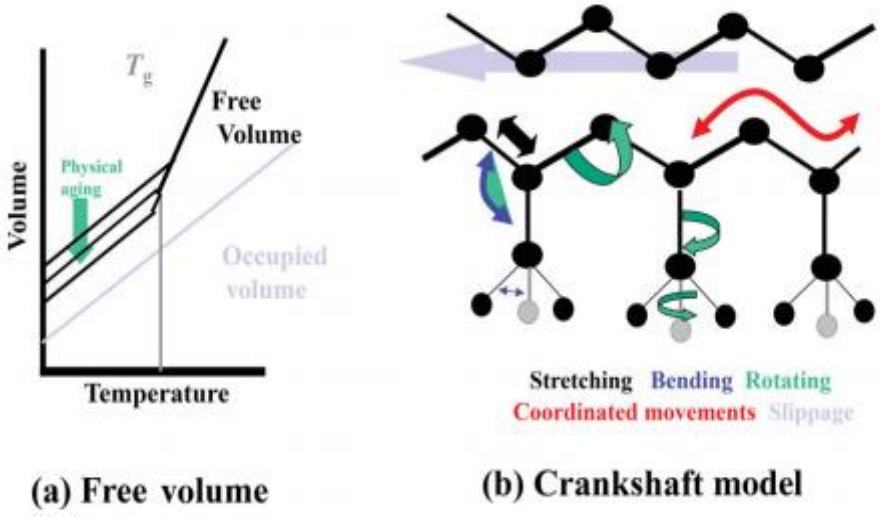

Fig. 5. Free volume and molecular motions in polymers.

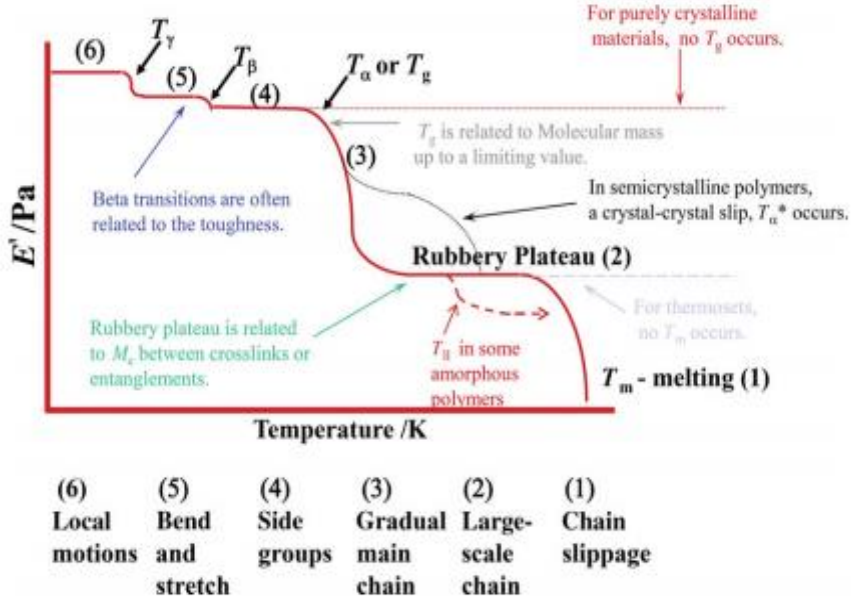

Figure 3.7: Changes in polymer´s properties with temperature (62)

3.2.6.2.Instrumentation

In DMA a thermocouple is used as a temperature sensing device. The temperature is changed by using a cooling circuit with liquid nitrogen for low temperature and a furnace in order to increase the temperature above ambient temperature.

The sample is held by clamps, which can have different geometries, such as torsional or axial configuration, in order to get different mechanical information.

There are two different analyses in which either the stress or the strain are controlled. When the stress is controlled a set force is applied by using a force balance transducer, whereas when the strain is controlled the probe is moved at a set distance (62) (63).

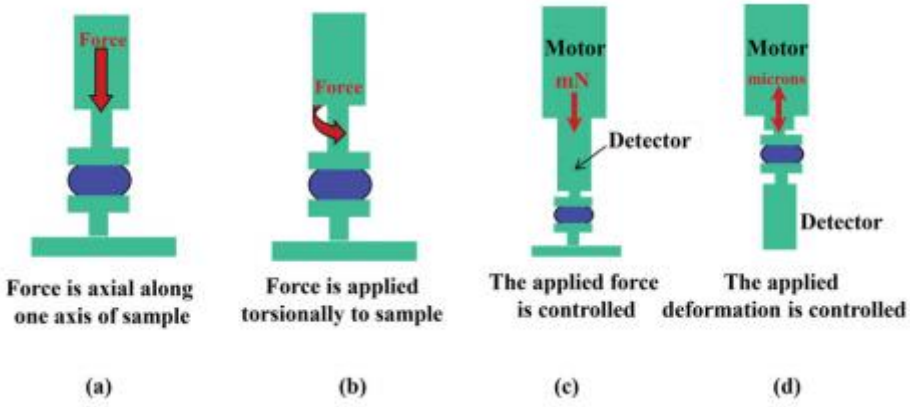

Figure 3.8: Different clamping configuration in DMA (62)

In the experiments, a DMA Q800 was used. The thin films were cut in rectangles of 5x20cm. The ends where glued on both sides to a cardboard. The cardboard was then adjusted to the DMA instrument in tensional conformation at different temperatures (from -90ºC to ambient temperature) and different frequency (1, 5 and 10 Hz) in order to perform the experiment.

Figure 3.9: TA instrument DMA Q800 (university of Oxford, Engineering department)

CHAPTER 4. CURING DEGREE

In this chapter the interaction between reactive species coming from different curing sources (E-beam and plasma) and a polymer thin film will be analyzed. For that purpose, the degree of cure and the thickness will be studied when varying different process parameters such as injection rate, volume, gas flow or power.

4.1 Curing degree when using different characterization techniques

First of all, the comparison of different characterization techniques when it comes to measuring the degree of cure will be performed.

4.1.1 FTIR vs Soxhlet

When comparing the degree of cure using the two different methods, it has been found that the results follow the same trend. However, the degree of cure is a bit higher when using Soxhlet extraction. In Soxhlet, the unreacted material is removed from the polymer network. This comprises the low molecular weight oligomers and monomers, which would dissolve in the solvent, toluene. Hence, only the not-bonded material is measured by calculating the thin film´s weight before and after the Soxhlet extraction. With FTIR, in contrast, both, the unreacted material and the chain ends are measured. This technique measures the absorbance of a specific bond, in this case the -C=C-, and this bond is not only present in the uncured material but also at the polymer´s chain ends. In both cases, the same baseline is used, the thin film (cured + uncured material).

In the following figure (Figure 4.1) a comparison of the degree of cure between the two characterization techniques has been made. In order to do so, the degree of cure of the

thin films obtained by using different process parameters had been used. In this case the process parameters including the curing source don´t play a role, given that what is measured would be the same in every case: the difference between the -C=C- of the unreacted material versus the ones comprising the unreacted material plus the ones comprising the chain ends.

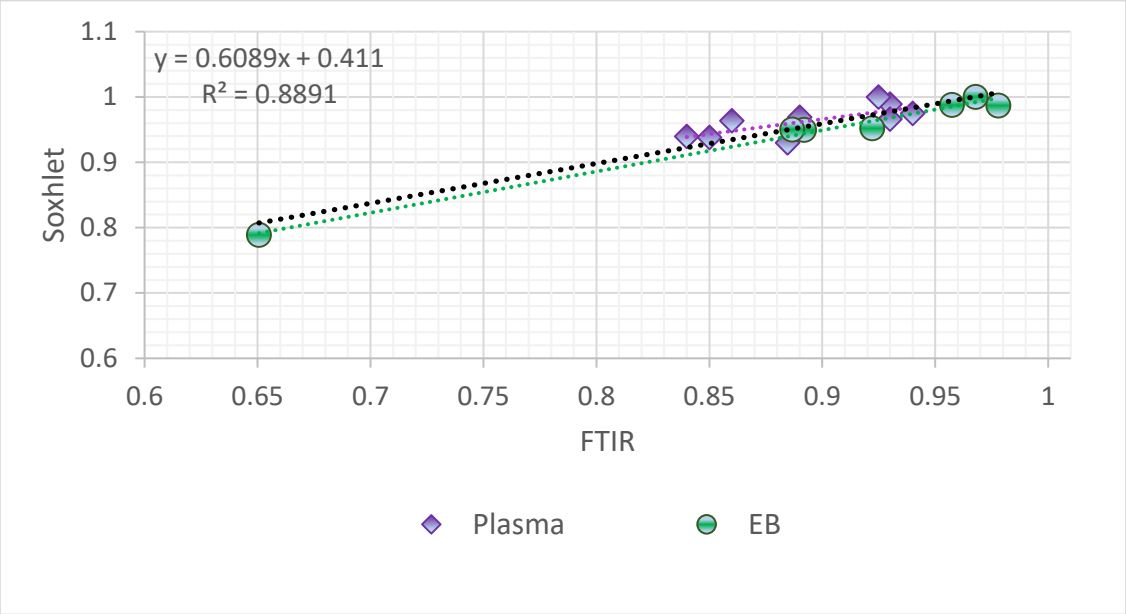

Figure 4.1: Degree of cure measured by FTIR and Soxhlet (for E-beam and plasma cured samples)

It was observed a linear correlation between the experimental data obtained by the two different characterization techniques (with a correlation coefficient of 0.9). In both instances the degree of cure was represented (Equation 4.1):

$$degree\ of\ cure = \frac{thin\ film - unreacted\ material}{thin\ film}$$

Equation 4.1: Degree of cure equation

So, now, in order to obtain only the -C=C- proportion, the following equation has been used:

$$\frac{unreacted\ material}{thin\ film} = (1 - degree\ of\ cure)$$

Equation 4.2: -C=C- proportion using the polymer network as a baseline

In the following figure (Figure 4.2) a representation of the -C=C- by using both characterization techniques has been done. The -C=C- represent different things depending on the characterization techniques (Eq. 4.3 and 4.4).

$$1 - Soxhlet = \frac{unreacted\ material}{thin\ film}$$

Equation 4.3: unreacted material measured by the use of the Soxhlet extraction method

$$1 - (degree\ of\ cure)_{FTIR} = \frac{(-C = C-)_{monomers} + (-C = C-)_{chain\ ends}}{Polymer}$$

Equation 4.4: -C=C- measured by the use of the FTIR method

The aim is being able to better understand the proportion between the uncured material versus the contribution of the chain ends and uncured material.

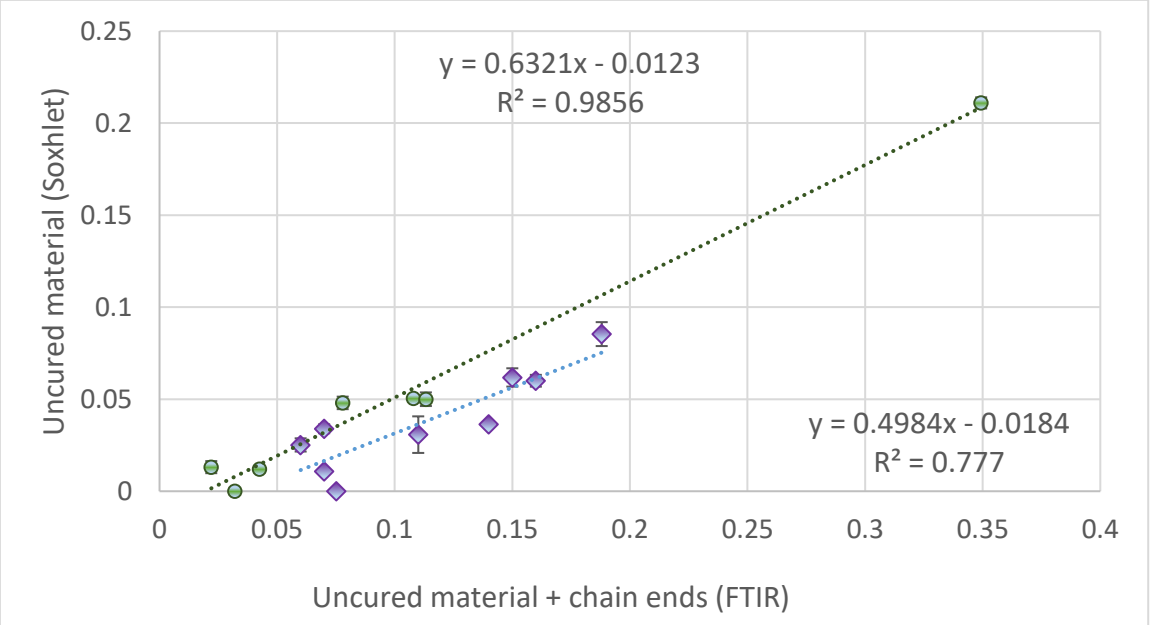

Figure 4.2: -C=C- measured by FTIR and Soxhlet (for E-beam and plasma cured samples)

Hence, by a adding a trendline the gradient would indicate the uncured material obtained by Soxhlet with respect to the uncured material + chain ends obtained with FTIR. So, using equations 3 and 4 the gradient is obtained (Equation 4.5):

$$Gradient = \frac{\frac{unreacted\ material}{thin\ film}}{\frac{(-C=C-)_{monomers} + (-C=C-)_{chain\ ends}}{thin\ film}}$$

$$Gradient = \frac{unreacted\ material}{(-C=C-)_{monomers} + (-C=C-)_{chain\ ends}}$$

Equation 4.5: Gradient equation

In plasma case, a gradient of 0.5 is obtained, suggesting that 50% of the unreacted acrylic end groups are not connected into the network and can be dissolved away. (Figure 4.2) The remaining 50% corresponds to the end groups of the polymer. In EB however, the proportion of uncured material represents a 63%, with a lower proportion of chain ends compared to plasma cured samples.

4.2 Plasma

In this study, the power of the plasma curing source, total volume of acrylate deposited, acrylate injection rate and gas flow into the curing source have been varied in order to understand how the different parameters affect the resulting coating degree of cure and thickness.

4.2.1 Current

Regarding the current, one can expect that the greater the power, the greater the degree of cure must be. When increasing the current for the same voltage, the power is increased in

consequence, and more plasma-derived species are created, which would theoretically increase the reactive sites, and in consequence, the degree of cure.

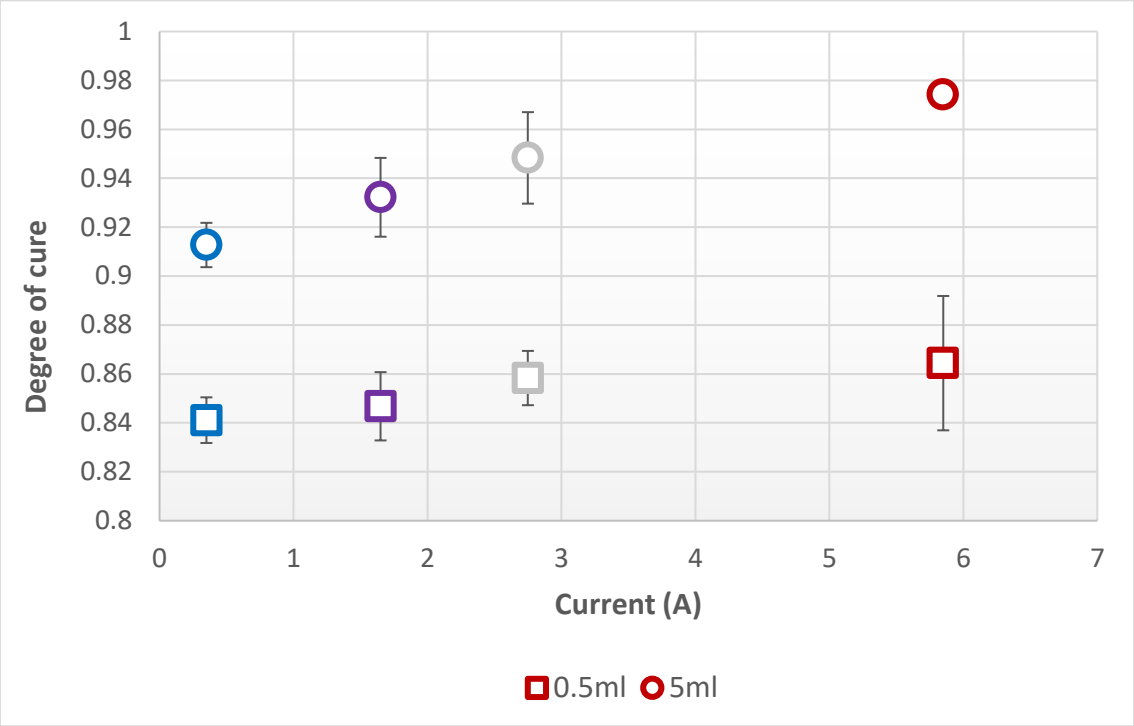

Figure 4.3: Degree of cure dependence of the current for the following volumes: 0.5ml (squares) and 5ml(circles) at 0.5ml/min of injection rate (error bars estimated by the standard deviation of each of the experimental values coming from 3 samples and 3 measurements)

As we can see in figure 8 the hypothesis fits the results when analyzing the degree of cure versus the current for a constant voltage of 250V, and at the intermediate injection rate of 0.5ml/min. In addition, it was observed a linear and proportional relationship current-degree of cure for both of the volumes analyzed: 0.5 and 5ml, so, as the number of reactive species is increased, the degree of cure will increase proportionally.

4.2.2 Gas flow

In addition, following the same logic, the degree of cure should increase when increasing the gas flow. When the gas flow is increased while the power is maintained, the current passing through the gas remains, however, more gas atoms would be subjected to ionization.

The gas flow influence on the degree of cure was only studied for one condition (Plasma 5ml 1000W 0.8ml/min), given that in this particular case the aim was to get a qualitative impression on the trend gas flow-degree of cure.

It was proved that when reducing the Ar gas flow from 200sccm[1] to 100sccm for the same conditions the degree of cure decreased linearly as the gas flow decreased. Therefore, it was demonstrated that the gas flow has an impact on the degree of cure as well as current. But also, that this impact is proportional to the overall degree of cure obtained. This linear trend was expected since the greater the gas subjected to ionization, the more reactive species interacting with the material.

However, this phenomenon was not explored any further, so during all the experiments the gas flow was maintained at 200sccm, not adding this variable in the overall analysis.

[1] sscm: standard cubic centimeters per minute

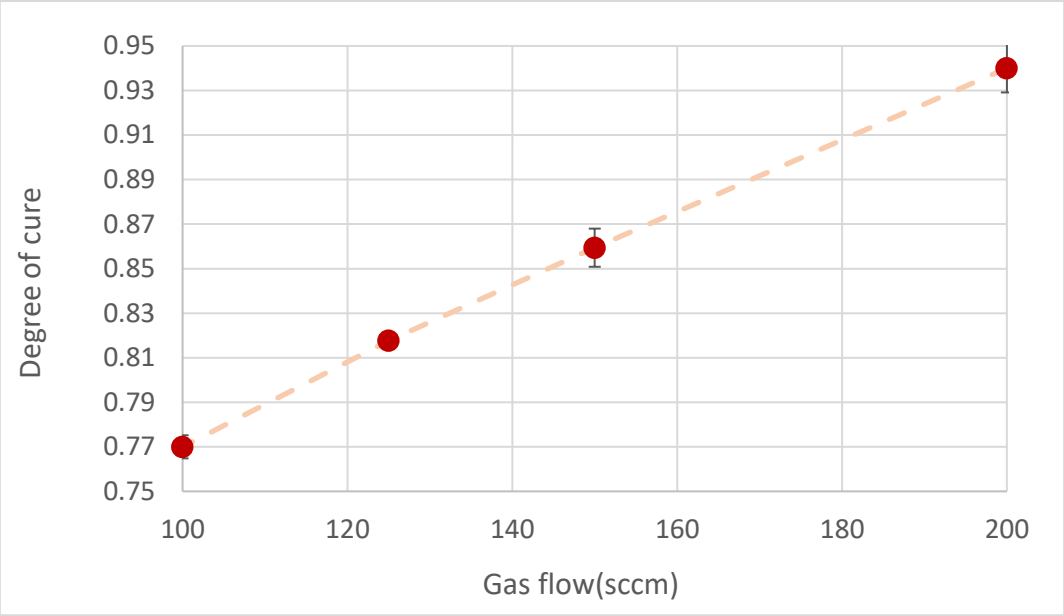

Figure 4.4: Degree of cure dependence on the gas flow for the set conditions of 5ml 1000W (0.35A) 0.8ml/min

4.2.3 Injection rate

The injection rate refers to how much material is put down at every pass of the drum (note that the drum speed is constant). For a constant volume, because an increase in the injection rate means there are fewer passes needed to deposit all the material this reduces the amount of time the material is subjected to the curing source.

In the following figures it can be observed that in every case an increase in the injection rate causes a decrease in the degree of cure.

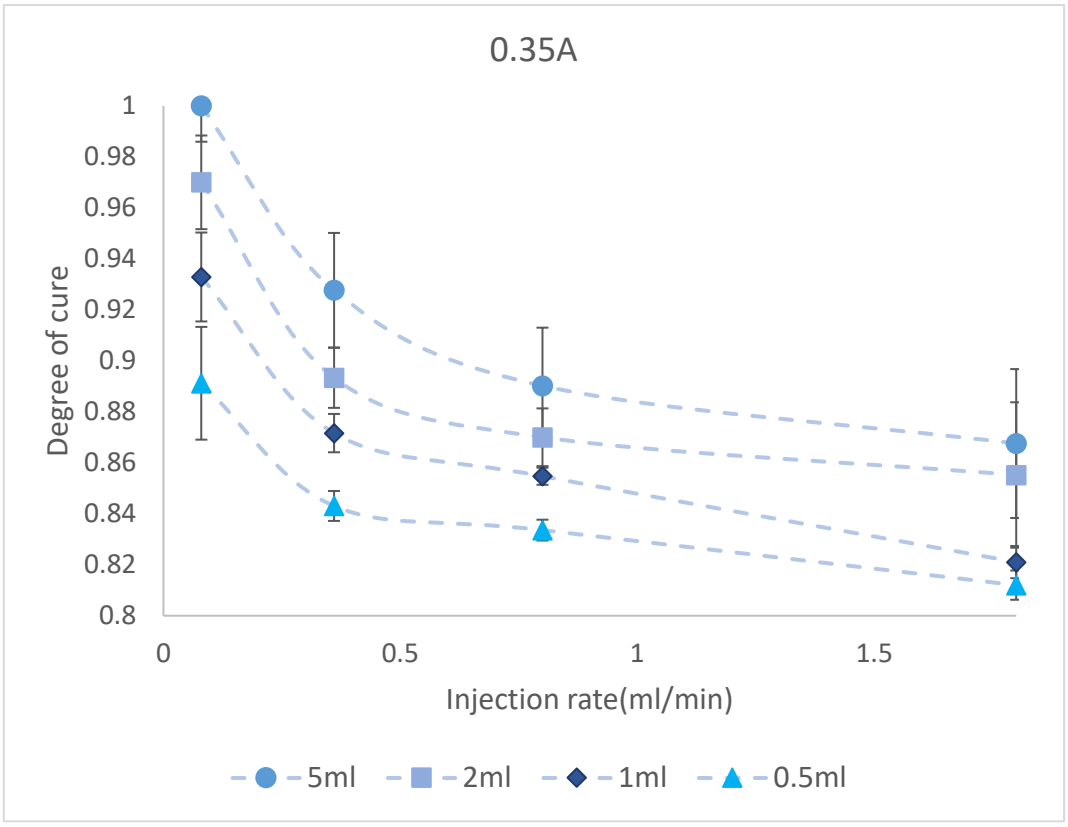

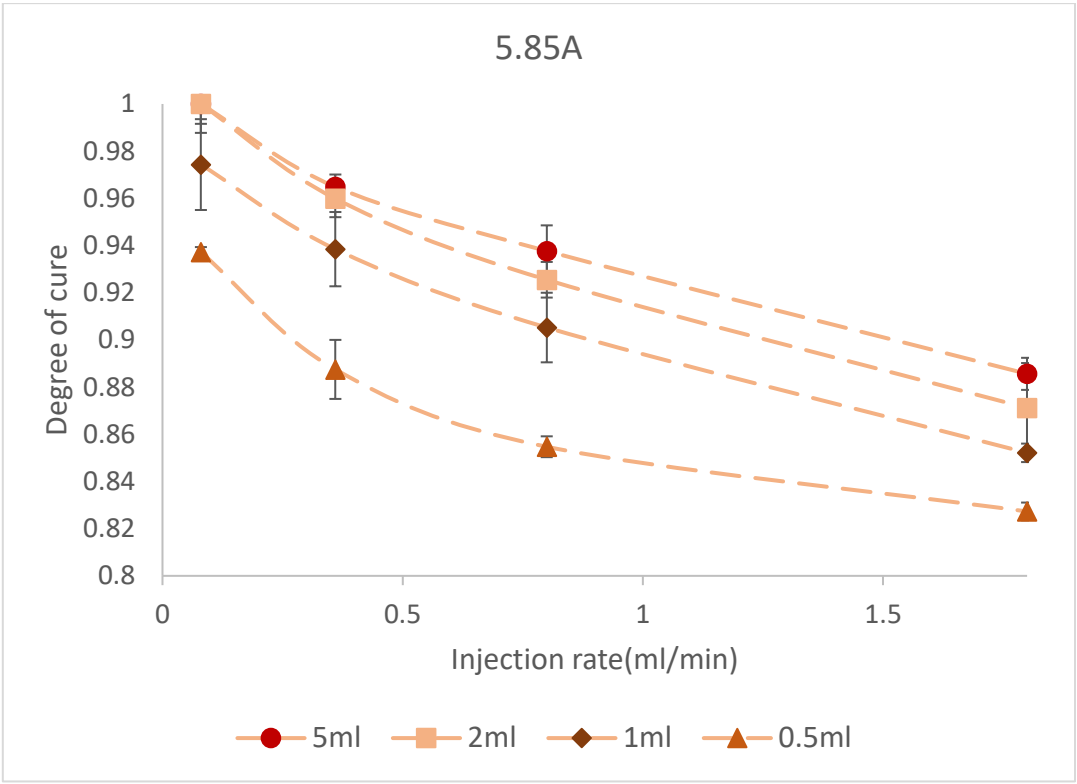

Figure 4.5: Degree of cure dependence of the injection rate in plasma cured samples (error bars estimated by the standard deviation of each of the experimental values)

Since there is an increase on the thickness of material that is put down at each pass of the drum, it may be that the plasma isn't able to penetrate enough into the material, meaning that the curing is non-uniform and only happening at the top of each layer, hence when each layer is deposited, the thicker it is, the greater proportion does not 'see' the penetrating radiation. In other words, the plasma curing could be limited by the thickness of the acrylate (A). Alternatively, the plasma species may be distributed throughout the thickness, but the difference in degree of cure may arise because the injection rate increases the overall exposure time to the plasma decreases (B). In both instances the data indicate that the cure is not complete in a single pass for plasma cure.

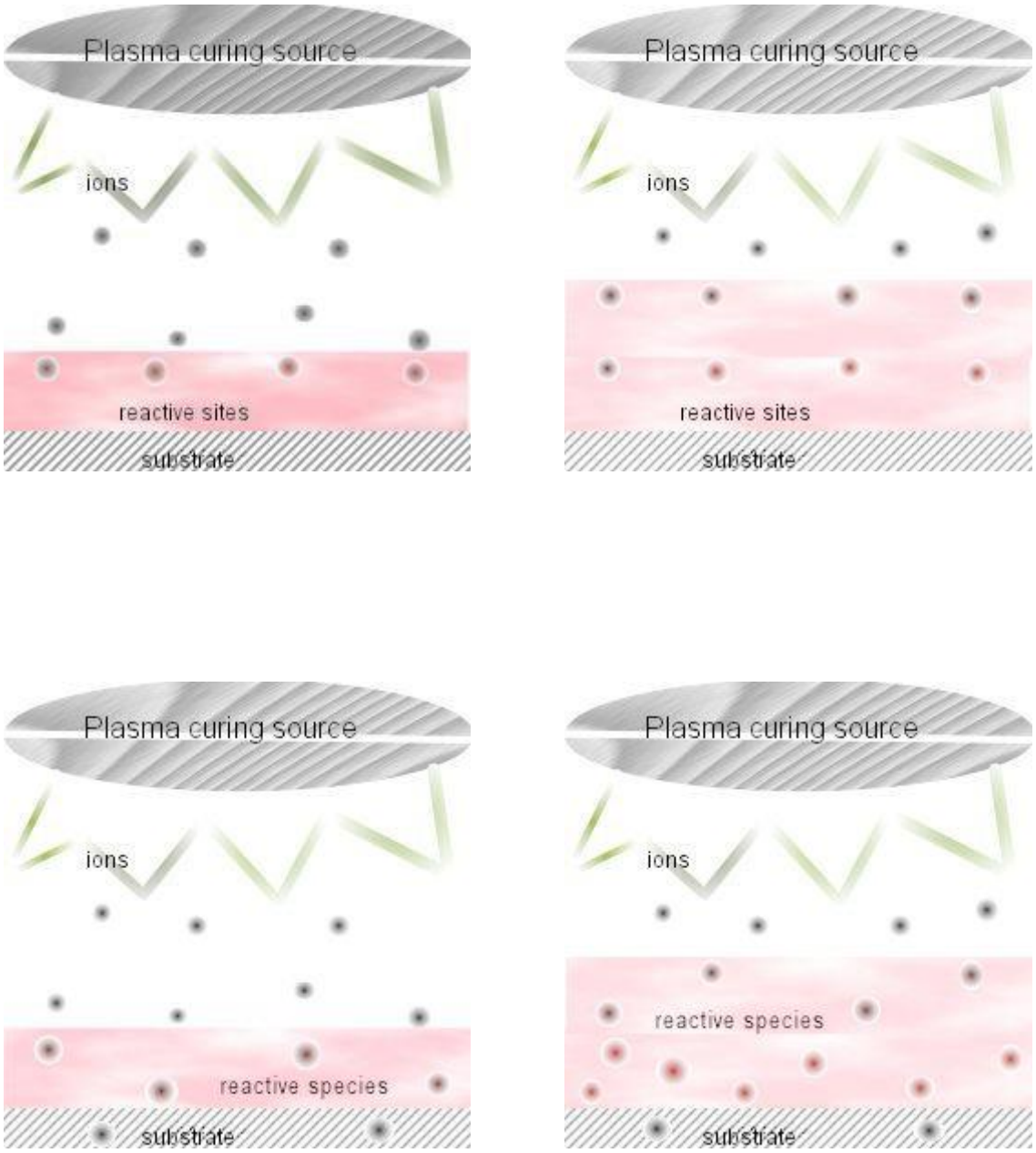

Figure 4.6: Schematic showing the possible plasma curing process. (A: upper images) For species forming the reactive centres being retained at the surface (B: lower images) species forming the reactive centres penetrating into the underlayers.

So, in the A hypothesis, the reactive species would be allocated on top of the layer in every case. Therefore, when increasing the injection rate, the films would be thicker and the reactive species would be the same. This would cause the same amount of reactive

species in the material, but for different amount of volume. When increasing the injection rate, the films are thicker but the reactive species are constant, creating a drop on the degree of cure.

On the contrary, in the B hypothesis, some ions would pass through the layer reaching the substrate, so, only some fraction of the ions would create the reactive species. When adding a second layer, the same number of ions would be retained on the new layer, but some would also be retained in the underlayers, increasing then the degree of cure of these underlying layers.

For the A case, an increase on the volume for constant degree of cure won´t change the degree of cure given that all the ions would be allocated on top of the layers. However, if what is really happening is the B case, the greater the volume, the coating passes under the source more times so there is more exposure to the radiation overall. In this case there would be "extra-curing", meaning that the underlayers would interact with a greater proportion of the radiation species as both, the overall thickness and the number of passes under the curing source increase.

4.2.4 Volume

In order to understand the reason for the differences in the curing behavior, (either case A or case B from the previous section), experiments at the same injection rate, but different volumes have been performed. In this case, the thickness at each pass of the drum stays the same, and the only difference is how long the underlayers are being subjected to the curing source.

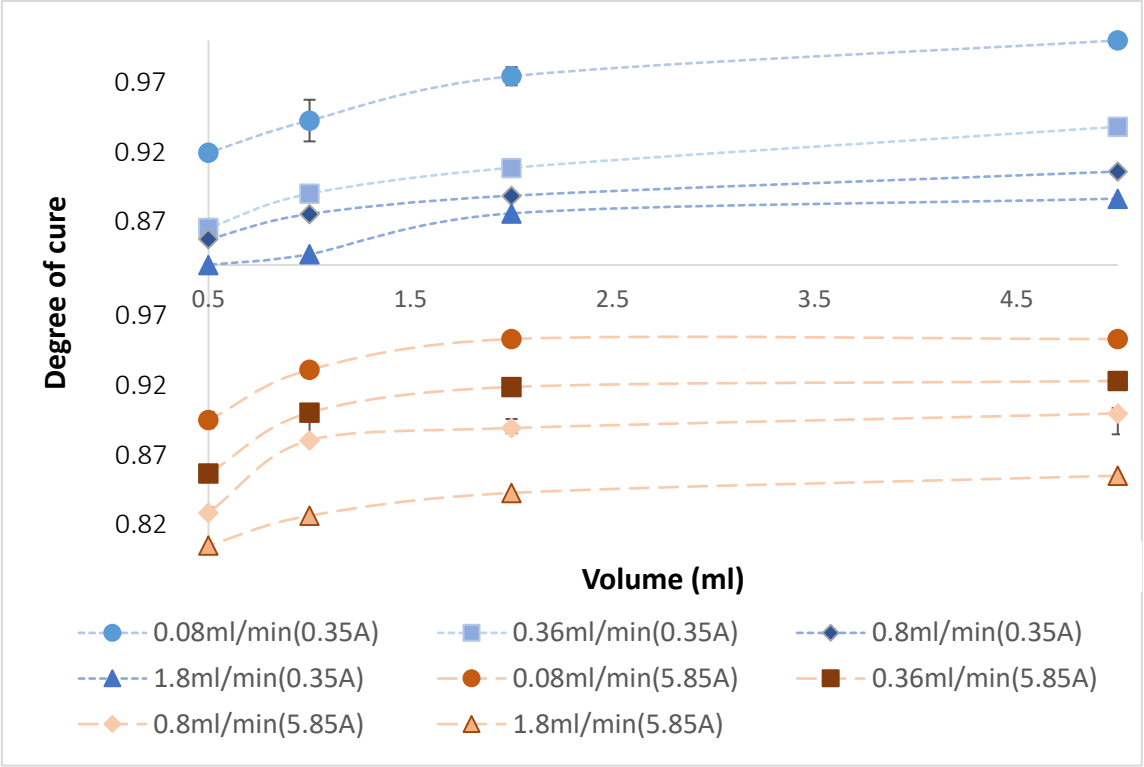

Figure 4.7: Degree of cure dependence of the volume for different powers and injection rates in plasma cured samples. (error bars estimated by the standard deviation of each of the experimental values)

So, by increasing the overall volume, at a constant injection rate and power, what it is being changed is the number of times a layer of material is being put down at the drum. Since the degree of cure increases as the volume does, it necessarily means that it must be some kind of post-curing mechanism of the underlayers. So, the reactive species do not only interact with the layers as they are put down, but also with the underlayers.

Therefore, the longer the material is subjected to plasma the better the curing degree will be. Then, it can be concluded the plasma species are distributed throughout the acrylate and not only on the surface of each layer. Therefore, plasma not only cures the layers as

they are put down but also the underlayers. This necessarily means that what is actually happening is the B case.

4.2.6 Model proposed

From all the conclusions from previous sections (Section 4.2.1-4.2.5), a model that describes the degree of cure was built. In order to do so, the following premises were considered:

- The amount of curing depends on the current of the curing source.
- The rate of cure is proportional to the amount of uncured material. Hence, for example, the "fresh layer" deposited on top of the drum will always have the same degree of cure, no matter the number of underlayers that are under it.
- The degree of cure is increased with the number of passes due to the "extra-curing" of the underlayers (Case B, as explained in section 4.2.4)

So, the main hypothesis is that the "fresh layers" will always achieve the same degree of cure, so, the reason for which the degree of cure increases as the number of times the material is subjected to the curing source increases, is due to the "extra-curing" of the underlayers. In the following figure (Fig. 4.8), this hypothesis can be observed:

In the first case, when the layer is just being deposited, the initial degree of cure (no "extra-curing") is 0.812 (Fig. 4.8A). Now, considering that when a new layer is being deposited on top of the first layer (Fig. 4.8B), the degree of cure of the "fresh layer" will be 0.812 as well. But, since the overall degree of cure is of 0.821 this increase might be due to the change on the degree of cure in the first layer.

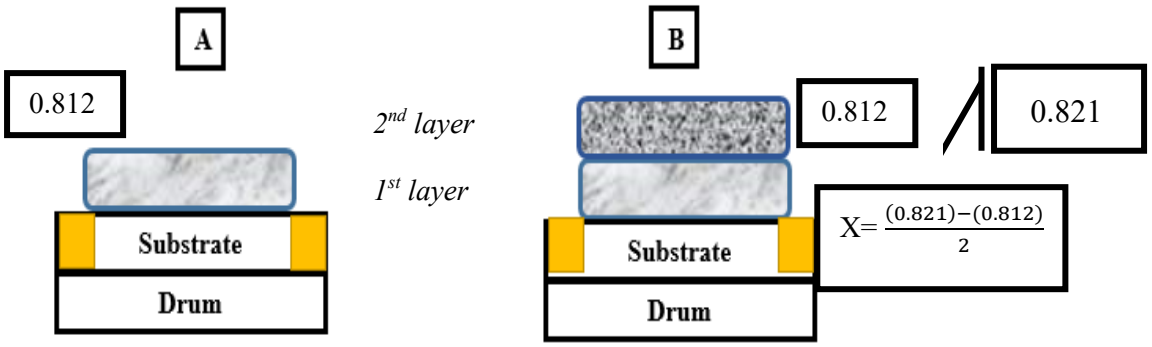

Figure 4.8: Schema of the deposition of two thin films. A- When one block of layers is being deposited, B-When two blocks are being deposited, one on top of each other. (data coming from the experimental values for 0.35A and 1.8ml/min)

So, in order to estimate the degree of cure rate with the number of passes, the following equation has been used:

$$\frac{dc}{dn} = Y(1 - c)$$

Where:

c is degree of cure

n is number of passes under the curing source that a particular layer has 'seen'

Y is a fitting parameter that would depend on the current

Equation 4.6: curing rate

This equation (Equation 4.10) is based on the hypothesis that the curing rate ($\frac{dc}{dn}$) is proportional to the uncured proportion within the thin film (*1-c*) i.e. that the curing rate

will be proportional to the number of reactive centers created, and that these can only be formed by the radiation interacting with uncured material.

Since the curing rate would depend on other factors apart from the uncured material, such as the current of the curing source, a fitting parameter Y is used.

The model at the moment, however, doesn´t take into account the reactive species concentration with depth. It was already observed that not only the number of passes, but also the injection rate plays a role when it comes to the degree of cure, reason for which the ions-matter interaction needs to be further investigated. First of all, solely the ions would be considered in the model, due to the limited effective charge or ionizing capacity of the electrons compared to ions for the same energy. (i.e 24 radical pairs for Ar+ ions versus 0.009 for e-beam for 1MeV (64))

Also, the probability of an ionizating particle to be absorbed by the matter won´t be constant with depth, but rather will be ruled by the absorption cross-section. This formula is based on the idea that there is a logarithmic decay on the number of absorbed particles as the depth increases, followed by the Beer-Lambert law, which establishes a direct relationship between the logarithmic decay of the radiant flux as the reactive species go through a material with the depth. If one divides the thin layer into slices, the probability of the deeper slices “to see” a reactive species is lower as some of them would have been already absorbed by the upper slices. When the thickness of each slice tends to zero, the

rate at which reactive species are being absorbed in that particular slice is proportional to the depth of the material the electrons had to travel prior to reach that particular slice.

However, as the absorption cross-section also depends on the material, curing source and energy, a shift on the logarithmic decay can take place. In this sense, according to different investigation treating the interaction ion-polymers it was shown that the depth-profile curves depend quite a lot from the ions used, and as well to the conditions (67) (68). The theory is based on the assumption that the slowing down of ions with depth is due to the binary collisions with the atoms in the material with straight mean free paths, which for structureless media depends on the density. The ions then will slow down as the contribution of the elastic (nuclear stopping) and inelastic (electronic stopping) mechanisms causing ionization. (64) (69)This means, that at the beginning only a small proportion of ions will stop, however, as they lose energy due to their interaction with target nuclei or target electrons, more will stop, causing crosslinking and scission processes as they slow down. Therefore, the probability of an ion stopping at a particular depth initially increases at greater depth and will then decrease again until at infinite depth the probability tends to zero. (65) So, in this case it was hypothesised that the overall probability of an ion to be absorbed by the thin film may be characterized by a simple Gaussian curve or the MonteCarlo model (66) (Fig.4.9).

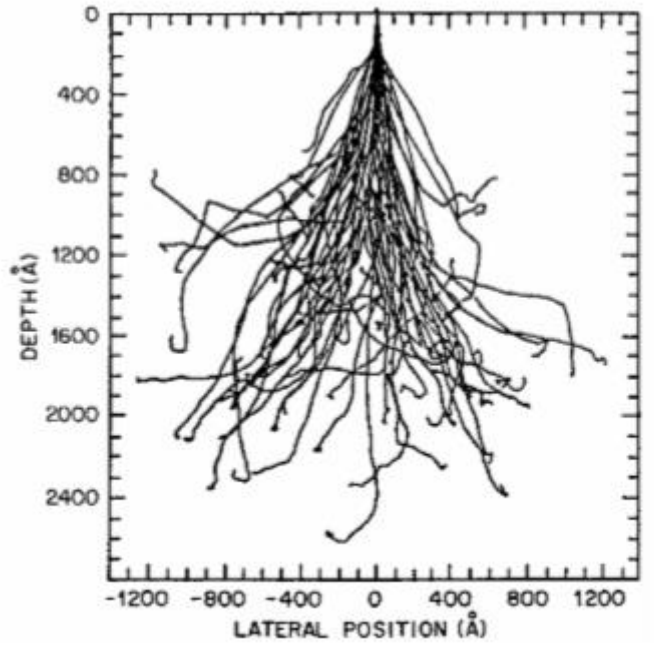

Figure 4.9: Penetration depth distribution of ions (66)

In this sense, SRIM is one of the most widely MonteCarlo type of codes for predicting the ions-matter interaction (70) In fact, previous research had already showed the good correlation between the predicting Ar+ distribution with polymer films. (71)

By running simulations for different ions energy Ar+-TGPDA using the SRIM simulation tool, it was observed that for every case, the ions distribution follow a Gaussian curve, being the penetration depth and the shape of the ions distribution dependent on the energy of the ions interacting with the monomer.

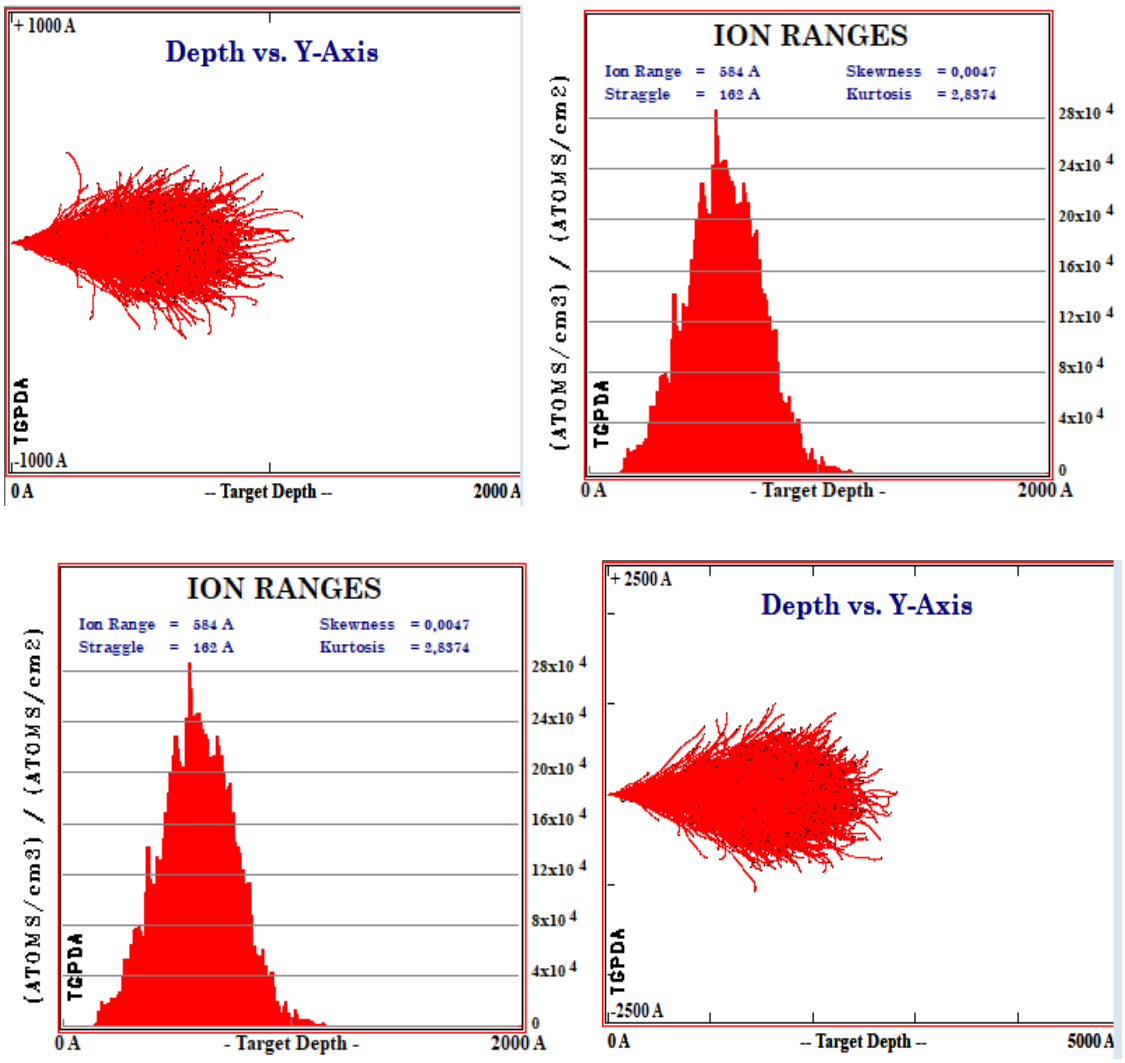

Figure 4.10: Penetration depth distribution of ions by SRIM simulation program for 25V (up) and 50V (down)

Regarding the curing model, it will be assumed that the curing rate depends on the ion depth distribution, but since the input ion energy is unknown all of the constants would be treated as fitting parameters. All in all, the ions distribution with depth will follow the expression:

$$ions\ distribution\ with\ depth = Y = A * e^{-\frac{(x-b)^2}{2d^2}}$$

Where:

A,b,d: constants

A: maximum ions concentration

b:depth at which the maximum ions concentration are obtained

d:wide of the function

*X: is the real depth, which in this case is n*i*

Equation 4.7:ions distribution

Now, by introducing equation 4.7 in equation 4.6, by assuming that the curing rate is proportional to the ions distribution with depth, the following expression is obtained:

$$\frac{dc}{dn} = A(1-c)e^{-\frac{(x-b)^2}{2d^2}}$$

Equation 4.8:curing rate

And by substituting x(depth) which is unknown for n times the injection rate, the curing rate formula is obtained:

$$\frac{dc}{dn} = A(1-c)e^{-\frac{(ni-b)^2}{2d^2}}$$

*Equation 4.9 :curing rate with depth (n*i)*

Where:

i: injection rate[ml/min]

n:number of passes

By integrating the expression, the degree of cure is obtained:

$$c = 1 - e^{-\frac{A*erf(\frac{ni-b}{d})}{i}}$$

Where:

i: injection rate[ml/min]

n:number of passes

Erf: error function

A,b,d: constants

Equation 4.10: Degree of cure

In the experiments, the working conditions were: ions (Argon), high voltages (or about 250V), and different currents. As the current increases, the dose of ions absorbed by the material increases, so it is expected an increase on the *A* fitting parameter with current.

The penetration depth is governed by the energy of the ion, the electric charge q (elementary charge) has an energy E = qV after passing through the potential V. So, it would be expected that the fitting parameters b and c remain constant in all the experiments. (72)

However, since the output energy is unknown, the Gaussian curve shape and the maximum penetration depth remains unknown. So, according to the theory, in this case, the probability of absorbing ions depending on the penetration depth depends on the voltage leading to an increase as the layers get thicker, up to some point in thickness in which the dose will start to diminish as the thickness increases. (b and c dependent). This would apply for every current, given the fact that the penetration depth is voltage-dependent.

Based on the assumptions of both simulations, and previous papers (71) it was assumed here that the penetration depth of the ions is low, with small b and c fitting parameters. This would lead, to different curing rates depending on the injection rate, increasing the curing rate as the injection rate is increased. However, up to a certain thickness the degree of cure no longer increases, given that the ions won´t be able to penetrate any further. This would most affect the greater injection rates, given the fact that the underlayers would be less times subjected to the ions due to their greater thickness per layer, so that the maximum depth until the ions interact with matter will be achieved for less times under the curing source as compared to the lower injection rates.

In the following figures it can be observed the “post-cure” of a single layer depending on the injection rate, curing and number of passes.

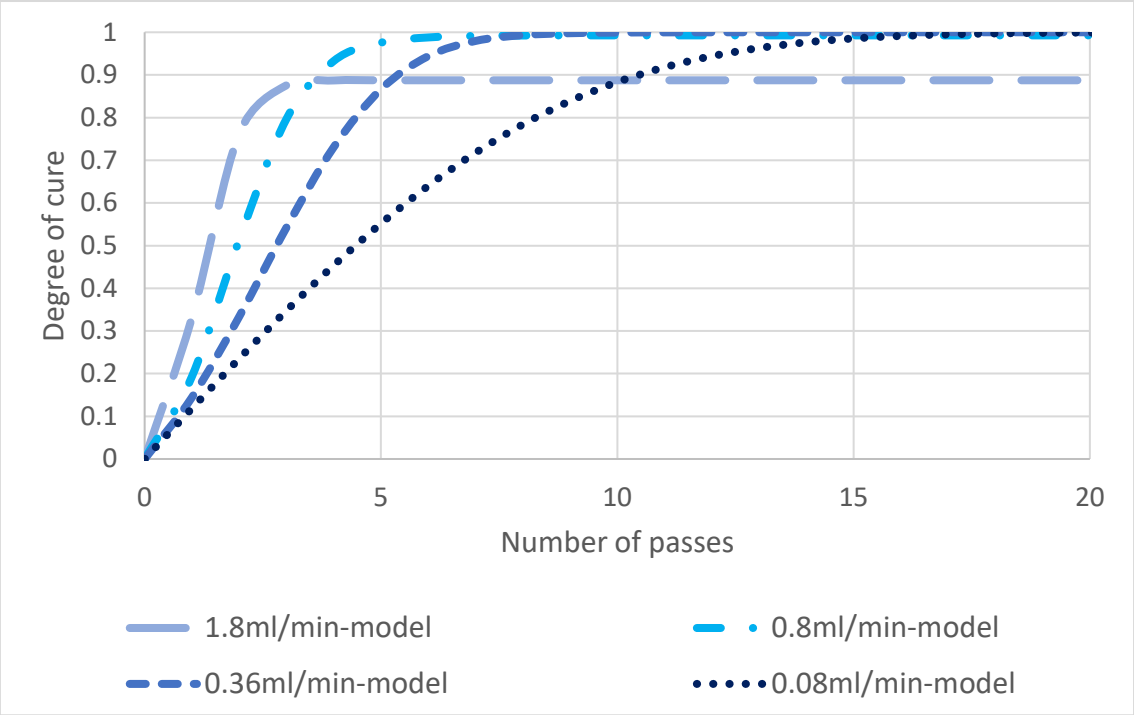
Degree of cure
1
0.9
0.8
0.7
0.6
0.5
0.4
0.3
0.2
0.1
0
0
5
10
15
20
Number of passes
1.8ml/min-model
0.8ml/min-model
0.36ml/min-model
0.08ml/min-model

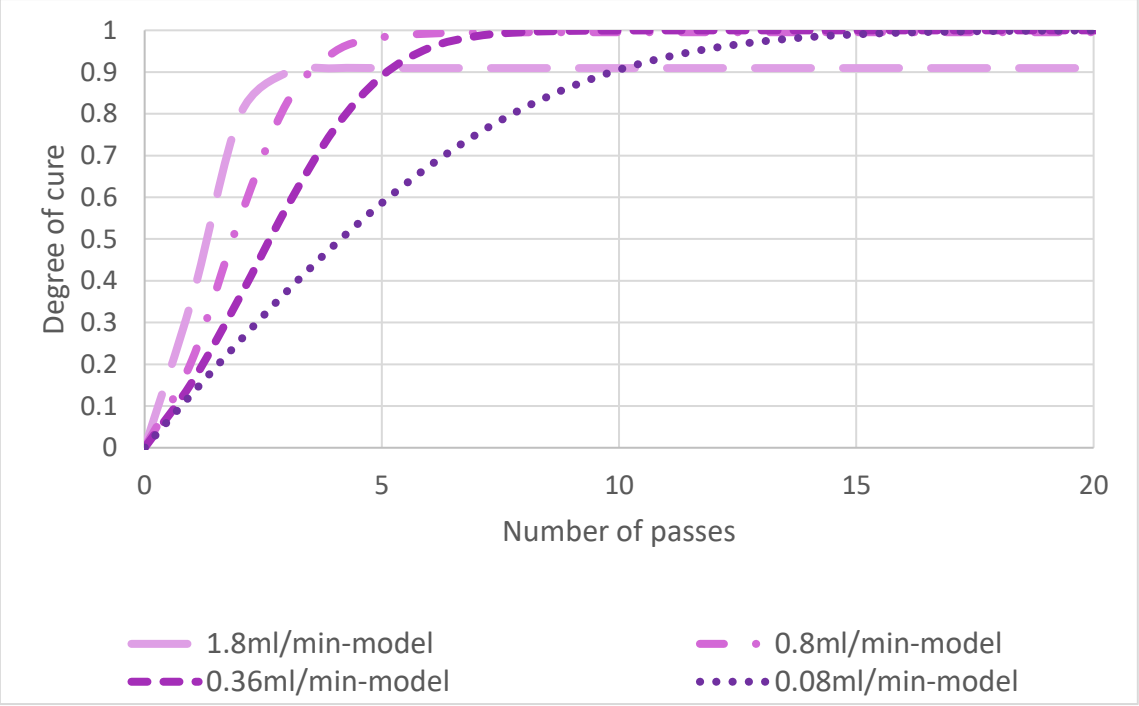
Degree of cure
1
0.9
0.8
0.7
0.6
0.5
0.4
0.3
0.2
0.1
0
0
5
10
15
20
Number of passes
1.8ml/min-model
0.8ml/min-model
0.36ml/min-model
0.08ml/min-model

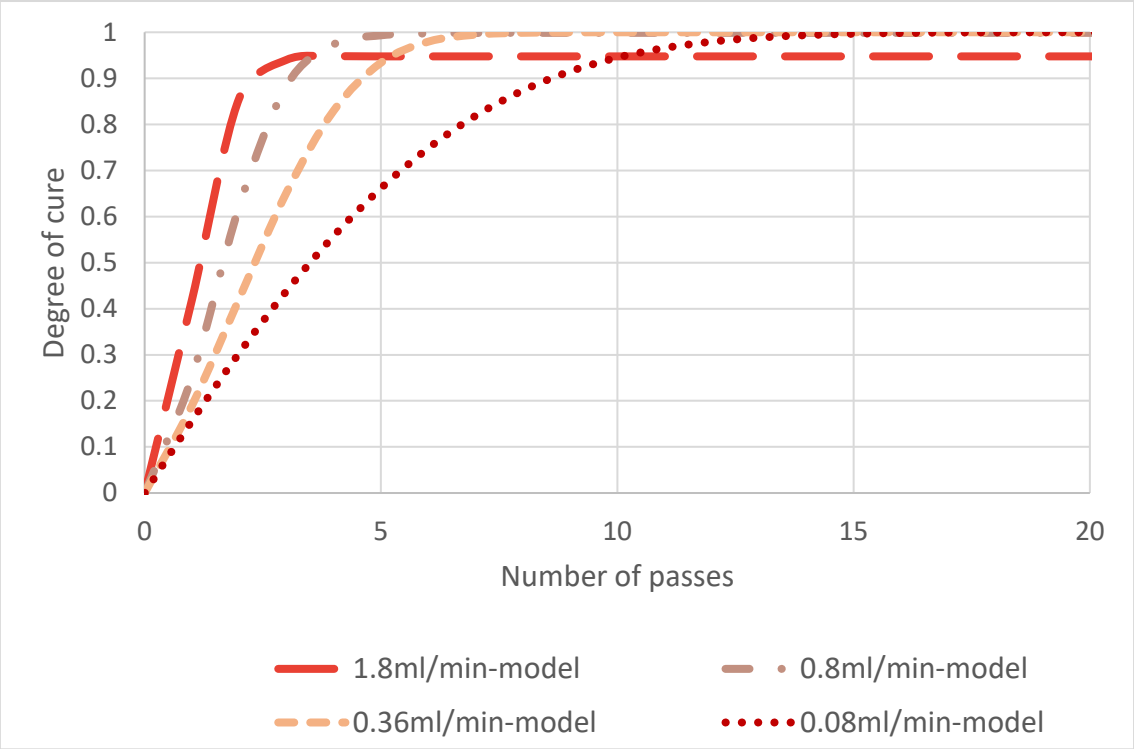

Figure 4.11: Extra-curing depending on the number of passes for 0.35A (blue), 1.65A(purple) and 5.85A(red) for different injection rates

At the moment the equation describes the 'extra cure' in each specific layer following a pass under the curing source. So, in order to get the degree of cure of that specific layer, it is needed to add the effects of the previous cures from every pass under the curing source. This consists of a summation of the effect the curing source will have on the thin film every time the plasma reactive species interact with the material. And then, the overall degree of cure is estimated by the average of the degree of cure of every layer that comprises the thin film:

$$d.c = \frac{\sum_i^n (c_i)}{n}$$

Where:

d.c : Degree of cure of the underlayer

c_i: Degree of cure of one layer after pass number i

n: number of layers

Equation 4.11: Overall degree of cure

By adding the effects of the previous passes of the thin film under the curing source, a set of data like this will be obtained:

	layer number	*1 layer deposited*	*2 layers deposited*	*3 layers deposited*	*4 layers deposited*
1st layer up	1	0.19	0.42	0.7	0.87
2nd layer up	2		0.19	0.42	0.7
3rd layer up	3			0.19	0.42
4th layer up	4				0.19
Degree of cure		0.19	0.31	0.44	0.54

Table 4.1: Increase on the degree of cure as the number of passes under the curing source are increased for 0.35 A, 0.8ml/min

So, as shown in the table, it means that at the first pass under the curing source 19% of the material is cured, then at the 2nd pass of the drum, the underlayer immediately below it will achieve an additional 23% (42-19) cure, as reactive species be formed in the underlayer due to penetration of the radiation, at the 3rd pass the degree of cure of the underlayer is increased by a further 28% (70-42), and so on.

At the moment, the degree of cure is just described depending on the number of passes and the density of ions. However, the hypothesis used for describing the model was that it does depend on the current of the curing source as well. This effect is included on the fitting parameter *A*.

As the current increases, the term on the equations decreases. Meaning, that as the current increases the degree of cure increases "faster" with the number of passes, given the fact that the term *A*, is included in a negative exponential equation (Equation 4.10).

Indeed, by plotting *A* versus the current a linear trend can be observed. As the current is increased the reactive species will increase proportionally, so the linear trend with current is not a surprising result, as this will at the end cause an increase on the degree of cure (Figure 4.12).

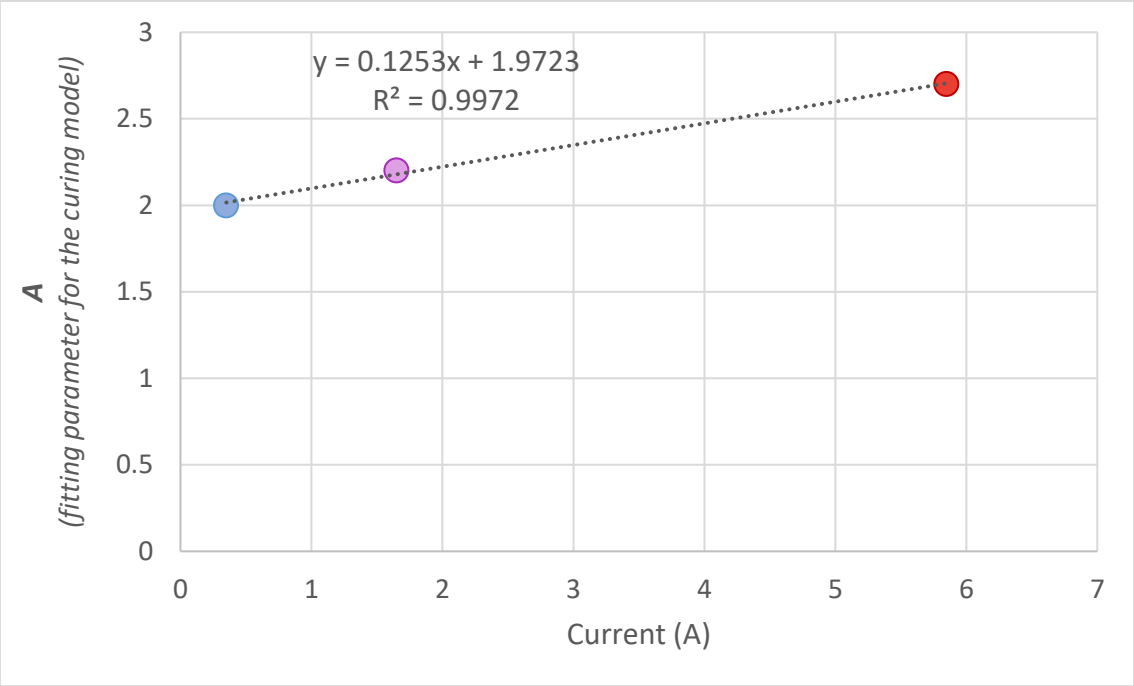

Figure 4.12: A (the prefactor fitting parameter for the proposed curing model) dependence with current

The degree of cure obtained by this equation allows for the very first time to numerically obtain the degree of cure through an equation without the need of performing many experiments. Since, as time increases so will increase the degree of cure of the thin films, the uncured proportion of the thin films will decrease.

The correlation coefficient of the model when using different currents was obtained by the following equation:

$$\rho = \frac{\sum_{i=1}^{n}(x_i - x)(y_i - y)}{(n-1)s_x s_y}$$

Equation 4.12: correlation coefficient

Where:

ρ: correlation coefficient

x: sample mean for the first variable (experimental data)

y: sample mean for the second variable (model)

s_x*: standard deviation of first variable*

s_y*: standard deviation of second variable*

n: number of data

In the following table the fitting parameters as well as the correlation coefficients of the overall degree of cure of the model with the experimental data.

Current (A)	**A fitting parameter**	**Correlation coefficient**	**B fitting parameter**	**D fitting parameter**
0.35A	2	86.3	3	2
1.65A	2.2	88		
5.85A	2.7	94.7		

Table 4.2: Fitting parameters and correlation factors for the plasma curing model

As an example, the model can be observed graphically for the greatest current in the following figure:

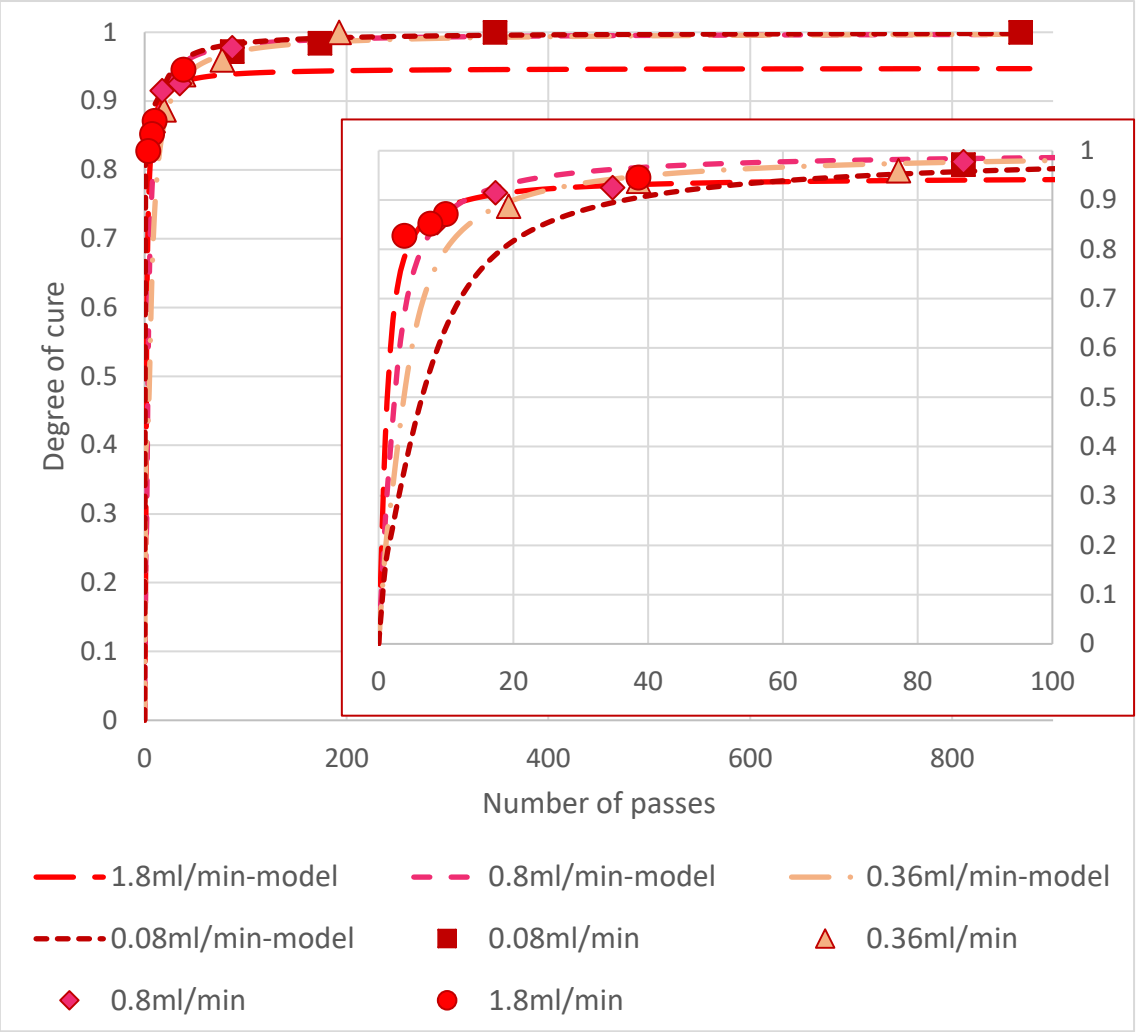

Figure 4.13: Curing model for 5.85A

In summary, by using the MonteCarlo model with penetration depth, the ions concentration will start increasing as the layers become thicker, and this would affect the curing, the number of ions interacting with the material will initially increase as the number of layers increases, but the curing would not only depend on the ions concentration interacting with matter, but also on the probability of a high energetic ion to reach a –C=C- , which will decrease as the uncured proportion drops. In this sense, considering the influence of time under exposure to the radiation to the films, the different research papers met at the same conclusion, once the films had reached a 60-70% of

curing degree, the increase on the degree of cure drops significantly with time. (73) (74) . And as seen before, these two effects would lead to decay of the degree of cure of a specific underlayer as it is further exposed to the curing source so that:

- As the degree of cure of the underlayer is increased, the probability of a plasma reactive species (ions, electrons…) of reaching a -C=C- is reduced, simply because the uncured proportion of the layer is reduced.
- But also, the propagation of the polymerization could be different as there will likely be less uncured neighbors in the proximity of a specific -C=C-.

The main conclusions of modelling the degree of cure under plasma treatment were that:

- The concentration of reactive species (ions) follow a Gaussian curve with depth.
- There is a post-curing effect, which depends on the time the underlayers are being subjected to the curing source, the current and the ions concentration.
- As the current of the curing source increases, the number of reactive species increases as well, causing an increase on the degree of cure on the layers on every pass under the curing source, leading to a linear relationship current- A fitting parameter of the model.

All in all, this model represents a great advance on the radiation curing (plasma) field, especially for industrial applications, as for all the applications the degree of cure must be above a specific number in order to ensure an optimal quality. So, the inverse equation could be obtained in order to obtain the process parameters for a specific degree of cure.

4.2.7 Thickness

The total thickness of the coating deposited would ideally be = (total volume of monomer) / (width of drum * circumference of drum), but the actual final thickness depends on a contribution of many physical processes that occur from the moment the material is injected until the material is cured. In the following figure, the injection and loss of material at every step of the process can be observed:

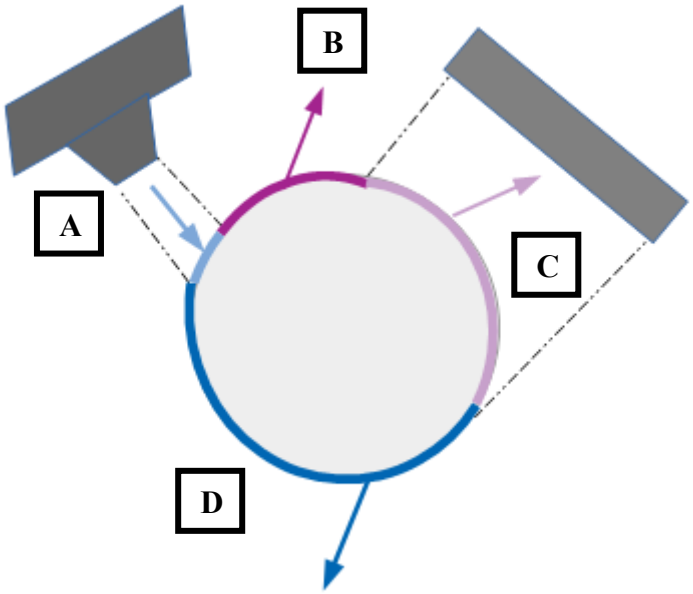

Figure 4.14: Schema of the vacuum deposition with the different steps that can make an influence on the resulting thickness

A: Material deposited onto the drum: Some monomer will never condense onto the substrate as it depends on physical variables such as the monomer vapor pressure or the substrate temperature.

B: Material re-evaporated before reaching the curing source: In a physical vapor deposition process, the vapor condenses on the substrate, however only a portion of the incoming material would be remain in the liquid phase, with the remainder re-evaporating before reaching the curing source. The re-evaporation which takes place between the monomer deposition slit and the curing source, refers to material which is completely uncured.

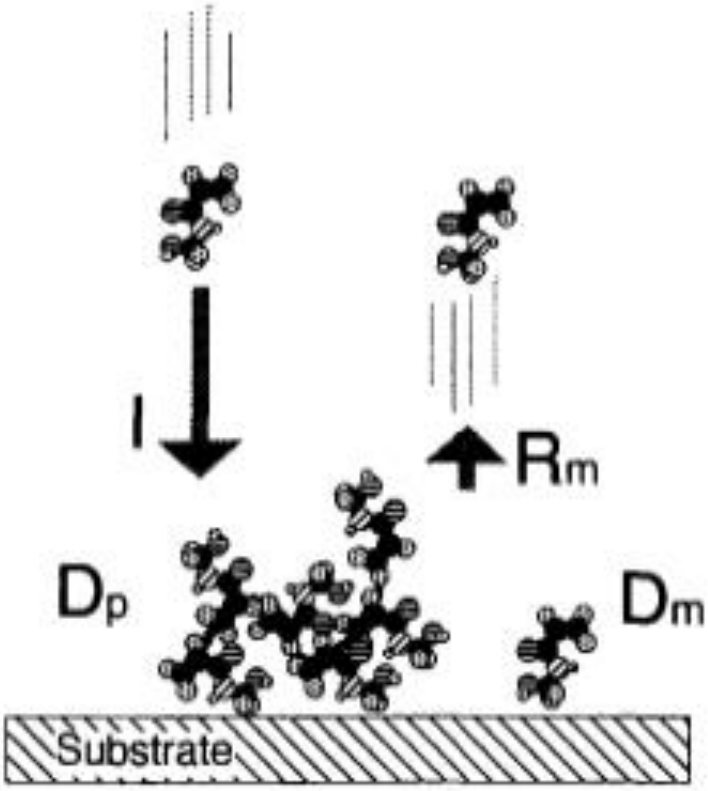

Figure 4.15: Re-evaporation and deposition schematic for physical vapor deposition (75)

There will always be re-evaporation due to the evaporator-to cure distance. but the amount of material lost will depend on some process parameters such as the injection rate, the monomer vapor pressure, the substrate temperature or the drum speed. (76) In this

research, the drum speed and substrate temperature are constant. So, the re-evaporation rate is estimated as a consequence of the changes on the injection rate, which would be directly related to the vapor pressure.

C: Etching : When the plasma reactive species are in contact with the material, not only curing but also etching can be produced on the thin films. The interplay of two competitive effects, etching and deposition processes can occur simultaneously when high excitation power and long exposure time are used (77).

However, the proportion of material which would be etched away as a result of the radiation from the curing source won´t presumably be homogeneous. An increase on the surface roughness was observed already by other researchers when the films were plasma polymerized, and it was attributed to the plasma etching. (78) (79) . (Further explained in the topography section) as a consequence of the fact that the uncured material will be removed much more easily than cured.

In the research, etching and curing occur at the same time, and in the same way as it was considered with curing, it is believed that the amount of etching will depend on the curing source power and the number of passes under the curing source as well.

D: Re-evaporation after curing – This refers to the low molecular weight species evaporating from the material as it passes around the drum between the curing source and the deposition slit (before the next layer goes down), not as a result of any interaction with the curing source. As well as the plasma being able to create reactive sites to cure the layer, it can also provide energy to re-evaporate material, in particular the low

molecular weight or unreacted components and so a part of the material will in consequence re-evaporate (Affinito, 1994) causing a reduction in final film thickness.

This will occur predominantly from the top layer of material at any given time and will depend on how well cured these top layers are.

In previous studies it was observed that not all the uncured species will re-evaporate given that a part of the liquid molecules will be embedded in the polymer. It was thought that the more uniformly the films are cured the less post-polymerization re-evaporation will occur. (75)

The curing homogeneity will depend on the curing source, so as far as the plasma thickness model is concerned, this won´t play a role in the thickness estimation, but certainly will when comparing curing sources.

E: Shrinkage of the material on curing. When the films are being polymerised, they can demonstrate a reduction in volume, shrinkage. When shrinkage occurs during curing, another effect is produced: the coatings are subjected to internal stress, when the degree of cure is low enough, due to the appearance of a gradient between the cured and non-cured parts of the films. Initially the curing may be homogeneous, but as cure progresses, these internal stresses relax, producing inhomogeneity in which cured and uncured species within the coating are separated. (80) The amount of shrinkage will depend on the average degree of cure of the whole layer, however the reduction of thickness expected by shrinkage is about 12-17%. (81). In this research, the degree of cure, is in every case above 0.8. Therefore, differences in the shrinkage between the films is very small and will be considered negligible in this work.

Thickness hypothesis:

The deposited thickness would be estimated using the following equation:

$$Thickness = (Material\ deposited) - (Material\ etched) - (Material\ re - evaporated)$$

Equation 4.13: Resulting thickness as a function contribution of the different variables that would affect it

4.2.7.1.Current

When studying the influence of the current on the thickness of the resulting films, an interesting result was observed. The thickness dependence on current was studied for the maximum and minimum volume of monomer, to get an overall idea of the trend the thickness would follow when using different currents, always using the intermediate injection rate of 0.5ml/min.

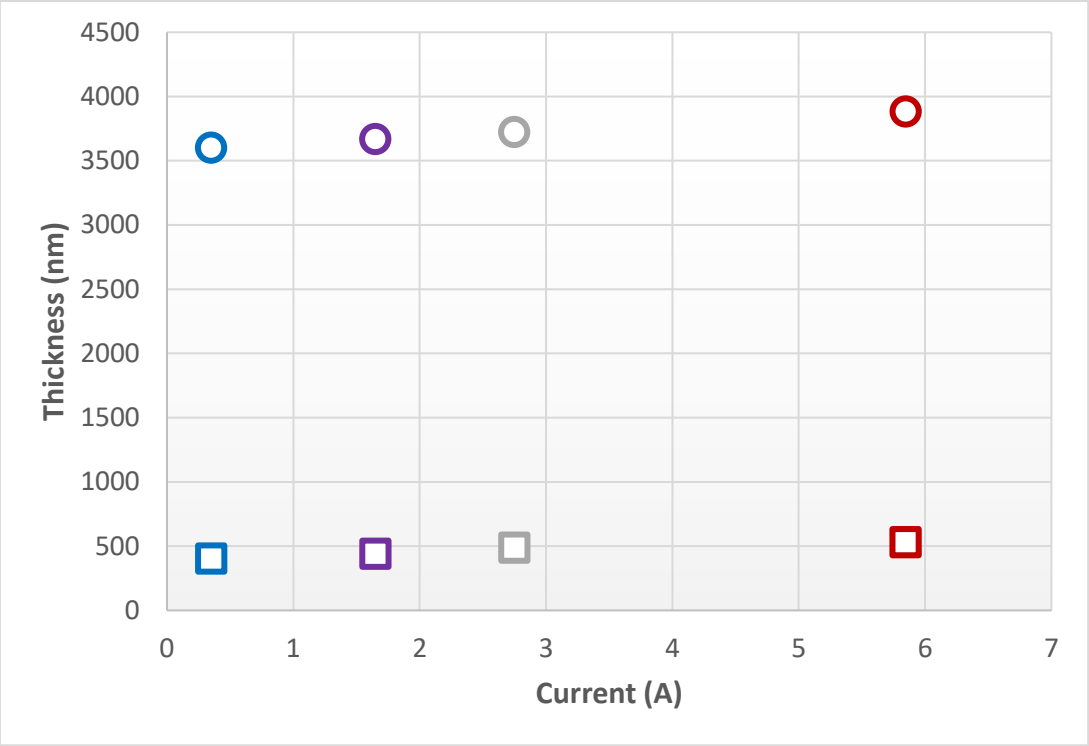

Figure 4.16: Thickness (measured by ellipsometry) dependence with power for plasma cured samples for volumes of 0.5 (squares) and 5ml (circles)

As can be observed in figure 4.16, an increase on the current, for the same voltage, slightly increases the thickness of the films for both volumes.

In this case, for constant injection rate, it would be considered that the proportion of material that re-evaporates before reaching the curing source is constant.

Current would have an effect on the other two variables:

- Etching: It would be considered that the etching is proportional to the current and number of passes, therefore the greater the current, and number of passes, the more material will be etched away, and we would expect the thickness to decrease with current.

- Re-evaporation after curing: As seen in the degree of cure model (Section 4.2.6), a greater current increases the degree of cure, and thus reduce the re-evaporation after curing, increasing the thickness with current.

So, as the current increases, less material re-evaporates but more material will be etched.

The first hypothesis would be considering that both, etching and re-evaporation only take place on the top layer, so that:

Etching: the etching rate is considered constant (different for each current), therefore the material etched is directly related to the number of passes, *n*, the material is being subjected to the curing source.

$$etching\ rate = \frac{Material\ etched}{n} = constant$$

Equation 4.14: Etching rate

In addition, it could be assumed that the material etched is linearly dependent on the current used. So, in order to use a general equation of the material etched, the current is taken into account using *B* as a fitting parameter:

$$Material\ etched = B * n * current$$

Where:

B: fitting parameter (constant)

Equation 4.15: Material etched

Re-evaporation: It will be considered that this will occur predominantly from the top layer of material at any given time and will depend on how well cured this top layer is. The degree of cure of the top layer was obtained from the degree of cure model (Section 4.2.6).

The overall re-evaporated material is estimated of n times the re-evaporated material at each pass of the drum, following the equation:

$$Material\ Re-evaporated = \frac{A * n * (d.c)_{top\ layer}}{volume}$$

A: fitting parameter

d.c: Degree of cure of the top layer

Equation 4.16: Material Re-evaporated per unit volume

So, at least from these results, it could be assumed that the curing of the top layer (current dependent) plays a more important role than the etching.

4.2.7.2.Injection rate

When analyzing the thickness with injection rate for different volumes, the same trend is obtained, as the injection rate increases, the thickness decreases. This trend applies for both powers (0.35 and 5.85A)

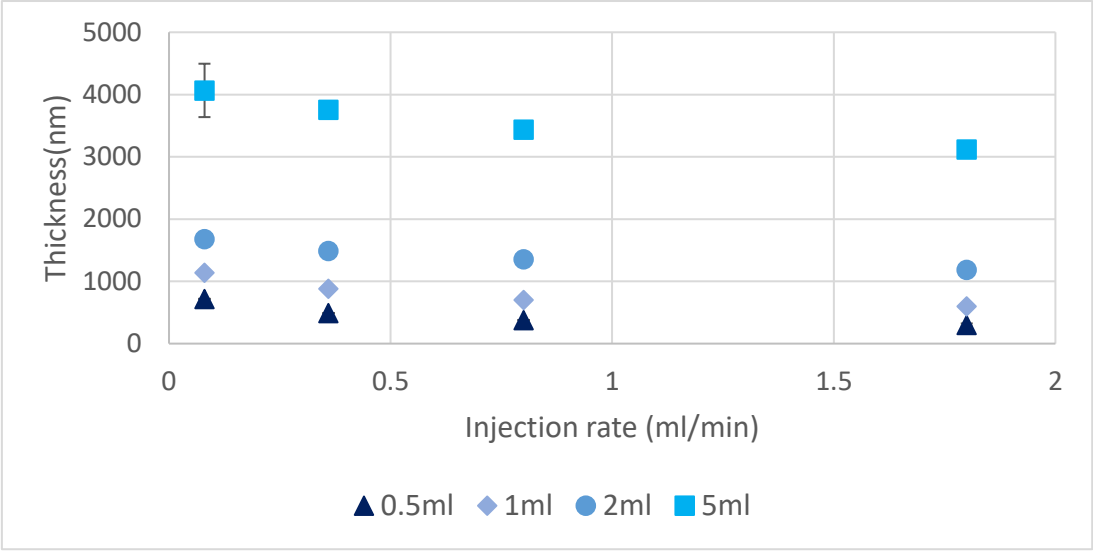

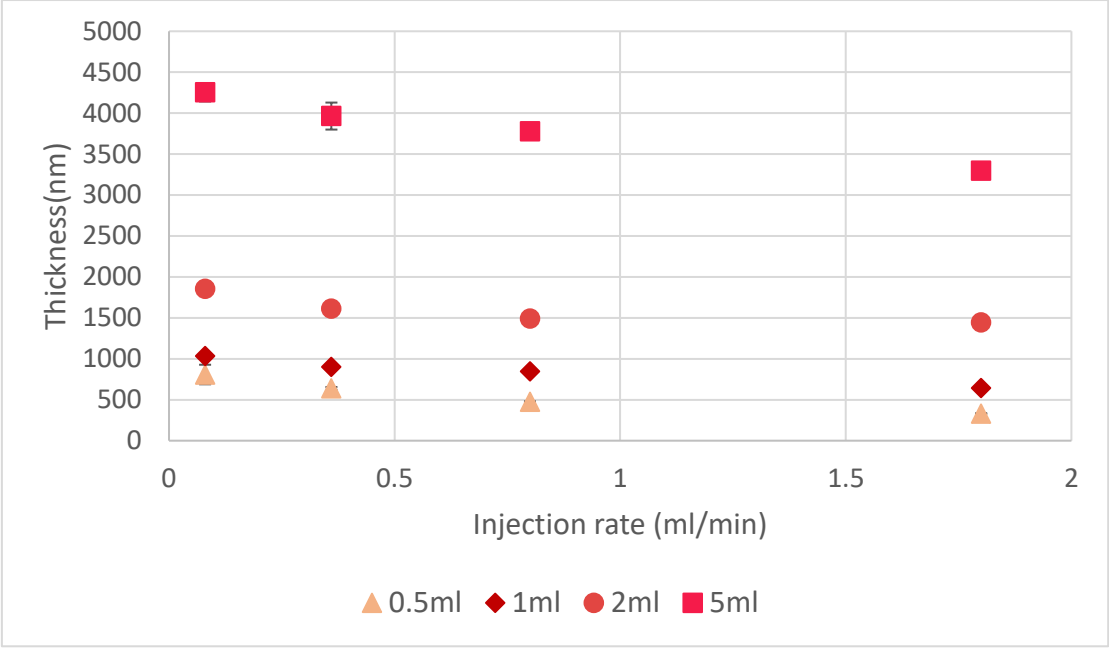

Figure 4.17: Thickness (measured by ellipsometry) depending on the injection rate for plasma curing samples using 0.35A (blue) and 5.85A (red) currents.

Based on the hypothesis that re-evaporation and etching only take place on the top layer, it should be expected that as the number of passes is increased more **etching and re-evaporation** should take place. For greater injection rate, each sub-layer is thicker, so to deposit a particular volume of monomer takes fewer rotations, subjecting the material

fewer times to the curing source , so we would expect that the re-evaporation and etching would be smaller, leading to thicker films rather than the decrease in thickness that we observe, with even more of a 60% of lost material, between the lowest and the greatest injection rate. This could be due to different reasons:

- **Re-evaporation**: It depends on the increase of the degree of cure with depth as well. Based on the curing model, the top layer is better cured (Table 4.3) as the injection rate is increased, because the top layer is thicker, so there is more ion interaction at the greater depth. However, when it comes to re-evaporation, it can occur from material within a certain *distance* from the surface. For a low injection rate, the top layer has the same amount of cure as the same thickness of material whatever the injection rate. The next layer down is now more cured because its been under the curing source one more time. Thus, it should reevaporate less, leading to greater thickness, as observed.

Current (A)	**0.08**	**0.36**	**0.8**	**1.8**
0.35A	0.12	0.15	0.19	0.34
5.85A	0.16	0.19	0.25	0.42

Table 4.3: Degree of cure of the top layers based on the plasma curing model

- **Deposited material:** By analyzing the thickness equation again (Equation 4.13), the other term that could potentially explain the trend is indeed the material deposited on top of the drum before curing, or in other words the thickness of the liquid film. By increasing the injection rate more material is put down at every

pass of the drum, and this would lead to different vapor pressures in the system, which would change the re-evaporation-impingement ratio (76) . In addition, there would be differences in the condensation, given that high injection rate means a larger ‘cloud’ emerging from the nozzle, therefore a smaller proportion of the monomer condenses onto the substrate, leading that the ratio thickness of the liquid film/injection rate is much smaller as the injection rate increases.

- **Etching:** It was considered that the etching would be constant, but if the degree of cure depends on the ion´s distribution, causing differences in curing depending on the thickness of the film, one should expect that the etching wouldn´t be constant with depth. Indeed, the probability of crosslinking/ scission depends on depth. In this regard, it has been suggested that the nuclear stopping mainly cause scission due to the atoms displacement, whereas the electronic stopping cause crosslinking (64) .So, by making a distinction between nuclear and electronic stopping mechanisms, it can be hypothesized that etching is indeed not constant, but rather dependent on the knock-on collisions caused by a nuclear mechanism, which increases with depth. (64) (82) . This would imply that not only the degree of cure of the top layer/layers would be greater, but the etching too.

4.2.7.3.Volume

When analyzing the volume vs thickness per unit volume, it is observed, that it decreases, as the volume is increased. Although, the trend differs depending on the injection rate, until the extent that for the maximum injection rate it is nearly constant no matter the volume.

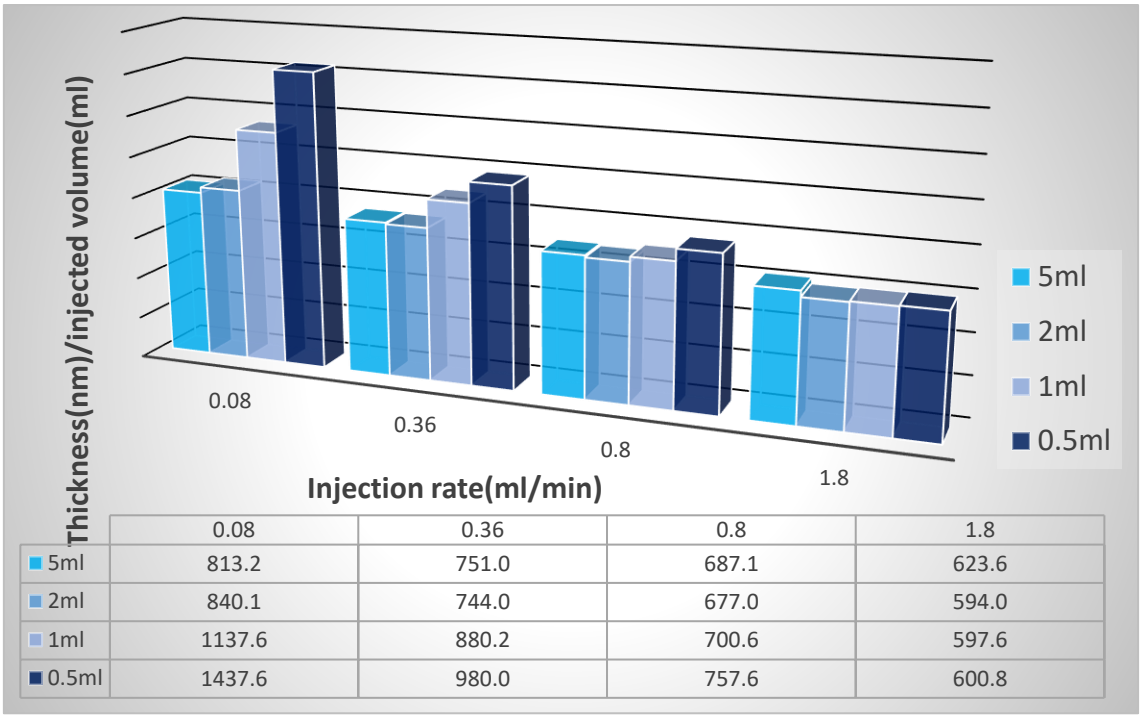

	0.08	0.36	0.8	1.8
5ml	813.2	751.0	687.1	623.6
2ml	840.1	744.0	677.0	594.0
1ml	1137.6	880.2	700.6	597.6
0.5ml	1437.6	980.0	757.6	600.8

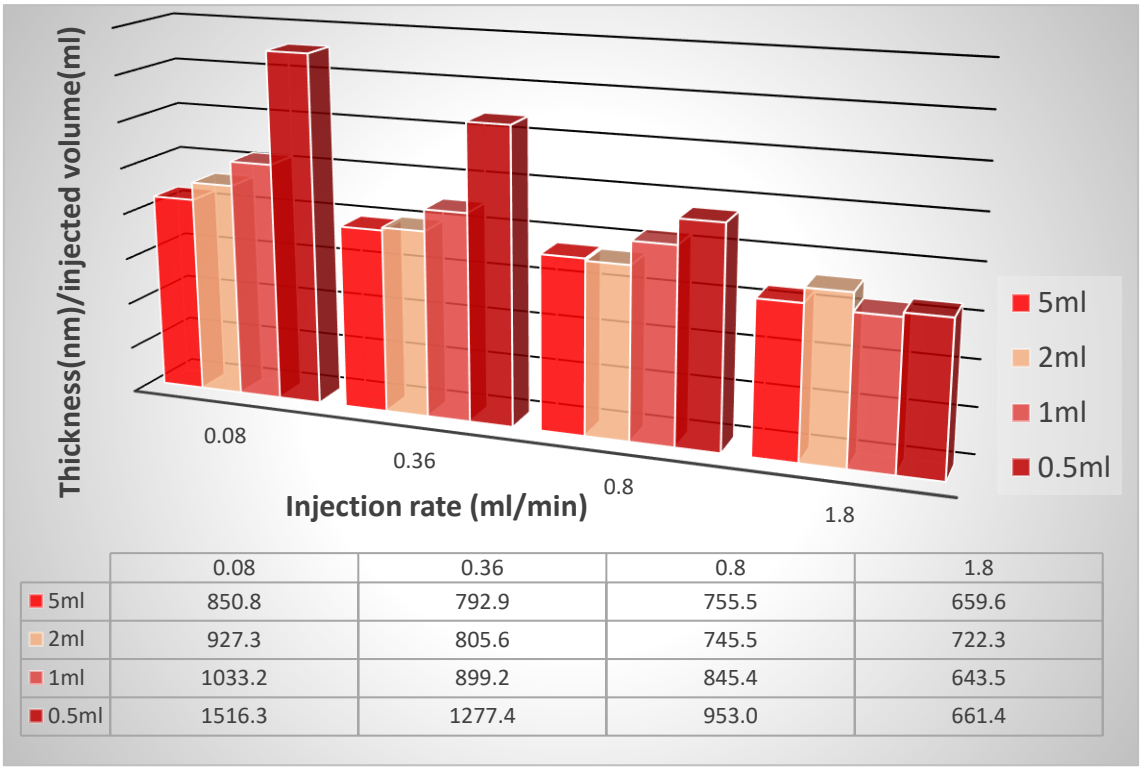

	0.08	0.36	0.8	1.8
5ml	850.8	792.9	755.5	659.6
2ml	927.3	805.6	745.5	722.3
1ml	1033.2	899.2	845.4	643.5
0.5ml	1516.3	1277.4	953.0	661.4

Figure 4.18: Thickness (measured by ellipsometry) per unit volume por plasma cured samples for different injection rates with 0.35A (blue) and 5.85A (red) currents.

Figure 4.18 suggests that indeed etching and re-evaporation come from the underlayers too.

From the curing model, it was demonstrated that the ions don´t solely interact with the "fresh-layer", but with the underlayers too. This further interaction causes a post-curing effect, increasing the overall degree of cure of the thin films. However, the ions not only cause crosslinking but also the scission of the chains. (64) (82) . So, the only left question is if the material not connected into the network would have enough time to diffuse towards the surface as the drum spins. In this sense, diffusion starts at 10^{-12}s, (64) , and it takes 4.32seconds for the drum to complete a full rotation, so it is plausible that some uncured or mobile fragments are able to diffuse towards the surface, finally escaping from the thin film.

As the injection rate increases thicker layers are put down on each pass until by about 1.8ml/min the etching and re-evaporation can only come from the newest top layer as this is so thick. Thus, the thickness/volume becomes about constant with volume by then as the material lost after condensation can only come from the newly deposited layer. For the lower injection rates some material can also be reevaporated or etched from one or more of the underlayers as this material is still close enough to the surface to escape. Thus, increasing the volume allows more material to be lost per unit volume as the drum rotates more times. This effect becomes larger as the injection rate decreases as more underlayers are involved.

Also, from the curing model, based on the MonteCarlo model, there is a limitation on the ions´ penetration depth, which follows a Gaussian curve. This means that up to a specific thickness the deepest underlayers won´t interact with the ions anymore, with not significant material lost from the layers deeper down. From the experimental results, it

can be observed that the thickness is maintained in the 2-5ml region, for all the injection rates, suggesting that the maximum penetration depth is reached in the thickness obtained in the region for those injected volumes.

In addition, it should be pointed out that the ions-matter mechanism causes a temperature rise (83) as a function of the ion-current density, due to the molecular motion of the chains. So, the underlayers would be subjected to a temperature rise due to the exothermicity of the ions-matter interaction. When the temperature of the "substrate/underlayers" increases, it could cause more re-evaporation of the "fresh layers" before reaching the curing source, which could cause that the liquid films get thinner given that more proportion of the material injected would re-evaporate as the underlayers´ temperature increases.

Regarding the power, it can be observed that the thickness is always greater with power, for all the process conditions, meaning that re-evaporation has a greater effect than etching. However, it was already hypothesized the importance of etching when it comes to determine the thickness. So, even though it´s true the more current the more number of ions, this doesn´t necessarily mean more scission, but on the contrary, as the energy is increased, according to the authors the ions would facilitate more crosslinks due to the closer distance between the reactive species, getting closer to the distance of the chains, so the probability for two radical pairs to be in neighboring chains is increased (64) .

4.2.7.4.Summary

The loss of thickness of the material is due to the contribution of:

- Monomer that never condense onto the substrate- The proportion of material that is able to condense on top of the substrate from the overall injected material increases as the injection rate decreases, leading to greater thickness per unit volume as the injection decreases, for all the process conditions.

- Shrinkage of the material on curing. The shrinkage produced in the film due to polymerization on TGPDA, is between 12-17%. (81) . It wasn't considered due to the small effect it has given the degrees of cure results obtained.

- Re-evaporation of monomer before reaching the curing source- The proportion of re-evaporated/ injected material in depends on the vapor pressure. So, as the injection rate increases, the re-evaporation /impingement ratio would be greater. But also, more material would be subjected to re-evaporate as the number of passes increase, due to the local temperature rise caused by the ions-matter interaction.

- Material etched: This is material removed as a result of the radiation from the curing source. Even though it was first believed that the etching only took place at the top layer, the thickness per unit volume results indicate that there is a proportion of lost material coming from the underlayers, so that the ions-underlayers interaction, not only causes "post-curing", but also "post-etching". It is believed to be a function of the nuclear stopping of the ions, which cause knock-out displacements. This mechanism increases with depth (64) (82) , so the etching increases as the layers get thicker.

- Material re-evaporated after curing: Thickness loss due to the low molecular weight species evaporating from the material as it passes around the drum between the curing source and before a new layer is added. This will depend on the degree

of cure of the top layers, number of passes and thickness per layer, as all of these factors determine the proportion of low molecular weight species that would be able to escape from the thin films.

4.3 Electron Beam

The influence of the process parameters on the degree of cure and thickness of the resulting thin films was studied. In an analogous way as when using plasma, the injection rate, volume and power were modified in order to better understand how the energetic electrons interact with the acrylate. In order to do so, volumes from 0.5 to 5 ml and injection rates from 0.08 to 1.8 ml/min were used. The power was modified by adjusting the current from 10 to 100 mA, obtaining then a power from 40 to 800W.

4.3.1 Current

In the following figure, the degree of cure is represented depending on the current used to cure the samples. The data had been subdivided in 3 groups depending on the volume of monomer injected, in all the cases the injection rate was set at 0.5ml/min.

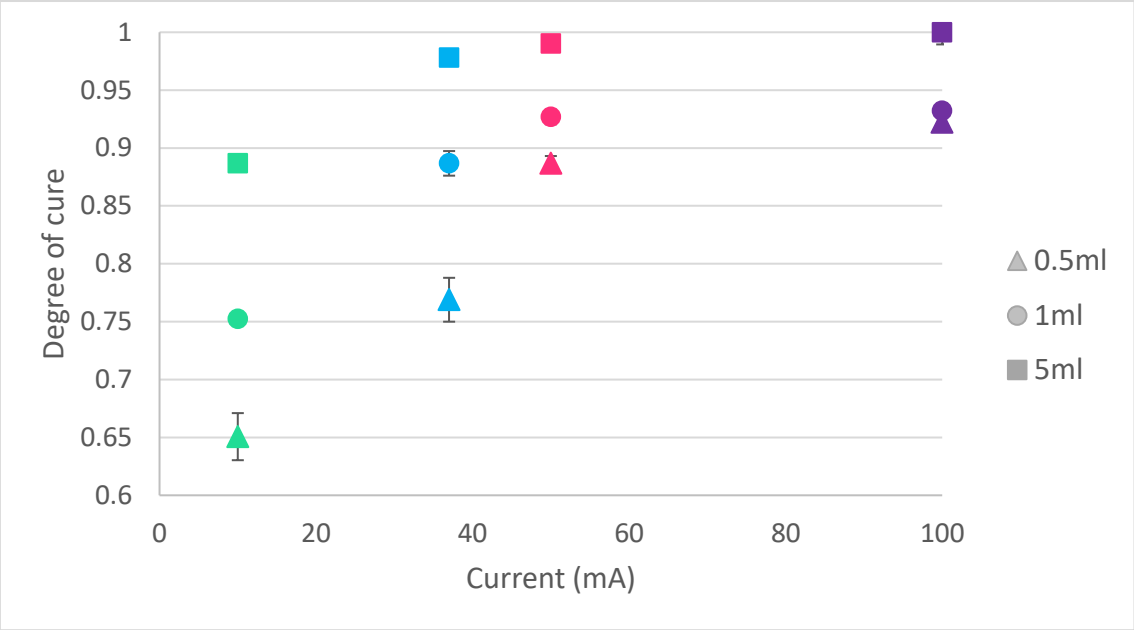

Figure 4.19: Degree of cure dependence with current for EB cured samples at different volumes (0.5,1 and 5ml) and at a fixed injection rate of 0.5ml/min

The trend in the degree of cure with current is similar for different volumes. As the current increases, more electrons interact with the coating, causing an increase in the degree of cure. However, the current does not have a linear effect on the increase on the degree of cure, with decreasing gradient as the current increases. So, the increase on the current has a positive effect on the degree of cure, but as the current increases, this effect diminishes. This could be due to the probability for an electron to reach a -C=C-, decreasing as the proportion of uncured material decreases. This hypothesis is supported on the observed gap 0.5-5 ml for different currents. The gap is reduced as the current is increased, or in other words, as the degree of cure increases. So, when the degree of cure is higher, it is less probable for the electrons to reach uncured material to form a reactive center.

In addition, it is clear that the degree of cure isn´t only influenced by the number of electrons generated, given the difference on the degree of cure observed by using different volumes.

4.3.2 Injection rate

Degree of cure as a function of injection rate was studied for different volumes by maintaining a current constant.

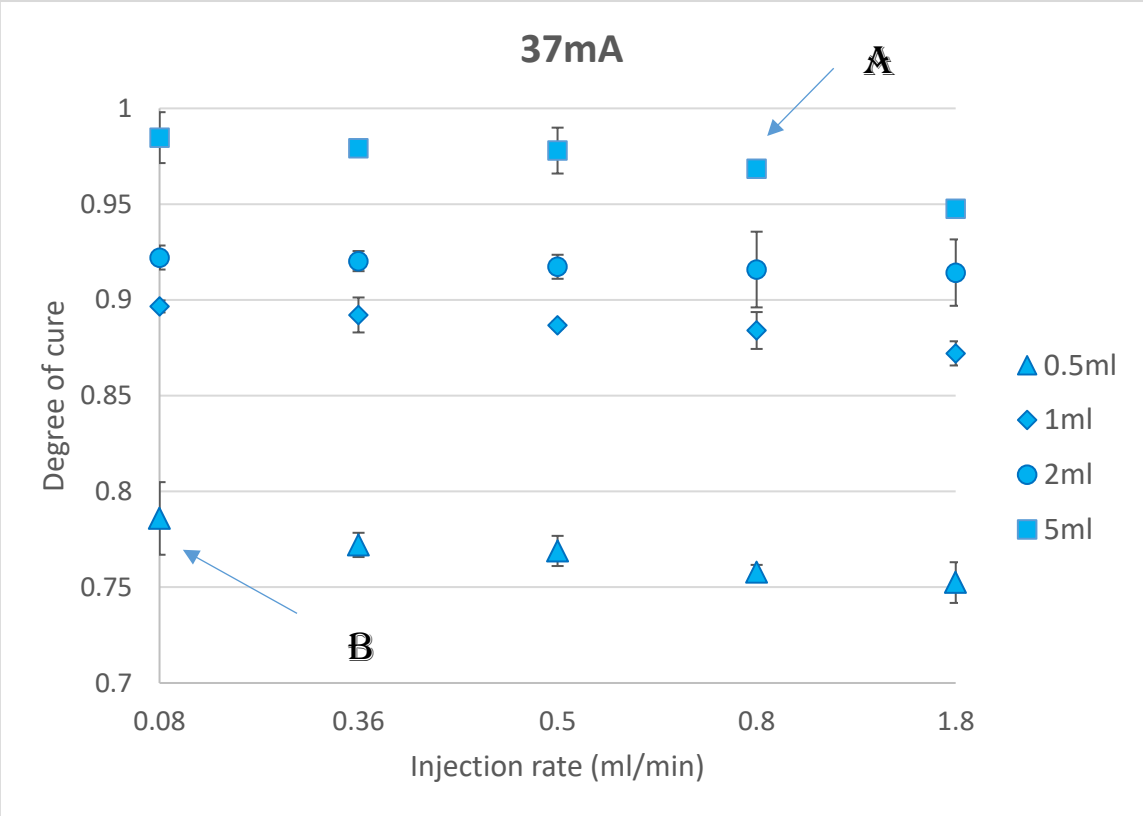

Figure 4.20: Degree of cure dependence with injection rate for EB cured samples for 37mA, with marks A and B indicating two samples in which were subjected to the same number of passes under the curing source

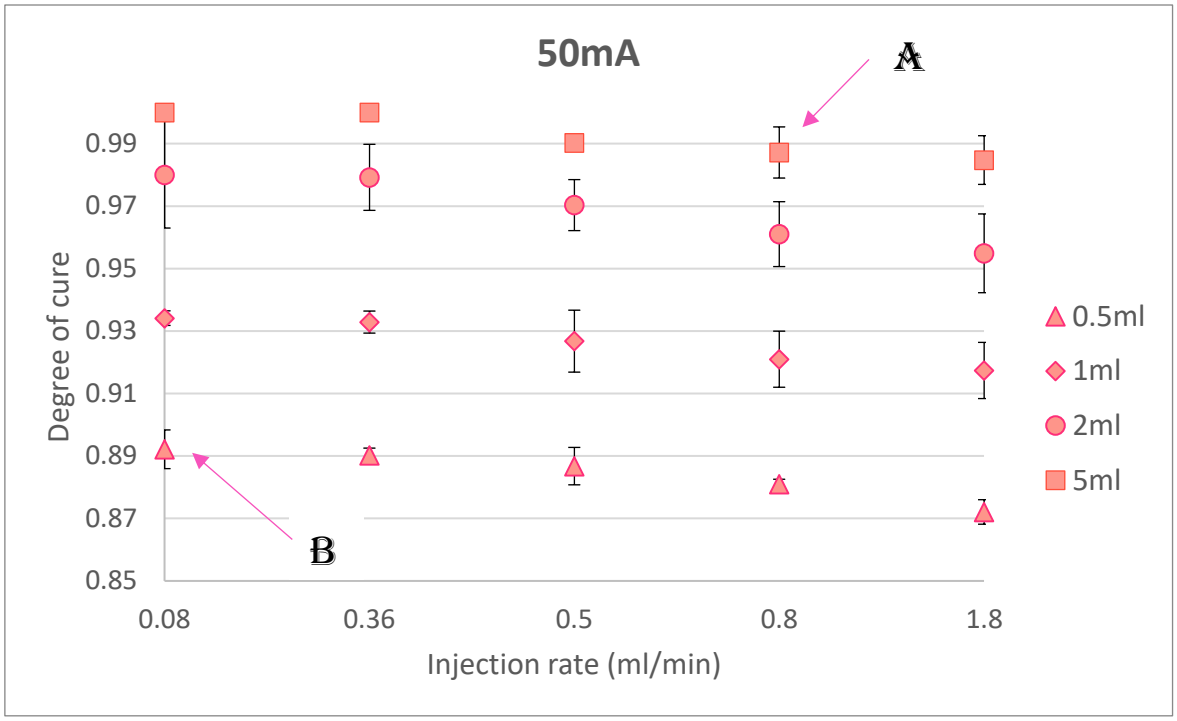

Figure 4.21: Degree of cure dependence with injection rate for EB cured samples for 50mA, with marks A and B indicating two samples in which were subjected to the same number of passes under the curing source

In contrast to the plasma cured material (Figure 4.5), the decrease of the degree of cure with injection rate is small. By modifying the injection rate, two variables are changed: the time the coating is being subjected to the curing source and the thickness of each layer that is put down on the drum. The density of reactive sites is not affected by any of these variables, given the fact that in both figures the power is kept constant. As the injection rate increases, the thickness of each layer would be greater, but it would be subjected by the curing source fewer times. So, the decrease observed in the degree of cure as the injection rate increases can be either by:

1) The electrons not being able to penetrate far enough through all the thickness of each layer or

2) Simply because it is being less times exposed to the curing source.

So, in order to better understand the electron-acrylate interaction the variable of volume needs to be analyzed.

4.3.3 Volume

Based on the previous figures (Fig. 4.20, 4.21) it is clear that the degree of cure is affected by volume, meaning that there must be "post-curing" of the underlayers, otherwise all the volumes at the same injection rate and power, should have the same degree of cure. This "post-curing" means that the electrons are able to penetrate in the underlayers.

Since for a given current and injection rate, the number of electrons created from the curing source are the same, what differs, for different volumes of material, is the number of times that electrons interact with the material and the overall thickness of the thin film.

So, firstly, the influence on the degree of cure of the number of times the material interacts with the curing source will be analyzed. However, by observing the marks A and B, in figures 4.20 and 4.21, it can be noticed that even though they are being subjected to the same time to the curing source, they have completely different degrees of cure. Therefore, time can´t be the only variable that explains the curing of the thin films. In fact, by plotting degree of cure versus number of passes, it can be observed that the data don´t fit a single trend.

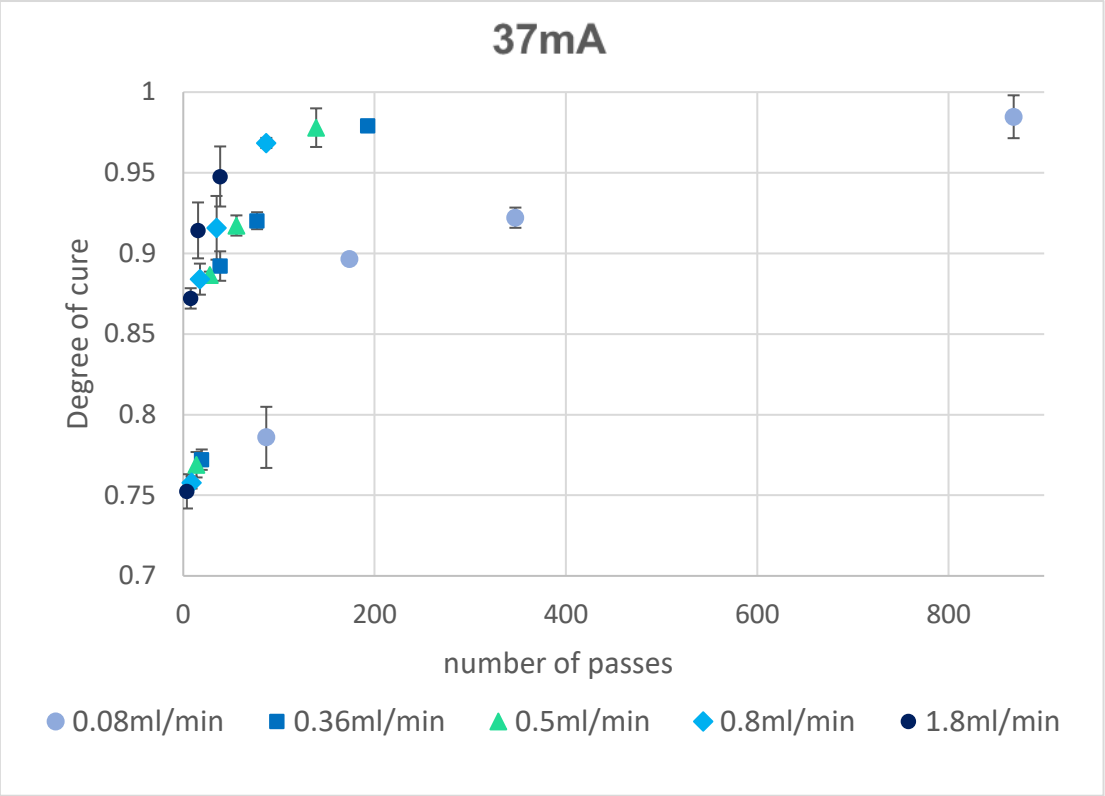

Figure 4.22: Degree of cure of EB cured samples depending on the number of passes under the curing source for 37mA

Building on this basis, another explanation for the modification on the degree of cure with volume needs to be found. Figures 4.23 and 4.24 suggest that, although injection rate has a minor influence, the trend in degree of cure is strongly related to volume.

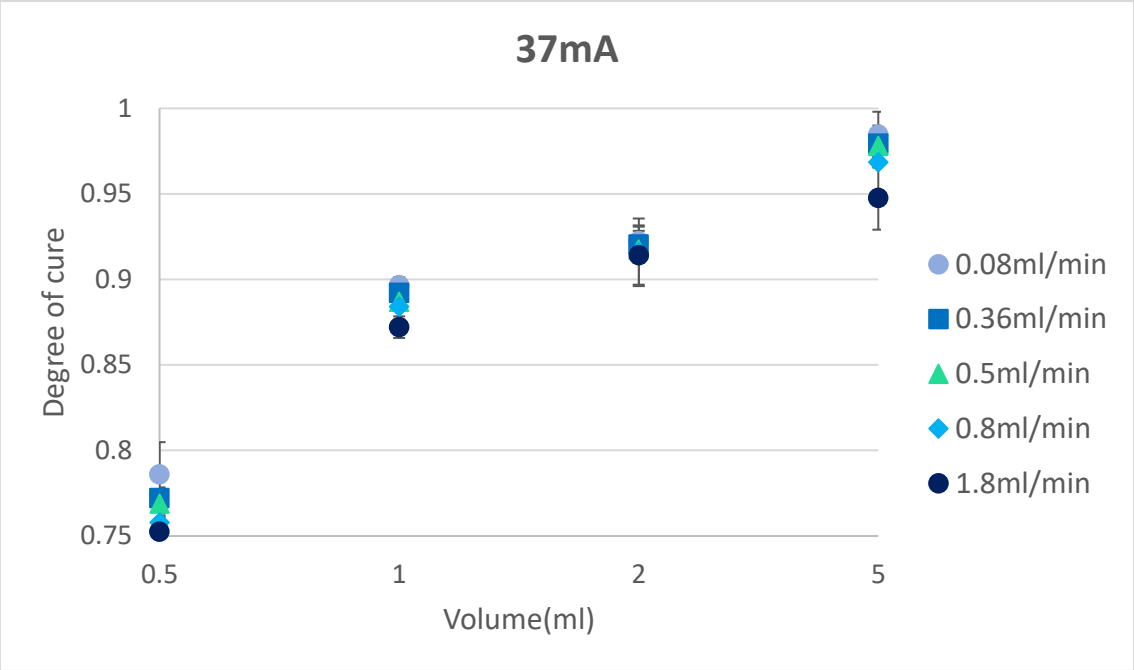

Figure 4.23: Degree of cure dependence with injection rate for EB cured samples for 37 mA

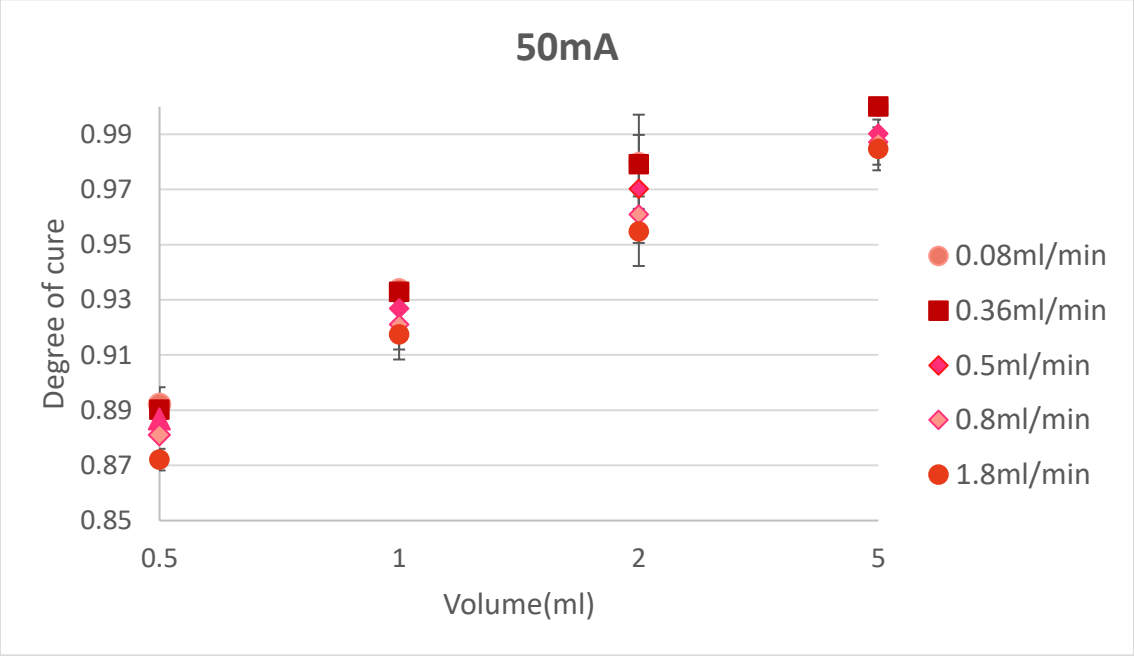

Figure 4.24: Degree of cure dependence with injection rate for EB cured samples for 50mA

The other thing changed with volume is thickness, understood as overall thickness, rather than each layer´s thickness.

The science behind the experimental results is that the electrons pass throughout the thickness of the film easily. Thus, some of the electrons will pass through the thin film without creating free radicals, so for which the greater the volume, the resulting thicker films increases the probability that the electron will create a radical, leading to a greater degree of cure. This was already concluded by other authors when studying the penetration depth of electrons in SEM polymer thin film: it was concluded that the probability of the electrons stopping at the surface causing inelastic scattering events was really low, so, most of the electrons passed deeper into the sample before causing any damage. (84) This phenomenon is energy dependent, as it can be observed in the following figure.

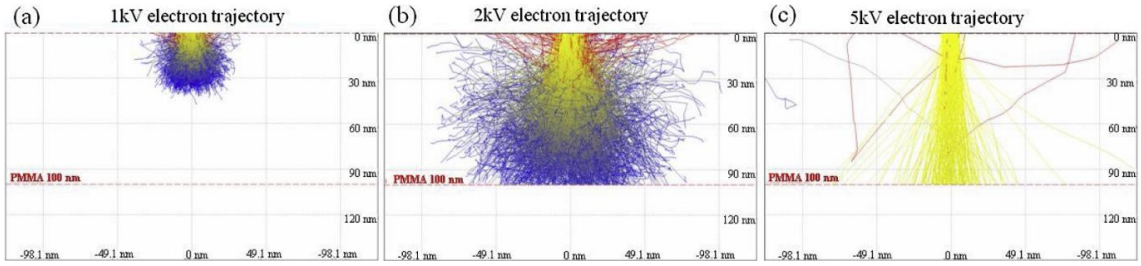

Figure 4.25: Electrons penetration depth for different accelerating voltages (84)

In fact, by simulating the energy of the electrons depending on depth by the CASINO program based on the MonteCarlo model, it can be observed that in the region near the substrate the electrons do not interact with the material, whereas they start slowing down after a certain depth, due to the hits with the material which would be the causative of ionization, and ultimately, polymerization. In the following figures, the energy

distribution of the electrons with depth and the increase on the probability of the hits matter-electrons with depth can be observed.

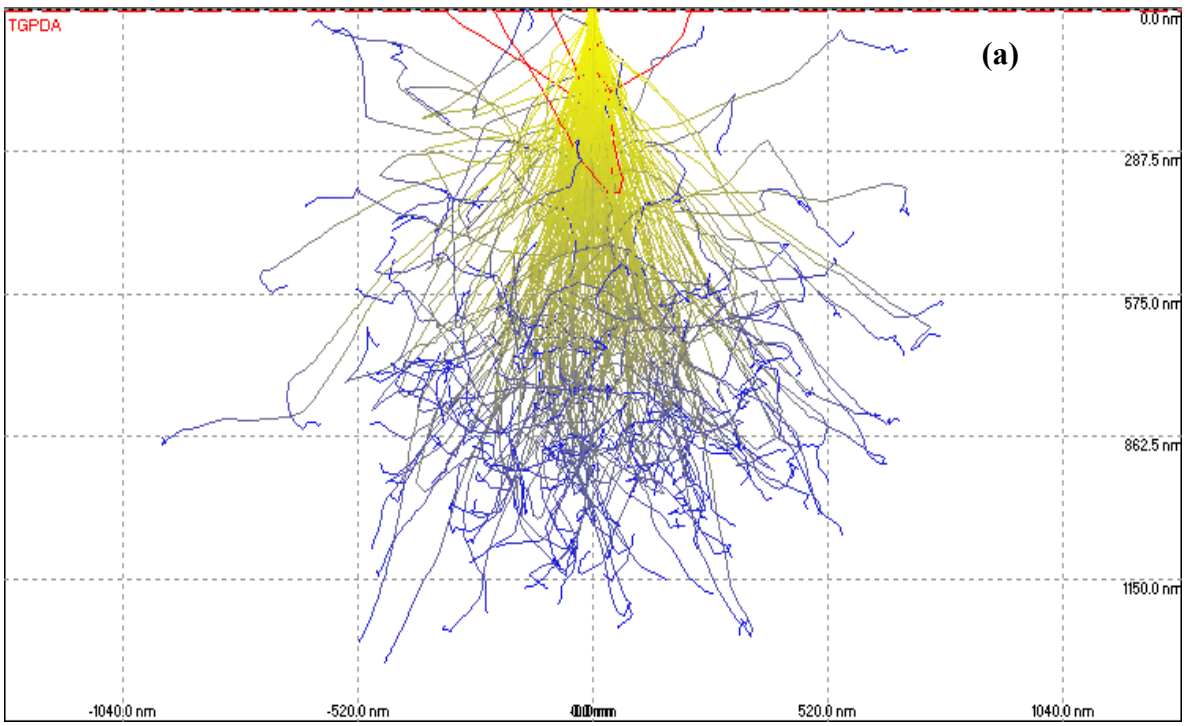

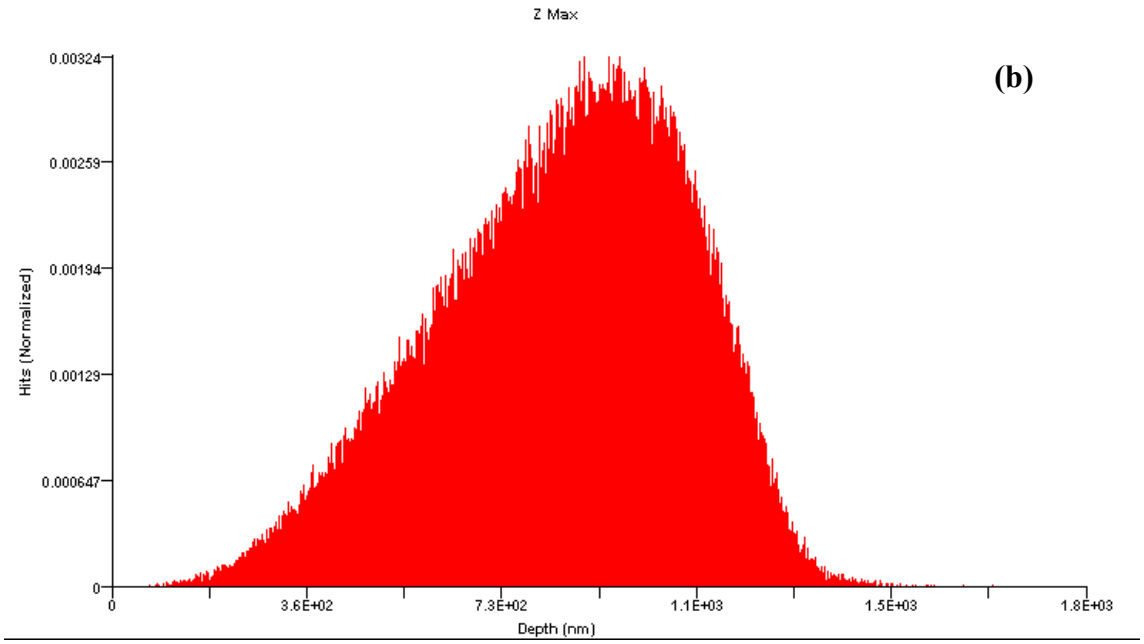

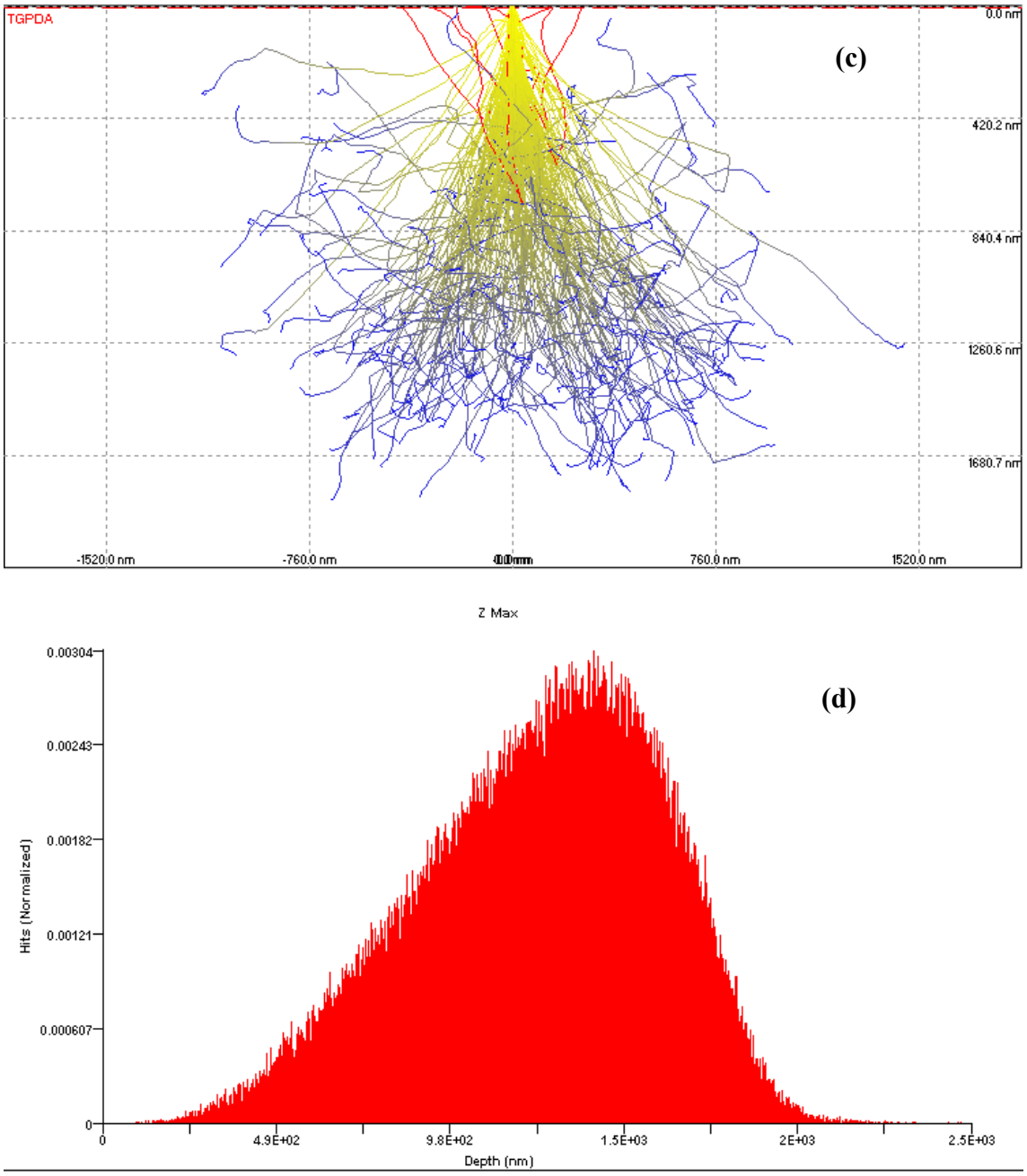

Figure 4.26: CASINO simulation of electrons-TGPDA interaction for: (a)(b) 50mA (5.98kV) and (c) (d) for 100mA (7.44kV). In (a) and (c) The red lines refer to the simulated tracks of backscattered electrons that exit the sample. The yellow to blue transition indicates the electron energy decreasing from the incident energy to lowest allowed energy, 0.0001 keV, in each simulated track.

The kinetic energy of the electrons starts decreasing when in contact when the coating, the velocity then, tends to zero underneath a certain point z, point in which the electrons would be able to interact with the material in such a way as to form radicals. Thus, the probability of speed of electrons tending to zero increases with thickness as there is more material they have to go through. So, the thicker the coatings the more electrons would be "stopped" in the coating, but also, the greater the accelerating voltage, the greater the penetration depth. (84) (85) (86) (Figure 4.26,4.27). At the same time, once the depth at which the interactions electrons-matter is the greatest, a logarithmic decay of the intensity as the electrons go further through the material was observed. This is a consequence of the reduction of the electrons transmission rate as they penetrate further, as some of them would had been already absorbed further up creating free radicals, following the Beer-Lambert law.

4.3.4 Injection rate and volume

By comparing the influence on the degree of cure of the volume (Figures 4.23, 4.24) and injection rate (Figures 4.20, 4.21), it can be observed that volume is the parameter that influences the curing degree the most. However, curing degree cannot be explained only based on the overall thickness, as it is not the only variable that makes an impact on the degree of cure. If that were true, no changes on the degree of cure would be noticed with injection rate.

In summary, the degree of cure is explained by number of passes and thickness of the layers. An increase on both variables, number of passes and thickness will cause an

increase on the degree of cure. The reason for which the volume has a greater effect on the degree of cure than the injection rate is:

- Volume: As the volume increases, both, the thickness and the number of passes increase, leading to a greater degree of cure
- Injection rate: As the injection rate increases, the number of passes is reduced, but at the same time, the thickness is increased, reason for which both effects will compensate, leading to a lower effect of this variable on the curing degree.

4.3.6 Model proposed

The conclusions made so far are that:

- The degree of cure mainly depends on the overall thickness of the layers at each pass of the drum as a consequence of the decay on the kinetic energy as the thickness is increased, following a Gaussian curve. (Figure 4.26,4.27)
- Also, the number of times the underlayers are subjected to E-Beam, the more curing degree will cause.
- The degree of cure increases as the power does, given that the density of electrons is increased.

Thus, the same premises as in the plasma modelling were used, resulting in the same expression. (Eq. 4.8-4.11)

The model was developed using two currents, 37 and 50mA, so, by adding the effect that every time the material interacts to the curing source (obtained from the model) to the degree of cure of a certain layer, the degree of cure for both currents is obtained:

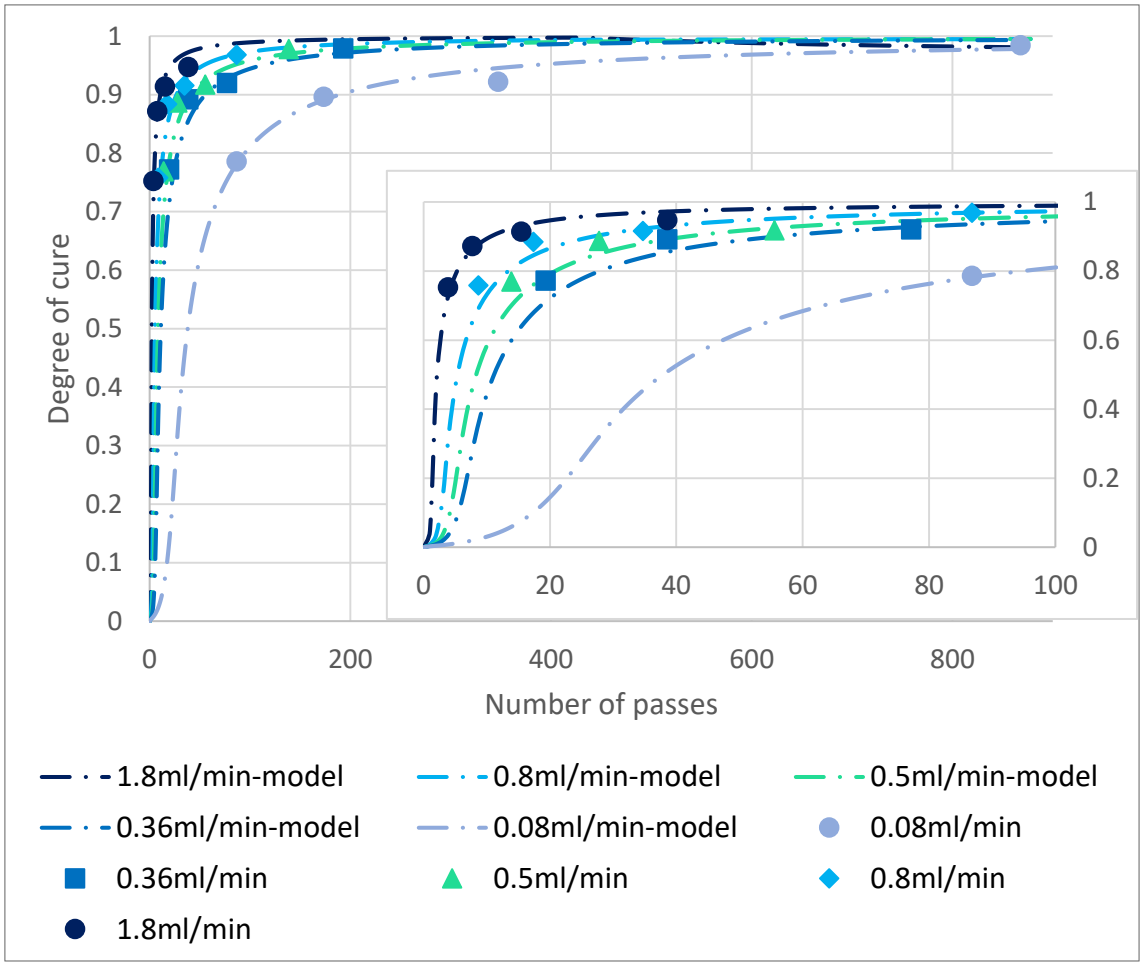

Figure 4.27: Curing model for EB cured samples (37mA,5.2kV)

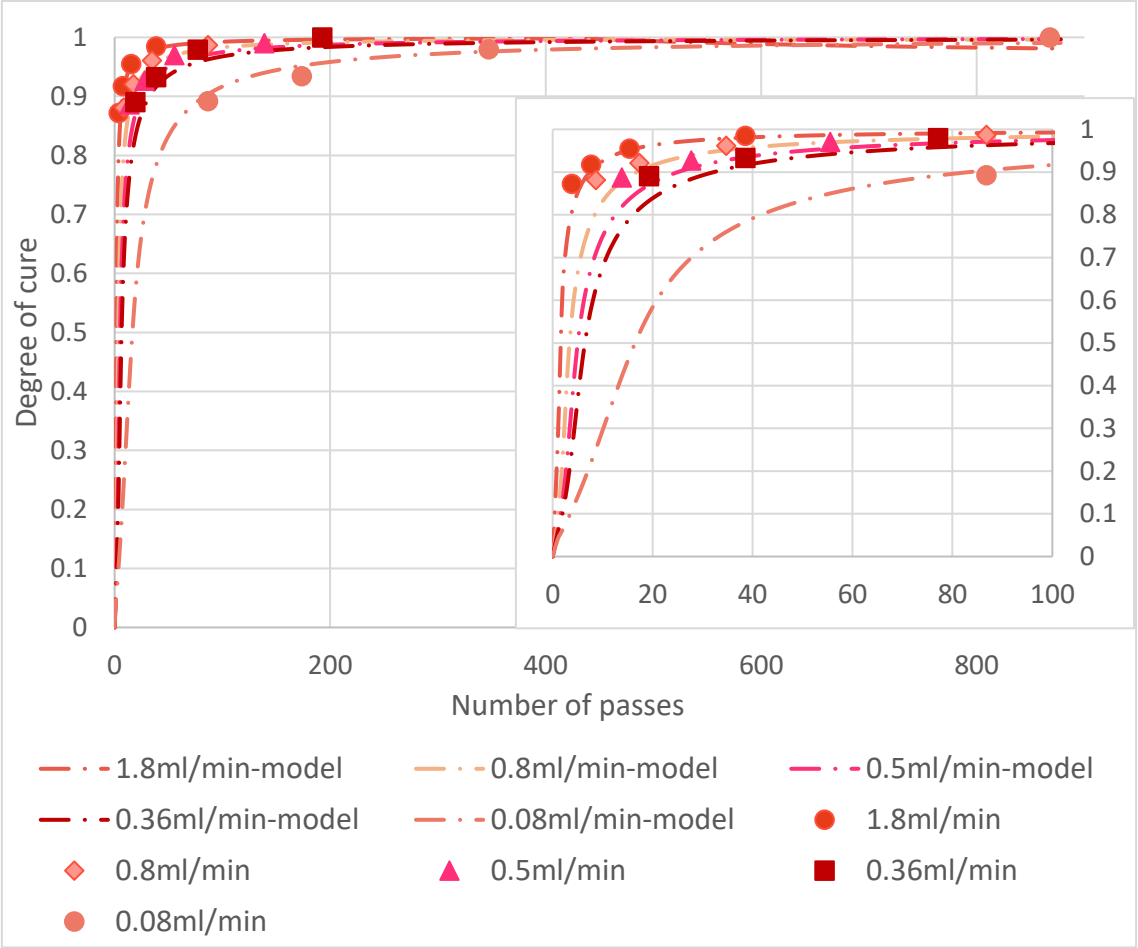

Figure 4.28: Curing model for EB cured samples (50 mA,5.98KV)

What differs with the plasma model, however, are the fitting parameters, which is a direct consequence on the deeper the electrons can travel through, which ultimately causes a greater interaction volume, when compared to plasma.

To better understand the models, the fitting parameters for both currents will be shown:

Current (mA)	*A*	*b*	*d*	*Correlation coefficient*
37	5,000	2.7	10	97.5
50	150,000	3.5	12	94.3

Table 4.4: Fitting parameters and correlation coefficients of both models

The physical meaning of the parameters is the same as in plasma, what changes however, is the relationship of *b* and *d* with respect to the power used:

- *A* is related to the increase on the degree of cure as the number of passes increase, so in other words, how fast the electrons will "post-cure" the thin films.
- *b* and *d*, describe the increase of the curing degree as the material the electrons have to go through increases, which is more related to the voltage.

So, as the current increases, not only the proportion of electrons interacting with the material at each pass of the drum increase, but also the electrons distribution with depth. In plasma however, the voltage was maintained throughout all the experiments, leading to a constant *b* and *d*.

Since only two sets of data for each current were big enough in order to build up a proper model, the numerical relationship of both parameters with current can´t be estimated.

Physical explanation

In this case, what needs to be understood is why does the absorbed dose mainly depend on the volume (0.78), in a lesser extent to the number of passes (0.65), and then with a 0.52 of correlation, by the current.

When electrons interact with the material, the electrons do slow down and their "stopping power" depends on the amount of material they are crossing. (87). The decrease in their kinetic energy is due to the inelastic scattering they undergo. But there is another variable that has an impact on the depth of electron penetration (x) which is the voltage (Potts, 1987, p.336). As the voltage is increased, the penetration depth increases as well, leading to a lower proportion of the electrons stopping at the surface. So, because of the electron beam mechanism, the current increase goes with a voltage increase. So even though the power has been describing as a function of the current, what actually causes the increase on the penetration depth is the change in voltage.

The most widely used model to explain the dose distribution along the material thickness is the MonteCarlo theory. It is based on the idea that electrons, do lose energy continuously, as in the plasma section, this means that their probability of stopping will increase until their rise an "optimum distance", up to this point it will decrease. (88)

Using this model, it was concluded, that for high energy electrons, their probability of interacting with the matter at the surface is almost zero, since most of the electrons will pass through. (84) . So, the idea that the degree of cure in this case, depends on the overall thickness is supported to the theory. (89)

Also, regarding power, it was concluded that for every volume and injection rate, an increase of power caused an increase on the degree of cure. This fits with the idea, that

when increasing the current, an increase on the dose absorbed occurs (89) , simply because more electrons will interact with the causing a greater number reactive sites.

4.3.7 Thickness

The process parameters do not only influence on the degree of cure, but also the thickness due to the differences on the re-evaporation and etching. For that reason, the control of thickness of the coatings with processing parameters is investigated.

4.3.7.1.Power

By plotting the thickness versus current for a constant injection rate (0.5ml/min) (Fig.4.30), it can be observed that for every volume the same trend occurs. At the beginning, the thickness increases as the power does. However, up to a certain point the thickness significantly drops. For the low powers, the curing source isn´t able to completely cure the coatings, resulting in a partial re-evaporation of the material. As the power increases, the degree of cure will increase as well, reducing then the re-evaporation. However, by further increase the power, more electrons will be generated, leading to a greater chain-scission resulting on more material being etched away from the thin film.

So, the maximum thickness is achieved at the optimum current in which both factors, etching and re-evaporation are best compensated.

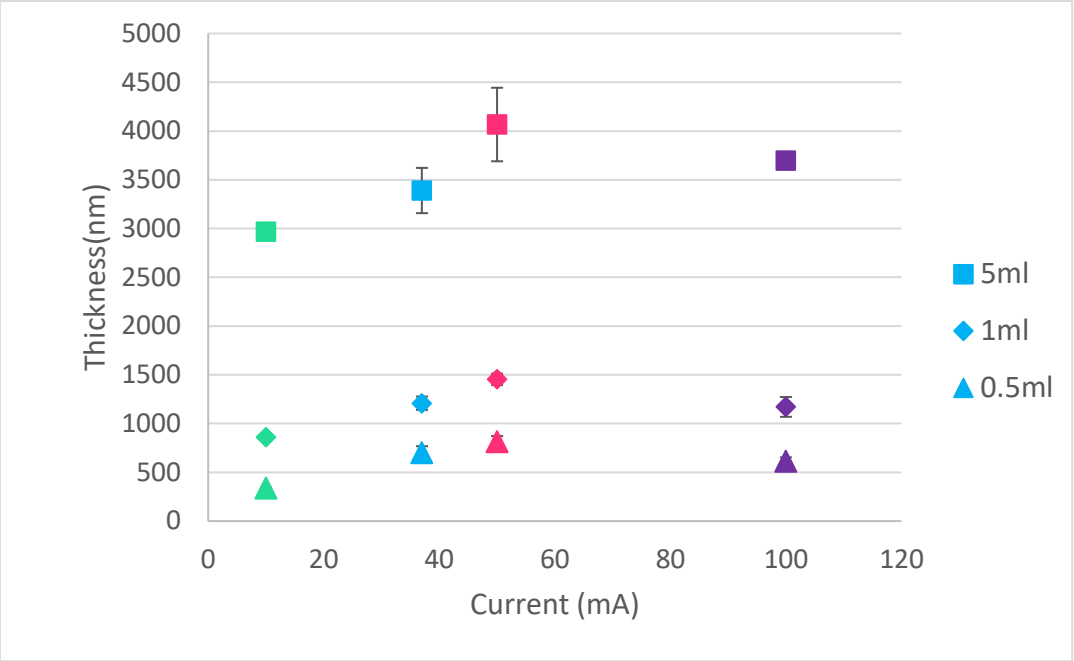

Figure 4.29: Thickness (measured by ellipsometry) dependence on current for EB cured samples at 0.5ml/min injection rate.

4.3.7.2.Injection rate

When analyzing the trend of the thickness with volume when using two currents (37 and 50mA), an interesting fact was observed. For the greatest volume, the thickness increases as the injection rate does. However, as the volume diminishes, the trend of volume against injection rate gets smaller until reaching the point in which the thickness trend is reversed, increasing as the injection rate decreases.

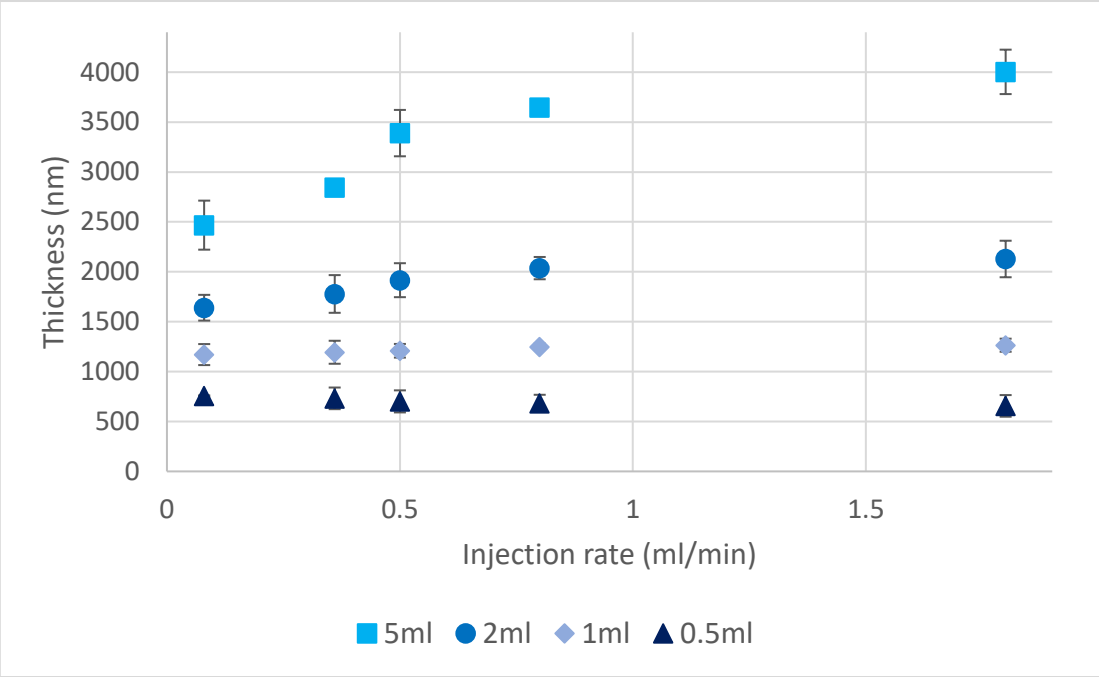

Figure 4.30: Thickness(measured by ellipsometry) dependence of injection rate for EB cured samples for 37mA

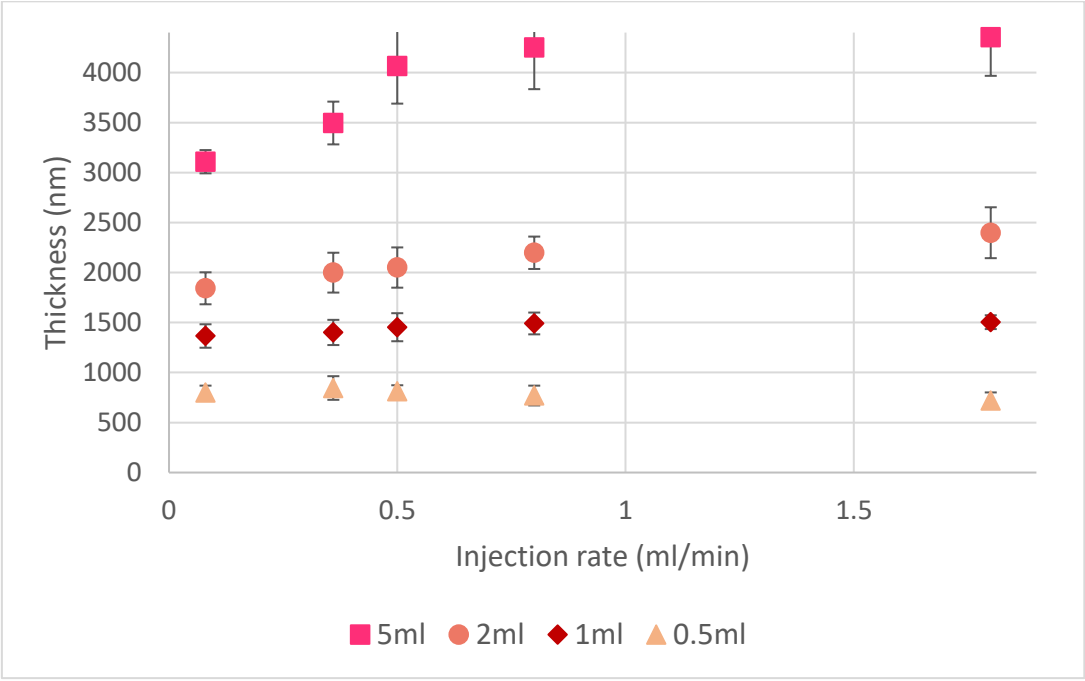

Figure 4.31: Thickness (measured by ellipsometry) dependence of injection rate for EB cured samples for 50mA

As in the plasma section, the differences on the injection rate will lead to different condensation ratio, so that the proportion of monomer that doesn´t condense against the monomer injected is greater for greater injection rate leading to thinner films.

Also, there is a depth of material from where the uncured species would re-evaporate, and it would depend on the number of passes but also the degree of cure of the layers on top. So the degree of cure, is more significant for lower injection rates (as the layers are thinner), hence at lower injection rates the thickness from which re-evaporation can take place has better cured material, so there will be less re-evaporation and the layer would be thicker. However, as the injection rate decreases, the material also passes around the drum more times for the same volume, so there will be more re-evaporation, hence thinner layers and the same will be true for etching.

What differs with the plasma section however is that in this case as the volume changes, the relative importance of these two effects changes, leading ultimately, to reverse the plasma thickness trend with injection rate.

4.3.7.3.Volume

When changing the volume for a given current and injection rate, it can be observed that there is a clear drop on the thickness per unit volume as the volume is increased, and this difference is greater as the injection rate goes down.

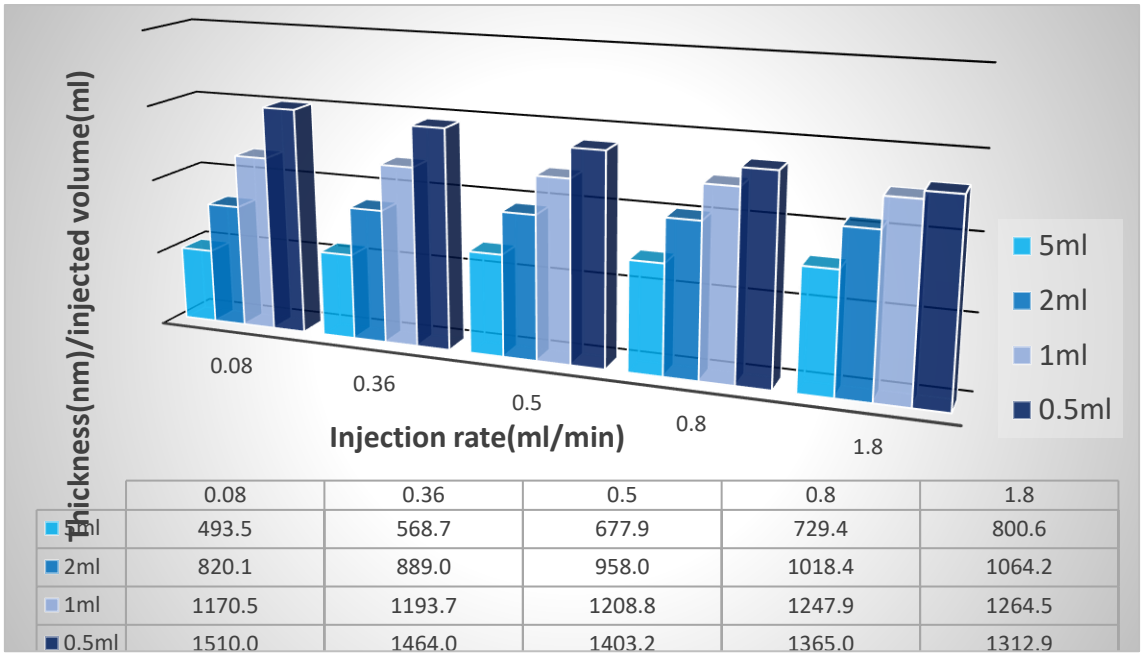

	0.08	0.36	0.5	0.8	1.8
5ml	493.5	568.7	677.9	729.4	800.6
2ml	820.1	889.0	958.0	1018.4	1064.2
1ml	1170.5	1193.7	1208.8	1247.9	1264.5
0.5ml	1510.0	1464.0	1403.2	1365.0	1312.9

Figure 4.32: Thickness (measured by ellipsometry) per unit volume for EB cured samples using 37mA

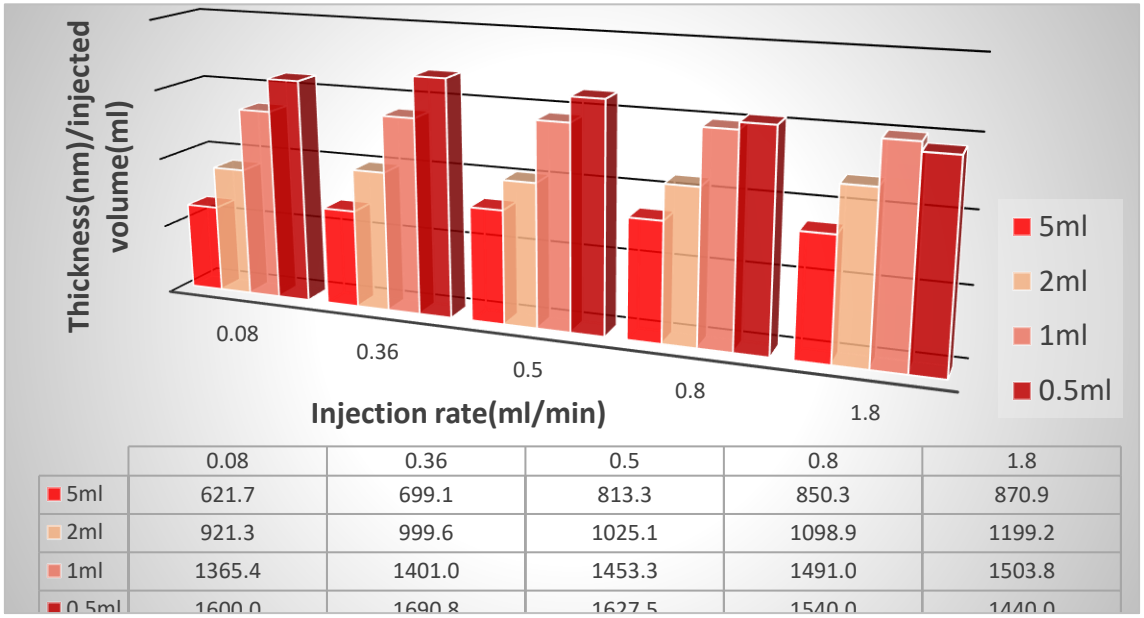

	0.08	0.36	0.5	0.8	1.8
5ml	621.7	699.1	813.3	850.3	870.9
2ml	921.3	999.6	1025.1	1098.9	1199.2
1ml	1365.4	1401.0	1453.3	1491.0	1503.8
0.5ml	1600.0	1690.8	1627.5	1540.0	1440.0

Figure 4.33: Thickness (measured by ellipsometry) per unit volume for EB cured samples using 50mA

So, if only considering the electrons distribution with depth (from the curing model), the decay on the thickness per layer as the volume goes up could be explained:

- First of all, the figures suggest that the lost material isn´t only coming from the top layer, but from the underlayers too. This effect is expected to be larger for lower injection rates as there are more underlayers involved.

- The interaction between radiation and matter causes an exotherm reaction generated inside the thin film As the number of reactive species increases the number of scattering events is greater, which not only causes the breakage of the C double bonds, but also the rise on the thin film temperature, causing an increase on the re-evaporation/impingement ratio, as the underlayers" temperature increases. This could explain, why the drop on thickness per unit volume with volume is greater for lower injection rates: because the underlayers had been subjected more times to the interaction with electrons.

- On the contrary than in plasma, where a levelling off was observed up to a certain depth, EB cured samples don´t reach the point in which this "equilibrium" is reached, suggesting that the effectiveness of etching (the depth over which it happens and the amount of material removed) will be different than the re-evaporation, and the difference between these two will be different between plasma and electron beam.

4.3.7.4.Summary

In this case, the variables´ influence on the thickness would be summarized:

- Power: As the current increases, more electrons will interact with matter. So, the power has a positive influence on the thickness, given the fact that it causes an increase on the degree of cure (due to the greater current), and therefore less material will re-evaporate. But up to a certain power, the increase on the etching doesn´t compensate for the decrease in the re-evaporation, resulting in thinner films.

- Injection rate: It was observed for both currents a change on the tendency of the thickness with the injection rate depending on the volume. For greater injection rates, the underlayers would be less times subjected to the curing source, resulting in less curing and scission, but since the layers per pass of the drum are thicker, the ability the low fragments have to escape will be lower too. The role these two effects play changes with volume.

- Volume: It was observed a decrease on the thickness per unit volume as the volume increased. It was considered to be a consequence of the etching and re-evaporation of the underlayers and the rise of temperature due to the inelastic scattering events produced by the electrons. The latter would increase as the interaction electrons-matter increases, causing a greater re-evaporation prior to curing. So that the layers will be thinner at each pass of the drum decreasing the overall thickness.

CHAPTER 5. INFLUENCE OF THE CURING DEGREE ON THE POLYMER´S PROPERTIES

In this chapter a comparison between the two curing sources (plasma and E-beam) will be made in terms of crosslinking density (Swelling experiments), storage modulus (DMA) and the topography (AFM).

5.1 Crosslinking density

The crosslinking was indirectly measured by swelling experiments. The results obtained were compared with the degree of cure obtained by different curing sources (Plasma and E-Beam), analyzing samples obtained at different injection rates.

5.1.1 Swelling experiments

According to studies by Asmussen and Peutzfeldt (48) (90) (91), polymers with a similar degree of cure may exhibit different crosslinking density. Degree of cure refers to an average value, but it doesn´t take into account the different areas of low and high conversion, hence, how homogeneously a polymer has been cured. A crosslinking density measurement on the other hand will be sensitive to heterogeneities. If a heterogeneous polymer is obtained in which highly cured regions coexist connected by less well cured, more linear chains, the crosslinking density will be measured as smaller than if the polymer was homogeneously cured, given that what crosslinking density measures is the number of links between polymer chains and the ability segments between crosslinks (or crosslinked regions) to unravel. In addition, it is believed, that a fast curing process favors

the formation of more centers of crosslinking, (92) or in other words, it has been speculated that a slow start of the polymerization, may result in a more linear polymer structure. Given that as the curing kinetics lowers, it favors the formation of extended polymer chains, allowing more time for molecular rearrangements and hence, reducing crosslinking. (91) (93) Given this explanation, it should be expected that as greater is the initial degree of cure, greater would be the crosslinking density.

Since this initial degree of cure depends in this case on the injection rate, the greatest and lowest injection rate cured samples had been measured. On top of that, a comparison between EB and plasma cured samples had been performed, as it can be seen in the following figure, where the crosslinking density had been estimated by performing swelling experiments, by following the equation 2.4 from section 2.2.2. (Figure 5.1)

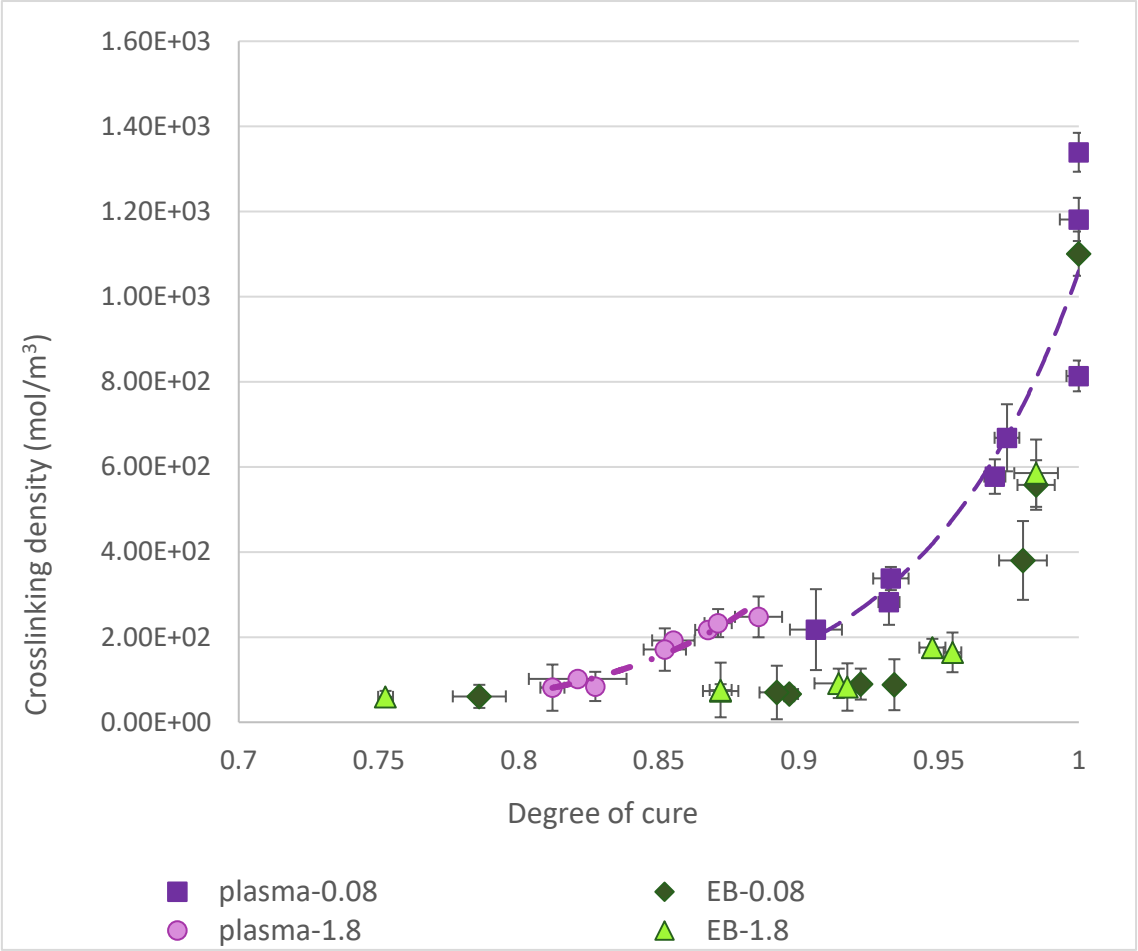

Figure 5.1: Crosslinking density of plasma and EB cured samples depending on the degree of cure

In EB cured samples, the degree of cure-crosslinking density relationship is independent on the injection rate. Similarly, the degree of cure itself wasn´t really affected by the injection rate, but rather by the volume. Most of the electrons would pass through without interacting with the material, curing it. This resulted in a really low start of polymerization for all the injection rates, according to the EB model (section 4.3.6), which will give rise to a more linear polymer network. As the underlayers are being further exposed to the high energetic electrons the overall degree of cure of the underlayers increase at different rates, however this doesn´t to cause big differences on the crosslinking density, it is only

when the degree of cure is above 0.95, that the crosslinking starts to increase significatively. These degrees of cure correspond to the greatest thickness and thus, the greatest density of electrons, promoting that the interactions electrons-matter results in crosslinks, simply because the probability of two electrons interacting with neighbor chains is increased with depth. (64).

The same trend degree of cure-crosslinking density was observed for different injection rates for EB cured samples, however the trend for plasma cured samples differed between injection rates. In EB the crosslinking density seems to be volume dependent, suggesting that the slower curing rate for 0.08ml/min is compensated by the increase in the number of passes, where the density of electrons will be greater leading to more chances of recombination. (94)

As for the plasma cured samples, different degree of cure-crosslinking density trends are obtained, to the extent that if the master curves drawn would be extrapolated, the crosslinking density couldn't be linked to the degree of cure without taking into account the injection rate, given the enormous influence the injection rate has on the crosslinking density of the plasma cured samples.

From the plasma section (section 4.2) conclusions, it was believed that the top layer is better cured as the injection rate increases, the post-curing of the underlayers is faster, due to the ions distribution with depth. So, at the start of the polymerization the degree of cure achieved is greater for greater injection rates, leading according to the theory to a greater crosslinking degree, and since the curing rate in the further interactions ions-underlayers is also greater for greater injection rates, simply because the ions density is greater, this could lead to a greater crosslinking density on the greatest injection rate samples even for smaller degrees of cure. However, once a certain volume is achieved the ions can´t further

penetrate in the underlayers, resulting in that the underlayers won´t be fully cured. So, in the same way up to certain degree of cure, the crosslinking density can´t further increased, meaning that the master curve drawn for plasma cured samples can't be extrapolated.

The greater crosslinking-density of plasma compared to EB even for greater curing degrees, may be attributed to the fact that in EB the pendant groups tied to the network could be further cured, however this wouldn´t result in an increase on the crosslinking density, just on the degree of cure. (95) (96) . As the density of radiation species is lower for EB, then fewer reaction centers are initiated, and hence there is lower probability that a particular reaction center initiated will be terminated. Hence there will be more propagation steps before termination and hence longer 'chains' (without crosslinks) in the rubber, leading to a lower rubber modulus. So, the conclusion is that EB will tend to form longer chain sections to start with before curing completes (once the chains become less mobile) so the degree of crosslinking is lower for EB than plasma.

5.1.2 DMA experiments

Mechanical properties are closely related to the crosslinking density, as the crosslinking density increases, the macromolecules become immobile, and hence, the material becomes stiffer, less flexible. However, when it comes to the degree of cure, this statement isn't necessarily true. Previous research studies of the relationship between degree of polymerization and mechanical properties such as storage modulus showed that higher degrees of cure did not always result in stiffer materials (97) (98) . Hence, samples with the same degree of cure showed different mechanical properties. The only difference between samples was the crosslinking density space distribution. The storage modulus at

the rubbery state depends on the crosslinking constraints which reduces the chain mobility. This process is defined by the phantom model, which is based on the assumption that the network junction motion determines the dynamic mechanical properties. “The junctions are fixed in space to move affinely with the whole network” (97)

So, in order to get an idea of how the mechanical properties (storage modulus) are influenced by the degree of cure and crosslinking density, 4 samples had been measured (3 plasma cured samples and 1 EB cured sample). The aim in this case is not a deep understanding of the thin films’ mechanical properties, but rather to get a first impression.

In the following figure the data obtained by DMA can be observed. While analyzing the results from the plasma cured samples it was noticed that the storage modulus at ambient temperature (the rubber modulus, above Tg) decreased as the degree of cure does, being the stiffer material the one obtained by using greater plasma power (a), followed by (b) which corresponds to the plasma cured sample when reducing the power, and finally, (c) which is the softest material, as it is the one obtained at the lowest plasma power and at a maximum injection rate. This is as expected: a lower cure gives a lower crosslink density and hence lower rubber modulus (section 2.2.2). However, when comparing these results with the EB cured sample (d), it can be observed that even though it is the better cured sample, it’s storage modulus isn’t a high as the highly cured plasma-cured sample, which aligns with the conclusions of the crosslinking density section: Eb cured samples have a lower crosslinking density even for greater degrees of cure when compared to plasma cured samples.

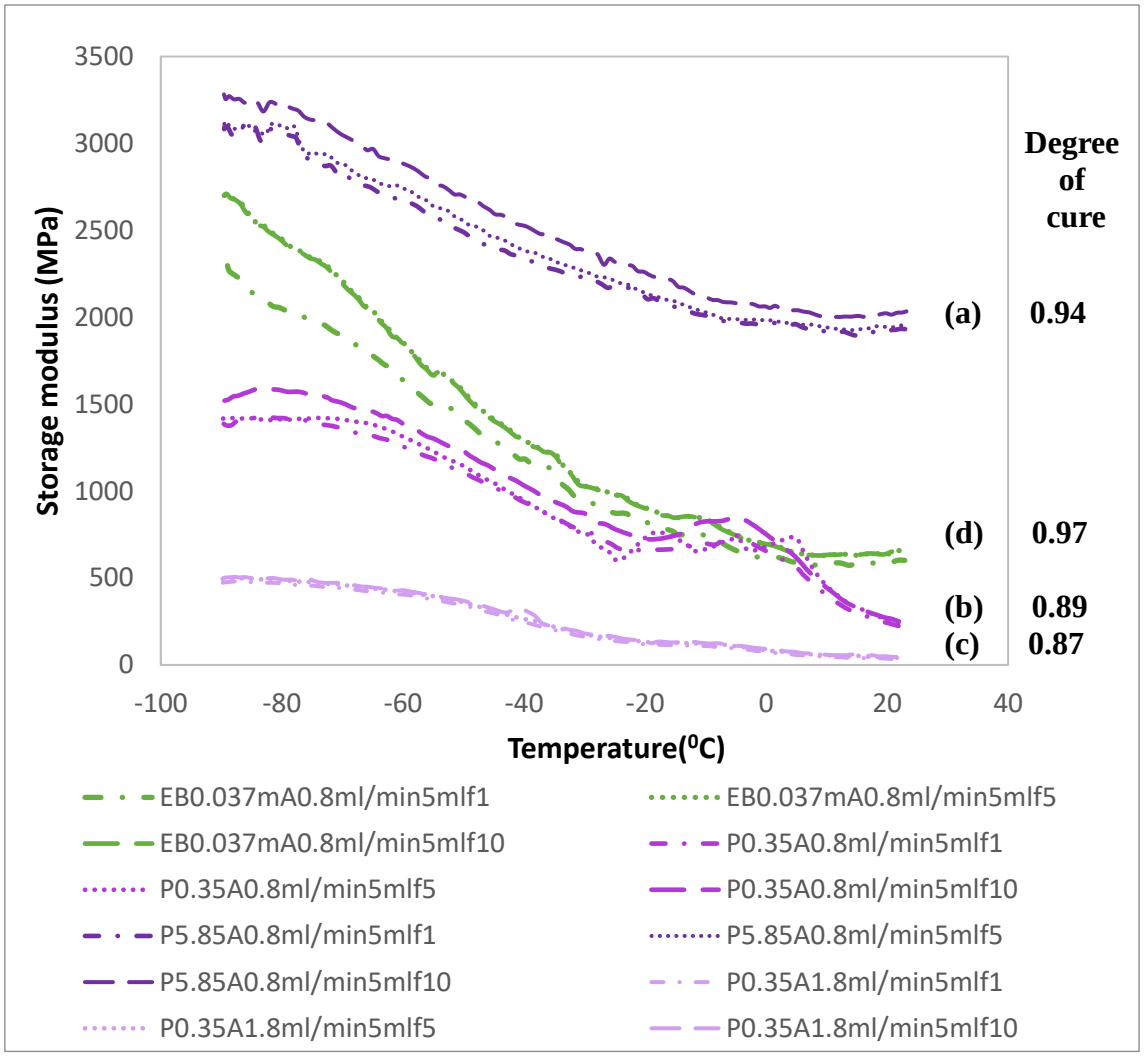

Figure 5.2: Storage modulus vs Temperature, (a) Plasma 1640W 0.8ml/min 5ml (b) EB 40W 0.8ml/min 5ml (c) Plasma 40W 0.8ml/min 5ml (d) Plasma 40W 3.8ml/min 5ml

5.2 Topography

In order to better understand how the topography of the acrylate coating is influenced by the curing conditions, measurements by AFM were performed. Roughness values such as the RMS was estimated:

- The root mean square value (RMS) of ordinate values within the definition area is equivalent to the standard deviation:

$$RMS = \sqrt{\frac{1}{A}\iint_{A}^{x,y} Z^2(x,y)dxdy}$$

Where:

A: area [nm^2]

x,y: corrdinates in the x,y axis [nm]

z: height[nm]

Equation 5.1: RMS equation

By plotting the RMS versus the degree of cure (Figure 3) and number of passes (Figure 4), it was noticed that other than some exceptions, the samples are really smooth. Also, the roughness obtained when using plasma and EB as curing sources are pretty similar, which contradicts Affinito et al findings: The published papers mentioned that EB-cured samples neither replicated the substrate defects nor reduced the roughness. It was believed to be a consequence of the electrostatic repulsion between the high energetic electrons in the liquid films. Then before the polymerization starts the film would be already distorted (6), however, this phenomenon wasn´t found on the plasma cured samples, resulting in ultra-smooth thin films, compared to E-Beam which had RMS values 10 times greater. (99). It must be noticed that those research papers referred to cured single layers, so it didn´t take into account either the effect of the underlayers or the partially cured samples.

In the same way as in thickness (section 4.2.7), the roughness would be influenced by numerous factors:

- Degree of cure and crosslinking density of the top layers: An inhomogeneous curing would lead to cured/non-cured areas, in which the monomers would flow towards the surface of the cured areas due to it´s greater surface energy. (50) (51)

- Shrinkage: When the films are being polymerized, they can experiment a reduction in volume, shrinkage. When shrinkage occurs during curing, another effect is produced: the coatings are subjected to internal stress, when the degree of cure is low enough, due to the appearance of a gradient between the cured and non-cured parts of the films. This produces at the beginning a homogeneity on the degree of cure, but as time passed by, this internal stress is transformed into relaxation, producing an inhomogeneity in which cured and uncured species within the coating are separated. (80)

- Etching: The etching occurring at the top layers due to the interaction of the radiation close to the surface. However, the proportion of material which would be etched away as a result of the radiation from the curing source won´t presumably be homogeneous. An increase on the surface roughness was observed already by other researchers when the films were plasma polymerized, and it was attributed to the plasma etching. (78) (79) . However, the roughening attributed to EB etching of acrylates is drastically reduced, when compared to plasma. (100)

- Re-evaporation: The proportion of uncured material that re-evaporates away from the surface. It is expected that RMS roughness would increase as a consequence of the removal of the uncured material, given the heterogeneity nature in radiation-cured acrylate networks. Thus, the re-evaporation would take place on the monomer-rich domains, leading to greater clusters. (101)

So, by plotting the RMS roughness against the degree of cure and the number of passes, it can be observed that the general trend shows a decrease on the roughness as the degree of cure and the number of passes are increased. (Figures 5.3 and 5.4)

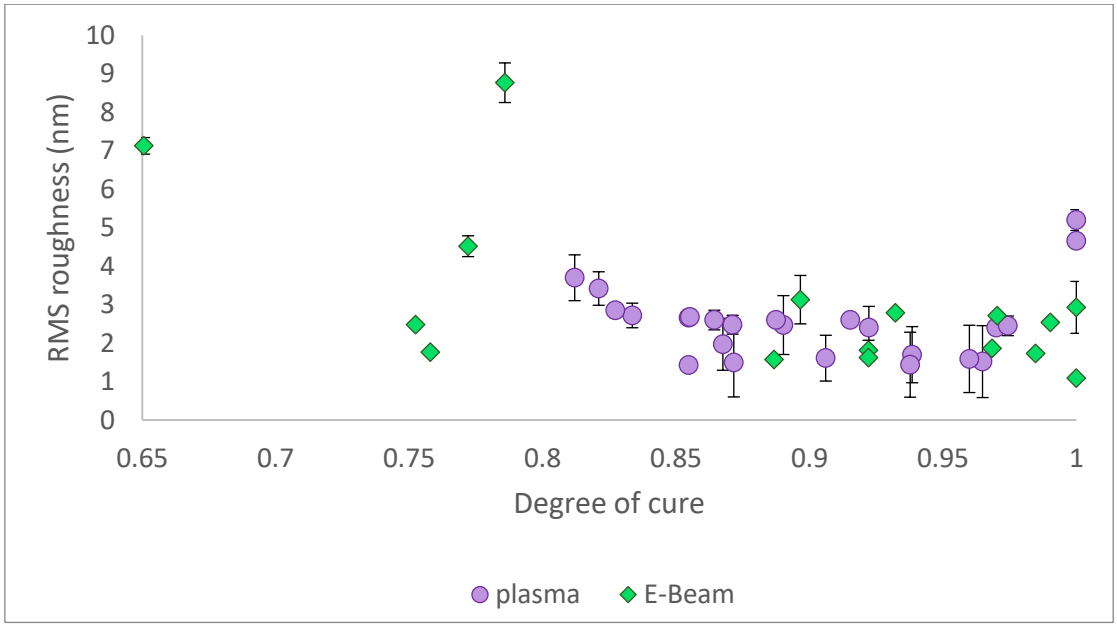

Figure 5.3: Root mean square dependence with degree of cure for plasma and EB cured samples (measured by tapping mode: 5000x5000nm)

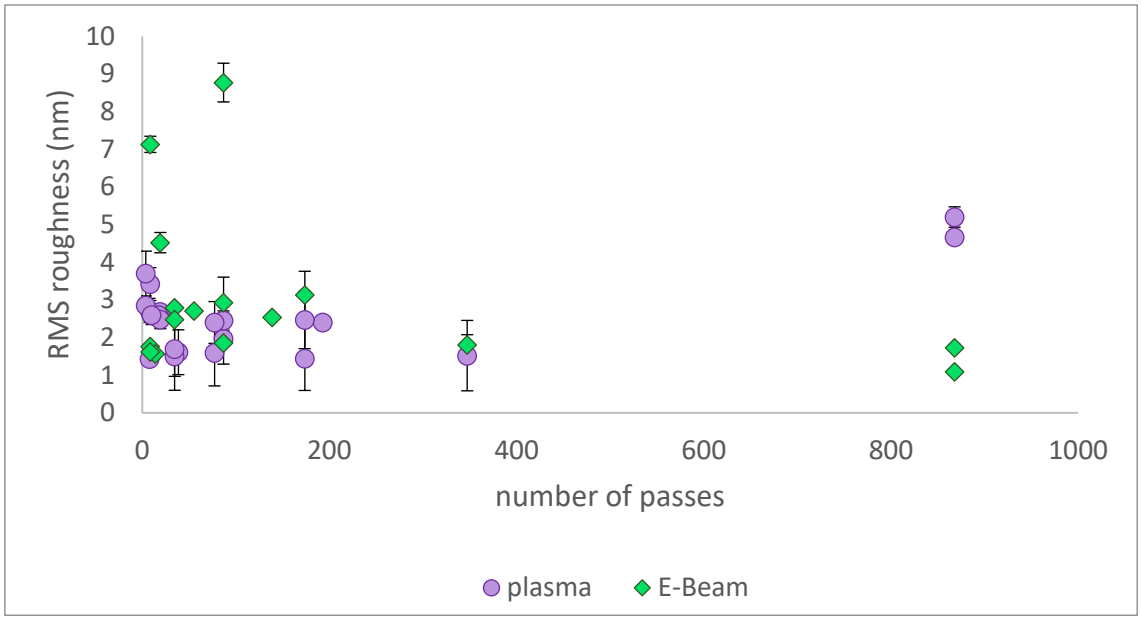

Figure 5.4: Root mean square dependence with the number of passes for plasma and EB cured samples (measured by tapping mode: 5000x5000nm)

The RMS experimental data (plasma and E-Beam) in general decreases as the number of passes and the degree of cure increases. However, RMS roughness only provides information regarding to the average roughness of the sample, but it doesn´t distinguish between wavy or spiky samples. In fact, when comparing the samples obtained by using different curing sources, the trend observed on topography wasn´t the same, as it can be observed in the following figures:

- In EB the samples with low injection rates and powers, showed greater peaks and valleys (Fig.5.7), but as the volume is increased, the topography becomes spikier (Fig.5.5), being the Fig.5.6 the most common topography obtained.

- In plasma however, the samples are spiky for the lower conversion degrees (Fig.5.8). And only as the degree of cure increases the sample starts showing a wavy and rough topography (Fig.5.9).

For this reason, EB and plasma curing would be analyzed separately.

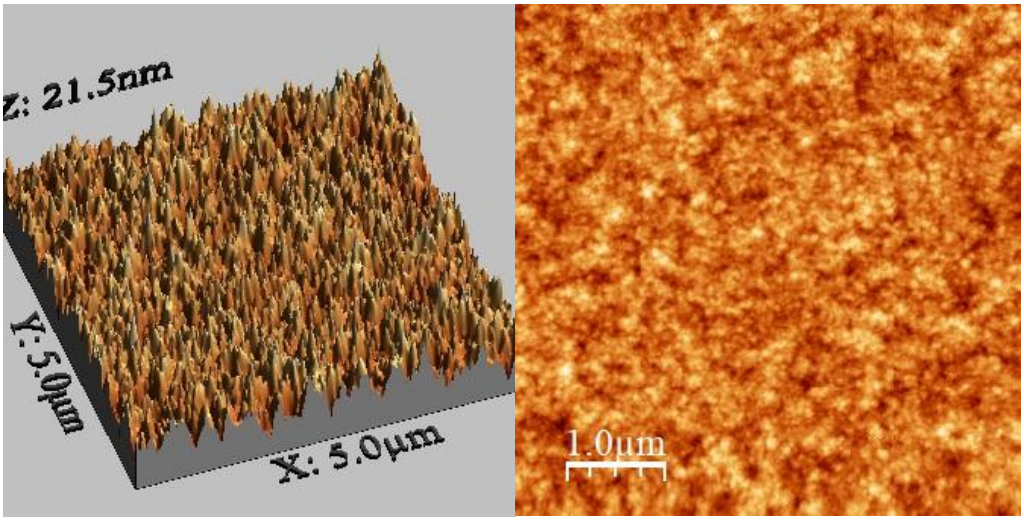

Figure 5.5: EB fully cured sample´s topography(50mA,0.08ml/min,5ml)

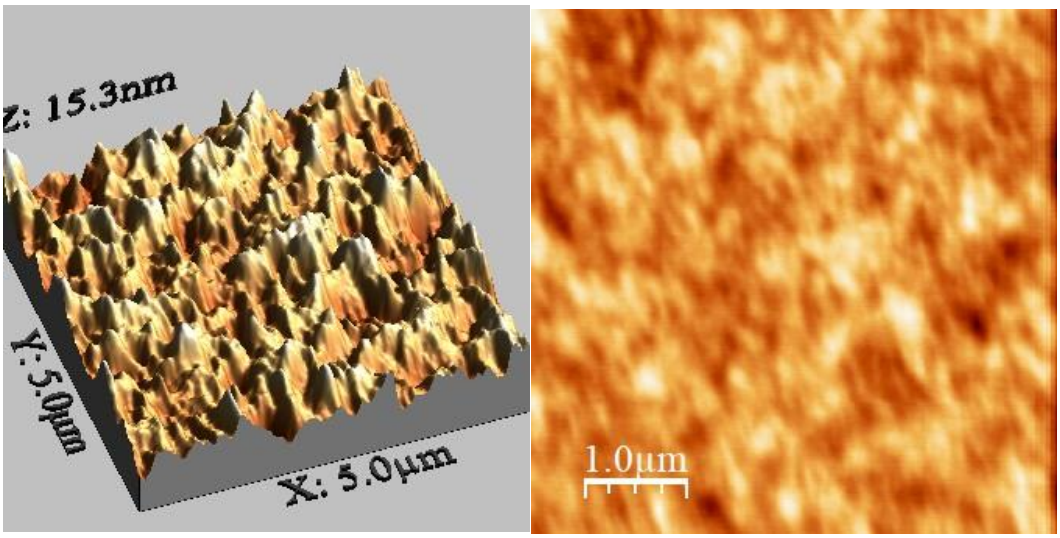

Figure 5.6: EB partially cured sample´s topography (degree of cure=0.87)(37mA, 0.8ml/min,5ml)

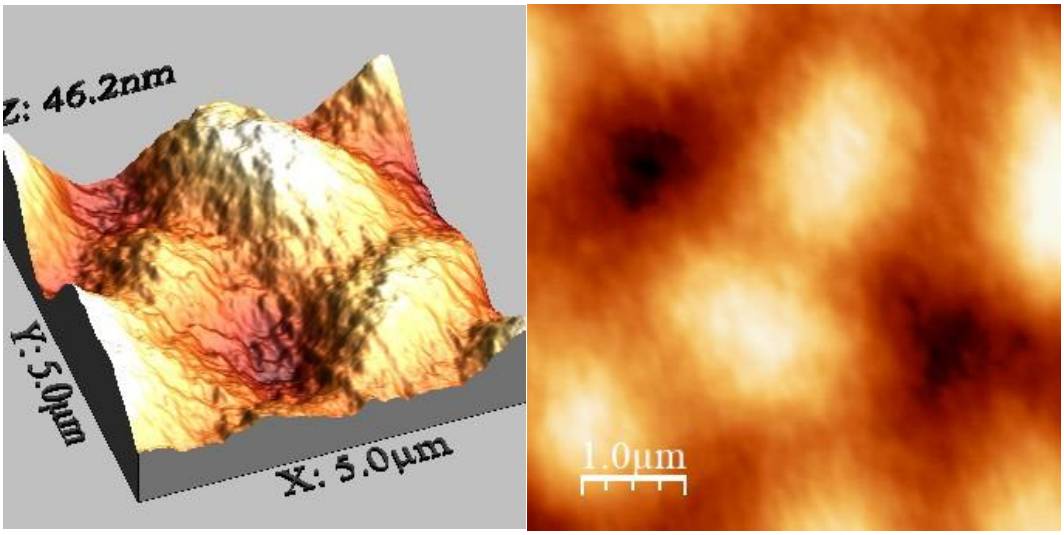

Figure 5.7: EB partially cured sample´s topography (degree of cure=0.78)(37mA, 0.5ml,0.08ml/min)

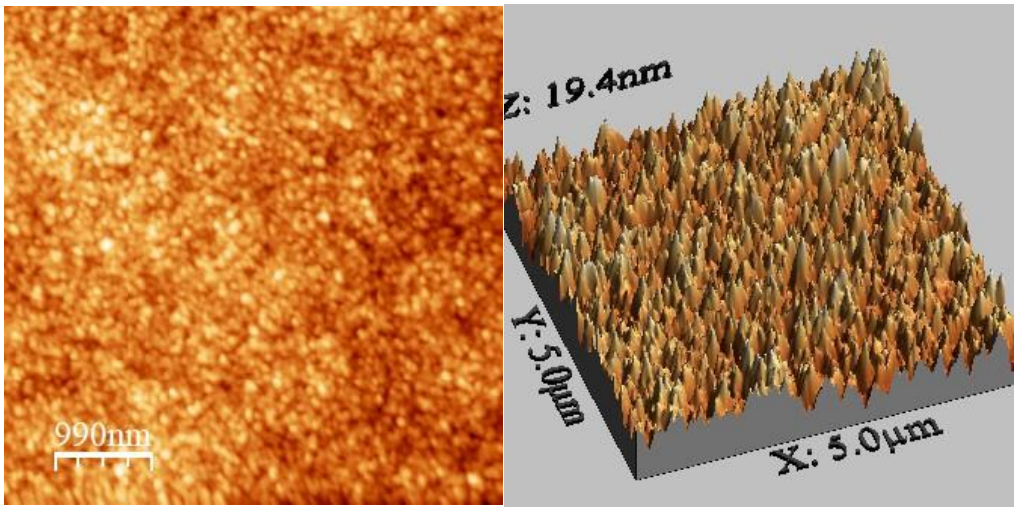

Figure 5.8: Plasma partially cured sample´s topography (degree of cure=0.93) (P1ml,5.85A, 0.08ml/min)

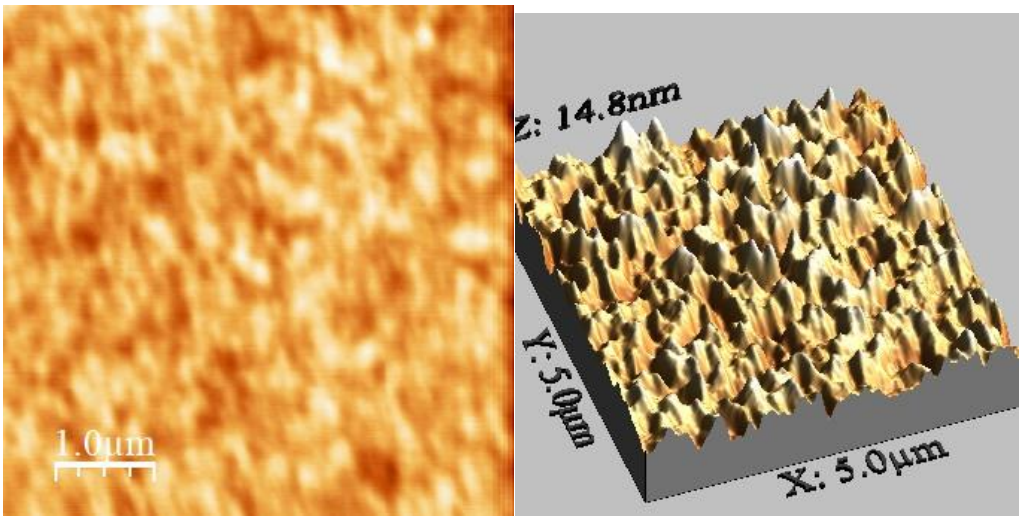

Figure 5.9: Plasma fully cured sample´s topography (P5ml,5.85A, 0.36ml/min)

5.2.1.E-Beam

Now, how do all the process conditions influence the topography?- By maintaining injection rate (0.5ml/min) and volume (0.5ml) while the current and voltage was changed, it was found that there were significant changes in the topography (Figure 5.10). As the current and voltage are decreased, the cured and non-cured areas become more visible, whereas for greater powers the surface becomes more homogeneous and spikier. In this case, the roughness decreases as power is increased, except for the greatest power. This can be attributed to that as the number of initiation sites is increased, the lesser the re-evaporation and the more homogeneous network would be obtained. (102) However, with the increase on power, the etching would increase too, so for the greatest power the etching would play a major role in determining the resulting roughness. These results do indeed, fit well with the thickness results (Sections 4.2.7,4.3.7).

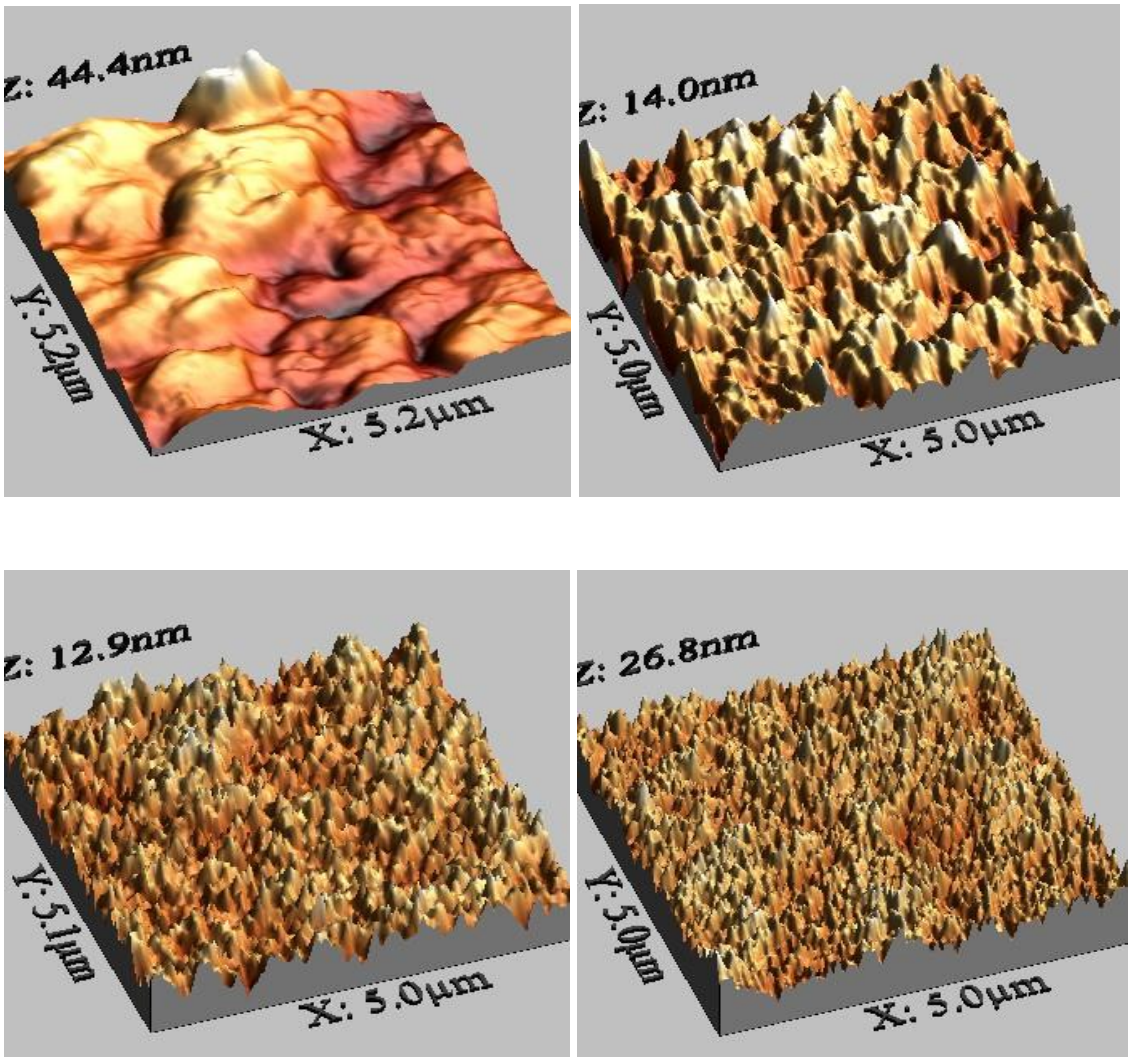

Figure 5.10: EB 10 (top left) ,37 (top right) ,50 (bottom left) ,100mA (bottom right), 0.5 ml, 0.5ml/min (RMS: 7.13,1.76,1.57,2.77)

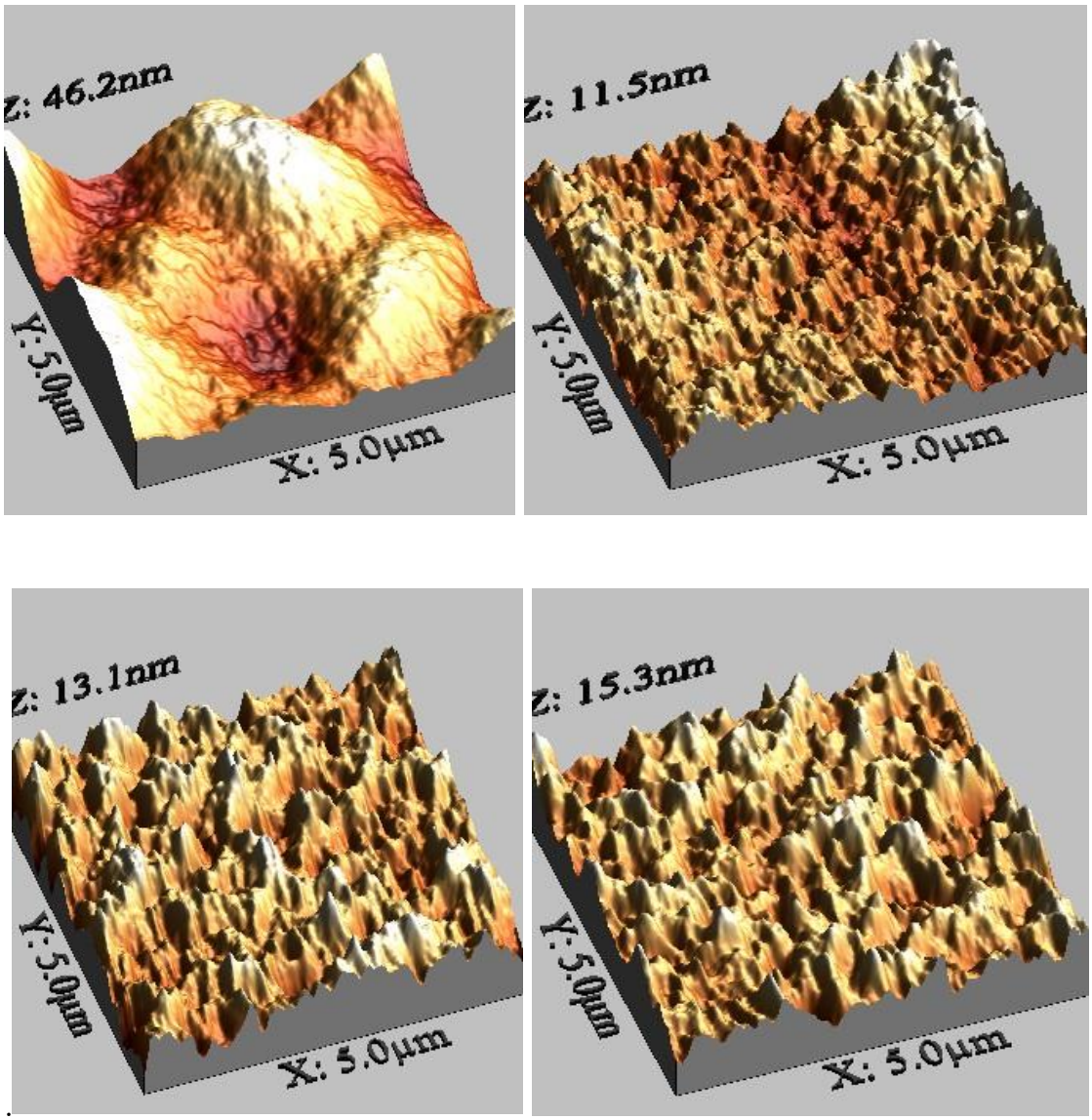

Figure 5.11: EB 37mA: 0.08ml/min (0.5ml-top left,5ml-top right) (RMS: 8.9,1.57), 0.8ml/min (0.5ml-bottom left,5ml-bottom right), (RMS: 1.71, 1.85)

When also studying the volume and injection rate (Figure 5.11), it was found that similarly, as the volume and injection rate is decreased, the size of the lumps are bigger. It is speculated that these lumps correspond to the cured/non-cured areas. (102) With these results it can be implied that this would be a direct consequence on how well cured the "top layers" are. In this sense, it can be thought that, when the films are partially cured

they will be rougher due to the accumulation of the uncured species towards the surface of the cured areas (78) (79).

So, in this case, according to the curing model, the last portion of material of top layers will have the same degree of cure for all the injection rates, what differs, however, is the time the uncured material will have to diffuse towards the surface of the cured areas, increasing as the injection rate lowers This would result in greater clusters as the injection rate lowers, roughening the surface.

The topography depends also on the volume, which indicates that what influences the topography not only happens in the last portion of material, but rather the topography is influenced by the underlayers too. The change on the topography with volume, was only observed when the injection rate was low, in the cases were there were more underlayers involved. It was already discussed that the high energetic electrons-matter interaction lead to a rise on the temperature. So, the change on the topography could be attributed to the fact that as the number of passes of drum increases, the greater the rise on the temperature. It would imply that the proportion of uncured material re-evaporating instead of diffusing towards the cured regions would increase with the number of passes, leading to smoother thin films.

5.2.2.Plasma

When analyzing plasma-cured samples, it was found that the power doesn´t influence much the topography, but the volume and the injection rate are very influential. Although, it has been previously observed that with plasma curing, when the power is increased too

much a portion of the polymerization happens in the gaseous phase. It results in an increase in the roughness, giving the samples a hazy appearance. (99) However, for the powers used in these experiments the topography isn´t changed, indicating that the polymerization takes only place in the liquid phase.

For the lowest volume, in every case (see examples in Figure 5.12) the samples present a spiky topography, but as the number of passes is increased due to the addition of new material deposited on top, the surfaces start getting a wavy appearance, except for the greatest injection rate, which keeps a spiky topography. It seems to be correlated to the thickness section, in which the biggest changes with volume were observed for the lowest injection rate, whereas for the maximum injection rate, the thickness per unit volume was constant.

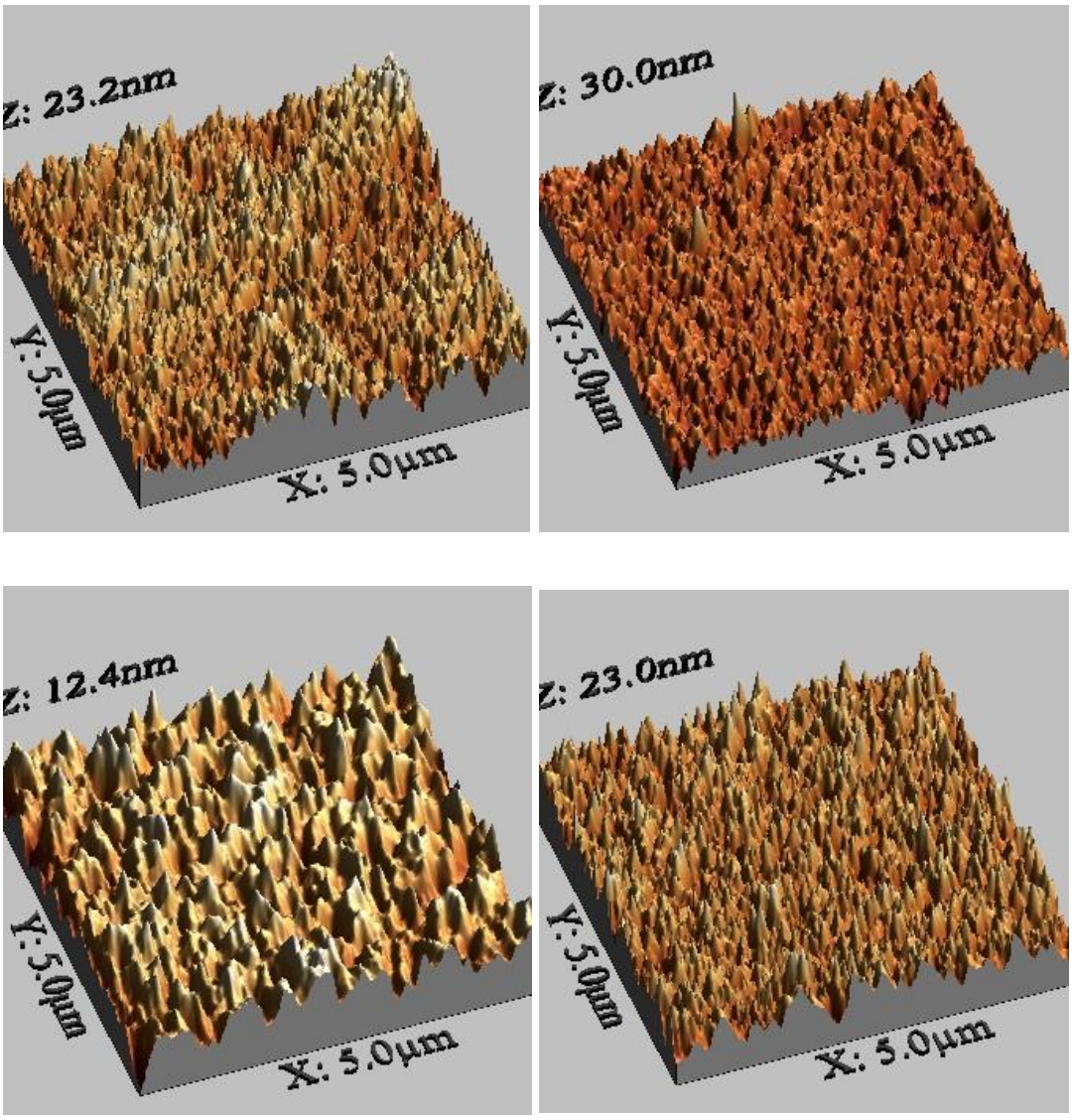

Figure 5.12: Plasma cured samples at 5.85A: 0.08ml/min, 0.5ml (top left) 1.8ml/min, 0.5ml (top right) 0.08ml/min, 2ml (bottom left), 1.8ml/min, 2ml (bottom right) RMS: 1.97, 2.38, 1.5,2.6

For the greatest volume and lowest injection rate, corresponding to the fully cured samples (Fig.5.13), it was observed the appearance of bigger and deeper depressions, which is thought to be a consequence of the etching. (103) (104).

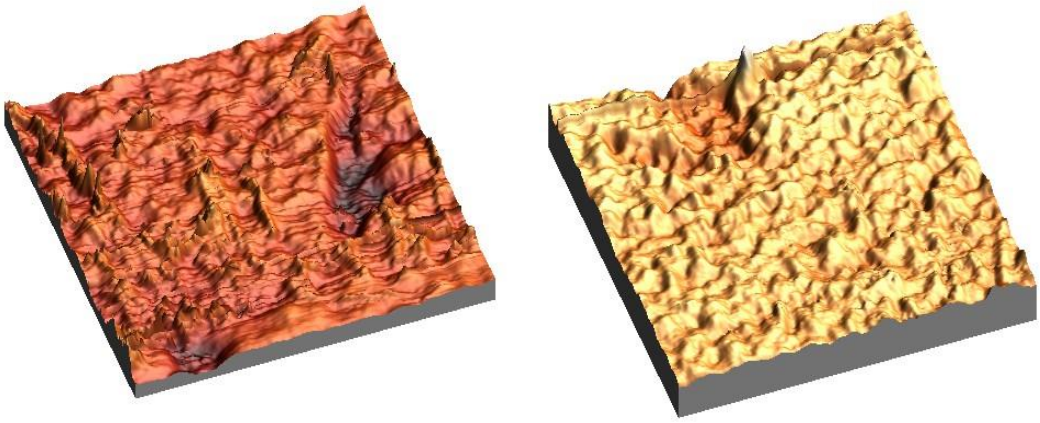

Figure 5.13: Plasma cured samples 3D topography for 0.08ml, 5ml, 5.85A (left), 0.35A (right) RMS:5.2,4.66

As the time the sample is being exposed to radiation is increased, so the topography could become rougher due the greater etching of the sample by the curing source. And as opposed as in the roughening induced by crosslinking, roughness features created by plasma etching are random in size and shape. (105) To test this, after curing the sample was exposed to different times of post-deposition radiation (Figures 5.14-5.16).

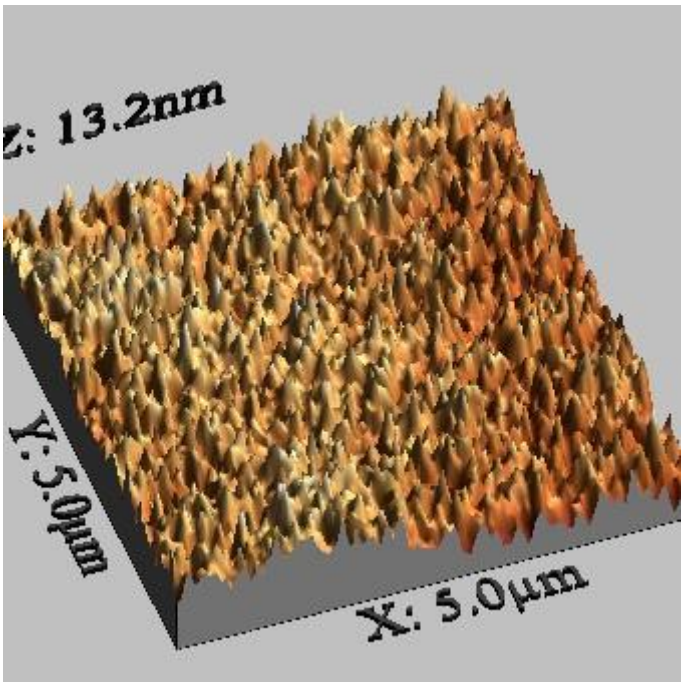

Figure 5.14: Plasma cured sample´s topography (for 1 min of extra exposure to the curing source) (P 0.5ml/min, 0.5ml) RMS:1.58

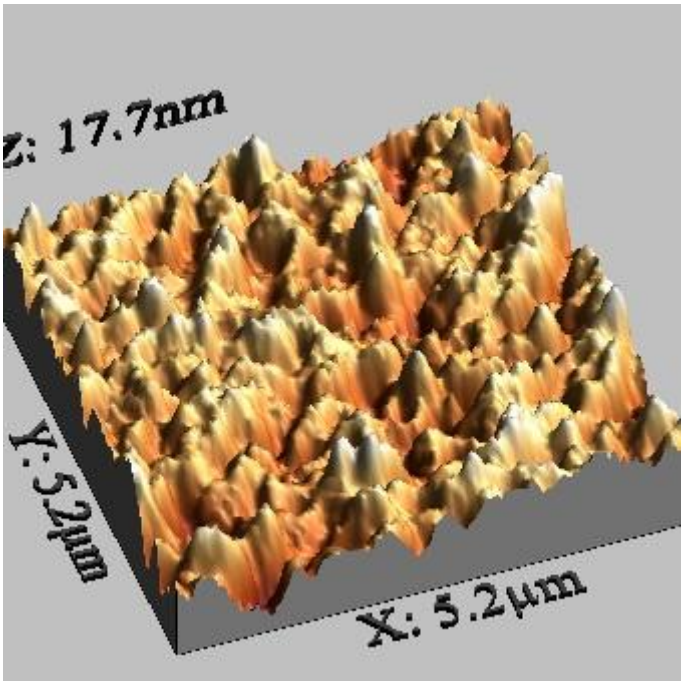

Figure 5.15: Plasma cured sample´s topography (for 2 min of extra exposure to the curing source) (P 0.5ml/min, 0.5ml) RMS:2.78

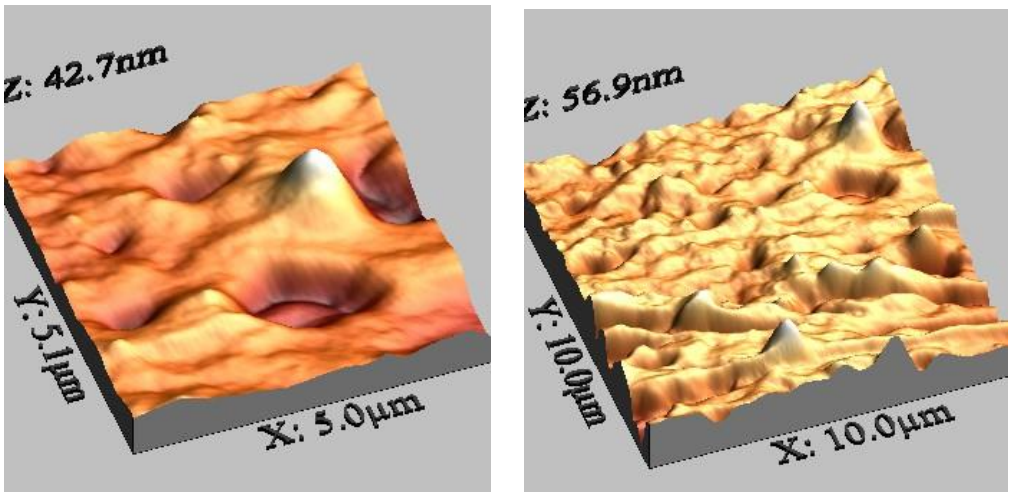

Figure 5.16: Plasma cured sample´s topography (for 10 min of extra exposure to the curing source) (P 0.5ml/min, 0.5ml) RMS:28.2,24.8

Indeed, in these images it can be observed that the etching is not homogeneous, hence it could be implied that the selective etching by the plasma reactive species is the principal cause of the changes in topography observed in samples subjected by long plasma exposure time.

5.2.3.Summary

The topography is mainly influenced by the degree of cure of the top layers, which would lead to differences: on the diffusion of the uncured material towards the surface of the cured regions, shrinkage, proportion of the uncured material re-evaporating away from the thin film, selective etching…All of these factors are influenced at the same time by the curing source, number of passes and thickness of the layers, reason for which the resulting topography can´t be explained by one factor only. However, depending on the

process conditions it was observed that the relative importance of those physical processes differ. In this regard:

- Localized variation on crosslinking density: Since the electrons tend to pass through, different concentrations of cured and partially cured areas will occur. Thus, the slower start of the polymerization would allow the formation of cured/non-cured areas leading to greater lumps, when compared to plasma.

- Etching: As the number of passes of the layers under the curing source is increased a selective etching was observed only for plasma, suggesting that EB etching might be more homogeneous.

- Re-evaporation: The changes of the topography with volume are greater as the injection rate goes down for both curing sources. This is thought to be as a result of more underlayers being involved, causing differences on the material re-evaporating away from the thin film. However, as EB samples get spikier with volume, the opposite effect was observed in plasma, suggesting that the relative importance of etching and re-evaporation differs between curing sources.

CHAPTER 6. CONCLUSIONS AND FURTHER WORK

6.1. Degree of cure

When comparing the behavior of plasma and E-Beam curing, it was observed an increase on the degree of cure with volume for the same injection rate, suggesting that both reactive species are able to further penetrate and interact not only with the "fresh layer" but also with the underlayers, post-curing them. What differ between both curing sources was their dependency on the overall degree of cure with injection rate: Whereas in plasma curing, a significant increase on the degree of cure as the injection rate diminished was found, EB cured samples weren´t affected significatively by the injection rate.

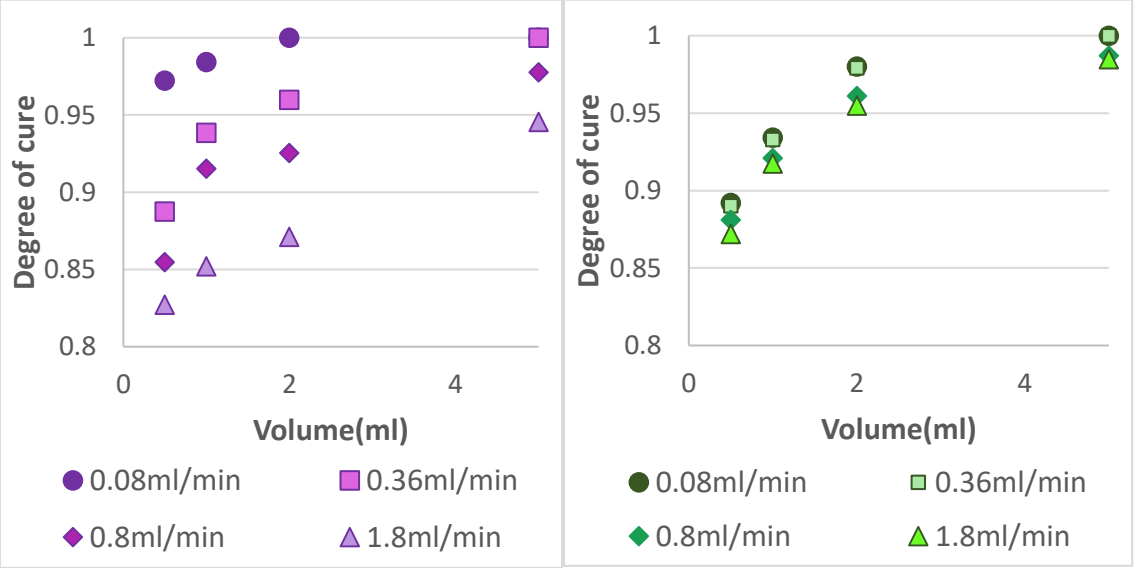

Figure 6.1: Degree of cure dependence with volume for different injection rates using plasma(left) and EB(right) as curing sources.

The science behind the differences on the trends between curing sources was thought to be as a result on the different penetration depth of electrons and ions. The penetration depth depends on the atomic mass and the energy of the radiation particles. So, due to the smaller mass of electrons compared to ions, the electrons will be able to penetrate in a larger depth for the same energy. Thus, ions stop closer together for a given thickness, while electrons are deposited in a larger range within a given depth (107) (108) (109). The slowing down, is in both cases caused by their interactions with matter, leading to ionization as the reactive species interact with the electrons of the monomer (64) (87) , resulting in the initiation of the polymerization.

In both instances, the curing rate was thought to be proportional to the density of reactive species with penetration depth, which is ruled by the Beer-Lambert law (described as a Gaussian curve according to the MonteCarlo model) and the proportion of uncured material (as the ability for the reactive species would depend on the proportion of double bonds left in the thin film (74) (73)). The fitting parameters obtained differed between curing sources. In fact, by plotting the increase on the degree of cure against the number of passes it can be observed that:

- The degree of cure of the top layer is lower for EB than for plasma, as the electrons will travel a greater distance without interacting with the material.
- The curing rate is more affected by the injection rate in EB than in plasma, which is a consequence on the greater proportion of ions interacting with the material near the surface.

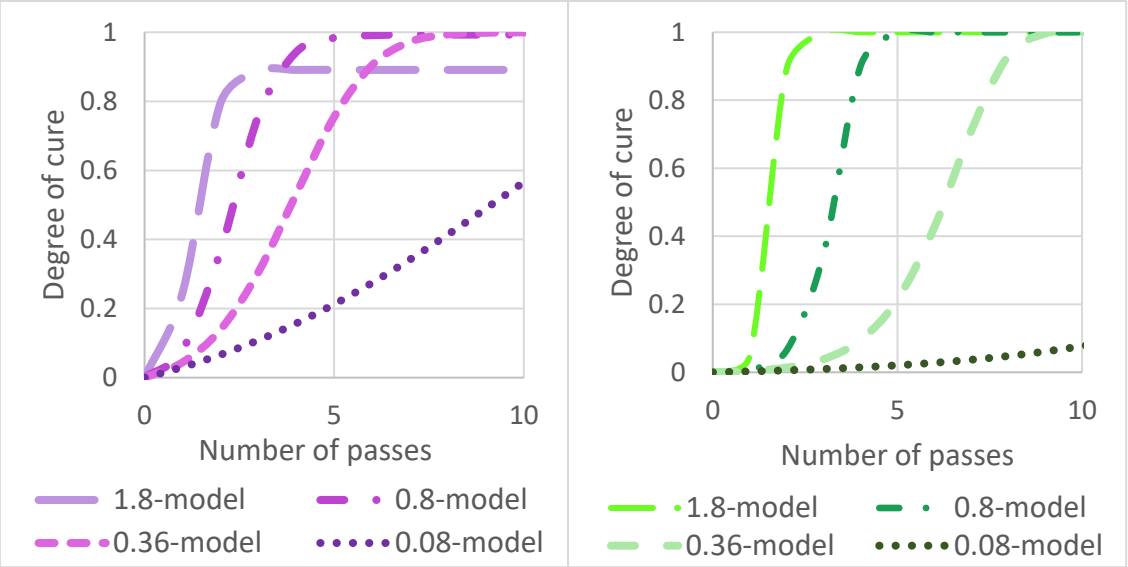

Figure 6.2: Curing rates model for different injection rates using plasma(left) and EB(right) as curing sources.

6.2.Thickness

The resulting thickness was believed to be a consequence of the contribution of the thickness of the liquid film arriving at the curing source (related to the physical vapor deposition process) and the material lost caused by the interaction between the reactive species with matter.

The thickness of the material prior to being subjected to the curing source was analyzed as a function of (76) :

- Substrate´s temperature: Radiation interaction with matter reacts exothermically, increasing then the temperature "substrate" (underlayers) at each pass of the drum.
- As the injection rate is modified, so will be the material that is being deposited on top of the drum. As a change in injection rate, leads to a change on the vapor

pressure, and thus, in the thickness of the liquid film before reaching the curing source.

- The distance travelled by the monomer from it´s deposition till the curing source is greater in plasma than in Electron Beam, so the re-evaporation is greater in plasma than in E-Beam.

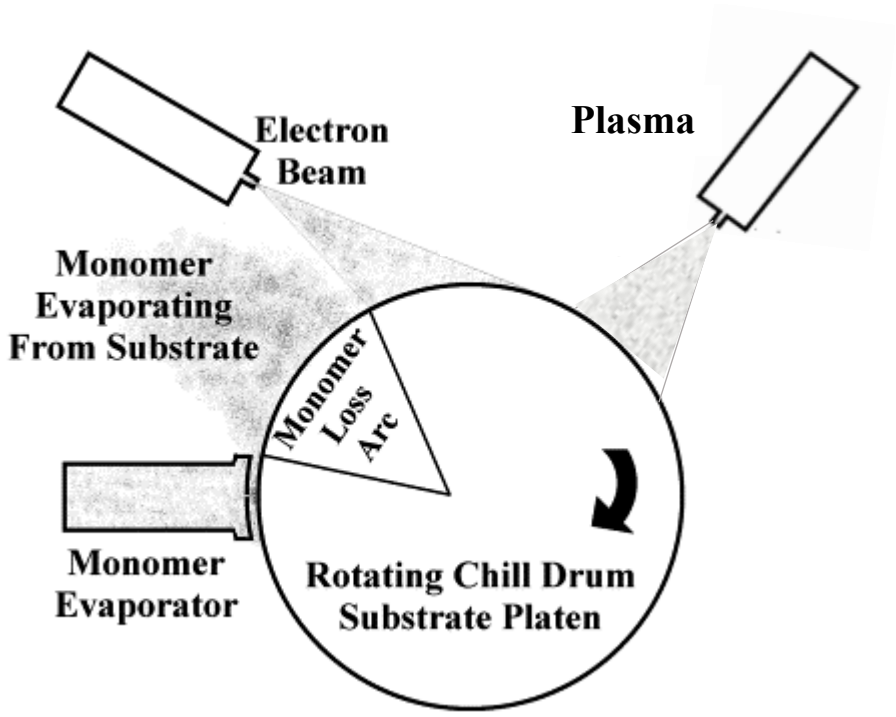

Figure 6.3: Roll-to-roll process followed by in line curing (76)

When the monomer interacts with the curing source, the reactive species won´t only cure the monomer but also etch it. So, if the degree of cure isn´t achieved at the first pass of the drum, re-evaporation can continue even after part of the material has been solidified. (75) Both processes will have an impact on the thickness of the material and both depend on the number of passes. Thus, the resulting thickness is obtained by the contribution of these two opposite processes. The re-evaporation which is directly dependent on the

degree of cure, and etching, which increases as the time of the material is being subjected to the curing source.

Even though shrinkage induces thickness changes, it was not significant enough to be considered, due to the high conversion degrees the samples presented and the low shrinkage that the polymer of interest has (81).

By plotting the thickness per unit of volume injected against the volume for the different curing sources, the main conclusions were made:

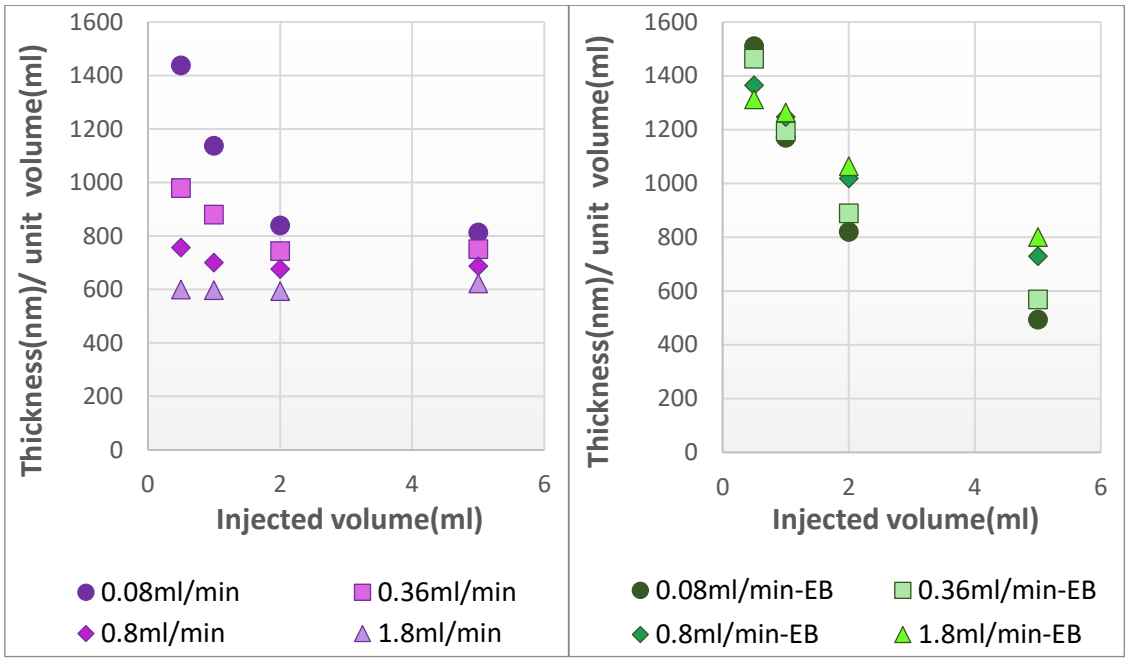

Figure 6.4: Thickness per unit of injected volume for different injection rates using plasma(purple) and EB(green) as curing sources.

In both cases, there is a general observation of a greater proportion of material lost as the volume injected increases, indicating that the underlayers play a key role in the resulting

thickness, otherwise the thickness per unit volume would be constant. This could suggest that:

1) The material is being lost from underlayers too. The underlayers are subjected to post-curing due to their further interaction with the reactive species. So, this further interaction could cause etching too. In any case, it would depend on the ability the low molecular fragments have to escape, which is dependent on:
    a. the time they have to diffuse towards the surface (dependent on the number of passes)
    b. the thickness the low molecular fragments have to go through, together with the degree of cure of the layer they have on top.

2) The interaction between reactive species and material would rise the temperature of the thin film, so that when new material is deposited on top, a greater proportion would re-evaporate.

What differs with the curing sources, however, is the thickness behavior observed for different injection rates. Whereas in plasma cured samples the decay in the thickness trends are completely dependent on the injection rate, in EB samples the thickness per unit volume follows similar trends with injection rate.

In both instances, as the injection rate is decreased for the same volume, the material would be subjected more times to the curing source, leading to a greater degree of cure of the underlayers. Thus, as the layers per pass of the drum are thinner, less re-evaporation will occur, simply because the underlayers would have been subjected more times to the curing source. But more number of passes would also mean more etching and more re-

evaporation due to heating. So, the difference on the thickness trends between curing sources could be explained as the relative importance that these effects (etching, re-evaporation and re-evaporation due to heating) would have on the resulting thickness.
In addition, plasma cured samples reach a volume up until the thickness per unit volume becomes constant, which fits with the hypothesis that the electrons are able to travel a greater distance than the ions. So that, this “extra thickness” of the deeper down layers that the electrons are able to interact with, allows the further removal of material either due to etching or re-evaporation due to heating, when compared to plasma.

By the study of other polymer properties such as crosslinking density or topography more information related to the ions/electrons interaction with matter was obtained.

6.3.Crosslinking density

The degree of cure provides information about the average -C=C- remaining in the film. And although it describes the effectiveness of the curing process, it does not provide information about the distribution of the linkage between the polymeric chains. Hence, it is feasible that two thin films with the same degree of cure present different crosslinking densities. (90) (91)

When comparing the crosslinking density of plasma and E-Beam cured samples, it was observed that the plasma cured layers exhibited greater density even for the same conversion values. This property is related to the distribution of the crosslinking centers. So, since the density of reactive species is greater in plasma than in E-Beam, it will give rise to a more linear network, since the propagation steps until the polymerization is

terminated will be longer in EB than in plasma. In addition, when comparing the relationship degree of cure-crosslinking density, it wasn´t really affected by injection rate for EB cured samples, as opposed to plasma:

In EB the degree of cure of the fresh layers is really low for all the injection rates, and it is mostly due to the post-cure that the degree of cure increases, given that as the depth the electrons have to travel is increased, the density of electrons is increased substantially, and this will cause an increase on the crosslinking density with volume for all the injection rates.

In plasma however, the trends are completely different, which could be due to the fact of the ions´ penetration depth. According to the curing model, the start of the polymerization is greater as the injection rate increases, leading to a greater cross-linking density, however, once a certain depth is achieved, the ions won´t be able to further cure or crosslink the thin films. For lower injection rates, the start of the polymerization will be rather low. But the number of passes would be greater, resulting in not only increasing the degree of cure, but also the crosslinking density.

By comparing the storage modulus at ambient temperature between curing sources, it was found that even though the EB cured sample exhibited a greater degree of cure, it´s storage modulus was much lower than the plasma cured sample. This finding aligned with the differences found when comparing the crosslinking density of EB and plasma cured samples, concluding that the electrons interaction with matter would lead to a more linear network as compared to plasma cured samples.

6.4.Topography

Finally, topography is as well affected by the process conditions. Films obtained by both curing processes exhibited a flat topography, with a general decrease on the RMS as the degree of cure is increased.

In both cases, it was observed that there were differences on the topography with volume, which suggests that the underlayers would have an effect on the topography. This difference was the greatest as the injection rate decreased. This could be linked with the greater thickness per unit volume trend as the injection rate decreased, since for lower injection rates a greater % of material will be lost due to etching and re-evaporation.

For EB cured samples the topography showed greater lumps, which was thought to be as a consequence of the low degree of cure of the top layers, leading to localized variations of cross-link density (106) . The uncured material would then diffuse towards the surface of the cured areas due to it´s greater surface energy (78) (79) . However, as the volume is increased a greater proportion of material will be lost. The rise on the temperature would then cause thinner films at each pass of the drum, so that a greater proportion of the uncured material will rather re-evaporate than diffuse.

In plasma however, the layers showed a spiky topography for low number of passes of the drum, which was attributed to the greater degree of cure near the surface compared to EB. But as the number of passes was increased, the layers started getting a similar topography as the plasma etched layers, concluding that even when more material is being deposited, the interaction between ions with matter causes selective etching in plasma samples when the thin films are subjected long enough to the curing source. (78) (104)

In addition, the main differences on the topography were observed for the lowest volume in EB and for the greatest volume in plasma. In addition, as opposed to EB, no differences were found on the topography with power in plasma cured samples, suggesting that the re-evaporation due to heating, etching or curing rates are really different between curing sources, aligning with the thickness conclusions.

6.5.Summary

All in all, it has been demonstrated that the process conditions, including the curing source affect the curing reaction, curing kinetics, re-evaporation and etching rates. All of these variables do directly affect the polymeric thin films such as degree of cure, thickness, crosslinking density, mechanical properties and topography.

The main difference between both curing sources is their penetration depth:

- As the electrons penetrate further before they start interacting with the material, it results in lower degrees of cure, and greater differences of the curing rates as the thickness of the material per number of pass is changed.

- The thickness per number of passes trend differs between both curing sources. Plasma cured samples exhibited a levelling off of the % of material lost with number of passes, so up to a certain depth no material is lost from the underlayers. EB cured samples however, never reached a depth up until the material lost is constant. These differences suggest that etching or re-evaporation due to heating are the main causatives of the lost material.

- The differences observed in etching and curing, had an enormous impact on the crosslinking density and topography between curing sources.

6.6 Applications and further work

But how could all the data gathered and analyzed be useful in terms of commercial applications?- In the industry, when using the roll-to-roll technique, the layers would be only subjected to the curing source once, reason for which the curing models become more handy. In this regard, for the conditions used none of them reached a complete cure when extrapolating the models back to one pass, which indicates that either an increase in the gas flow or current needs to be done.

Also, not only a complete cure would be desired, but also depending on the application a specific thickness needs to be achieved. For really thin layers plasma curing would have an advantage over E-Beam as the ions will stop closer together. However, as the thin films become thicker, a combination of both curing techniques would achieve better results, as ions and electrons will cover different penetration depths, achieving a greater overall degree of cure. If by either increasing the plasma current and/or gas flow or combining both curing sources, the increase on the degree of cure will imply an increase on the crosslinking density in the bulk and in the surface.

This implies greater mechanical properties and smoother films. Based on the analysis, the RMS was thought to be a consequence of the presence of heterogeneities in the crosslinking density, etching and re-evaporation due to heating. But since the two latest processes started to become important after the thin films had been subjected long enough

to the curing source, they shouldn´t be considered for one single pass, as no underlayers are involved.

In terms of further work, since the end-product will consist in multilayers, other properties such as adhesion or surface energy could be explored. Also, a deeper analysis of the mechanical properties related to the crosslinking density and degree of cure between both curing sources could be explored.

All the research was performed with one single monomer, TGPDA. And apart from the process conditions, another way to interfere in the thin film properties is by changing the chemistry. This could be done by changing the functionality of the monomer or even by the study of monomer mixtures.

BIBLIOGRAPHY

1. **Ding, Ziqian.** *Large area vacuum fabrication of organic thin film transistors.* 2014.

2. *Use of evaporated acrylate to smooth the surface of polyester ad polypropylene substrates.* **M. Roehring, D. Shaw, M. Langlois, C. Sheehan.** s.l. : Journal of Plastic film and sheeting, 1997, Vol. Vol 13.

3. **Tobin, V.** *Roll-to-roll deposition of highly flexible organic-inorganic barrier layers for printed electronics and photovoltaics.* 2018.

4. *Aluminium oxide barrier films on polymeric web and their conversion for packaging applications.* **C.F. Struller, P.J. Kelly, N.J. Copeland, V. Tobin, H.E. Assender, C.W. Holliday, S.J. Read,.** s.l. : Thin Solid Films, 2014, Vol. 553.

5. *Modification of the Carbon Fiber Surface by Oxygen Plasma and its Influence on Adhesion Strength in Acrylate-Based Composites Cured by Electron Beam and UltraViolet Light,.* **F. Vautard, P. Fioux , L. Vidal , J. Dentzer , J. Schultz , M. Nardin & B. Defoort.** s.l. : The Journal of Adhesion, 2013, Vol. 89.

6. *PML/oxide/PML barrier layer performance differences arising from use of UV or electron beam polymerization of the PML layers.* **J.D. Affinito, Stephan Eufinger, M.E. Gross, G.L. Graff, P.M. Martin.** s.l. : Thin solid films, 1997, Vol. 308.

7. *Photoinitiator-Free Plasma-Induced Polymerization and Microstructuring of Acrylate-Based Coatings on 3D Substrates.* **Christian Elsner, Alya Boulares-Pender, Martin Hahnel, Robert Konieczny, Christa Kuhnel, Michael R. Buchmeiser.** s.l. : Macromolecular materials and engineering, 2009, Vol. 294.

8. *A comparison of plasma and electron beam-sterilization of PU catheters.* **O. Mrad, J. Saunier, C. Aymes Chodur, V. Rosilio, F. Agnely, P. Aubert, J. Vigneron, A. Etcheberry, N. Yagoubi.** s.l. : Radiation Physics and Chemistry, 2010, Vol. 79.

9. **Martin, Peter M.** *Handbook of Deposition Technologies for Films and Coatings : Science, Applications and Technology.* 2005.

10. *High rate vacuum deposition of polymer electrolyte.* **J. D. Affinito, M. E. Gross, C. A. Coronado, G. C. Dunham, P. M. Martin.** 14, s.l. : Journal of Vacuum Science & Technology A: Vacuum, Surfaces, and Films, 1996.

11. **Bishop, Charles A.** *Vacuum deposition onto webs, films and foils.* 2015.

12. *Low dielectric constant polymers for microelectronics.* **Maier, G.** s.l. : Progress in polymer science, 2001, Vol. 26.

13. *Vacuum Deposition Coating Options for Finishers.* **Lampert, Carl M.** s.l. : Products Finishing, 2013, Vol. 77.

14. *Curing Methods for Advanced Polymer Composites - A review. .* **Dilmurat Abliza, b, Yugang Duana, Leif Steuernagelb, Lei Xiea, Dichen Lia, and Gerhard Ziegmannb.** s.l. : Polymers and polymer composites, 2013.

15. *High-energy radiation and polymers: A review of commercial processes and emerging applications.* **Clough, R.L.** s.l. : Nuclear Instruments and Methods in Physics Research Section B: Beam Interactions with Materials and Atoms, 2001, Vol. 185.

16. **Davidson, R.S.** *Radiation Curing.* s.l. : Rapra Review Reports, 1996.

17. *Vacuum deposited polymer/metal multilayer films for optical application.* **John Affinito, Peter Martin, Mark Gross, Chris Coronado, Eric Greenwell.** s.l. : Thin Solid Films, 1995, Vol. 270.

18. *Plasma-induzierte Polymerisation von Acrylaten Eine Alternative zu strahleninduzierten Polymerisationen von beschichtungen.* **Elsner, Christian.** s.l. : Vakuum in Forschung und praxis, 2010, Vol. 222.

19. *Vacuum production of OTFTs by vapour jet deposition of dinaphtho[2,3-b:2',3'-f]thieno[3,2-b]thiophene (DNTT) on a lauryl acrylate functionalised dielectric surface.* **Ziqian Ding, Gamal A.W. Abbas, Hazel E. Assender, John J. Morrison, Stephen G. Yeates, Eifion R. Patchett, D. Martin Taylor.** s.l. : Organic electronics, 2016, Vol. 31.

20. **Manepalli, Rahul.** *ELECTRON BEAM CURING OF THIN FILM POLYMER DIELECTRICS.* 2000.

21. *The curing performance of UV-curable semi-interpenetrating polymer network structured acrylic pressure-sensitive adhesives.* **Hyo-Sook Joo, Young-Jun Park , Hyun-Sung Do , Hyun-Joong Kim , Si-Yong Song & Kil-Yeong Choi.** s.l. : Journal of Adhesion Science and Technology, 2007, Vol. 21.

22. *Shrinkage studies in electron beam curable polyurethane pressure-sensitive adhesive,.* **Anil Kumar Singh, Utpal Kumar Niyogi , Sunil Sabharwal , Agnieszka Kowalczyk ,**

Zbigniew Czech & Dayal Singh Mehra. s.l. : Journal of Adhesion Science and Technology, 2013, Vol. 27.

23. *Acrylate Copolymer/Ultraviolet Curable Oligomer Blends as Pressure-sensitive Adhesives,.* **Takehiro Ozawa, Shinichi Ishiwata , Yoshihisa Kano,Tomoyuki Kasemura.** s.l. : The Journal of Adhesion, 2000, Vol. 72.

24. **G. K. Noren, J. M. Zimmerman,J. J. Krajewski, T. E. Bishop.** Mechanical Properties of UV-Cured Coatings Containing Multifunctional Acrylates. *Radiation curing of polymeric materials.* 1990.

25. **A.J., Bean.** Radiation Curing of Printing Inks . [book auth.] Pappas S.P. *Radiation Curing. Topics in Applied Chemistry.* s.l. : Springer, 1992.

26. *Effects of highly absorbing pigments on near infrared cured polyester/melamine coil coatings.* **Mabbett, Ian, Elvins, Jon, Gowenlock, Cathren, Jones, Paul, Worsley, D.** s.l. : Progress in Organic Coatings, 2013, Vol. 76.

27. *Cure-on-command technology: A review of the current state of the art.* **Ali Javadi, Hamideh Shokouhi Mehr, Masoud Sobani, Mark D. Soucek.** s.l. : Progress in Organic Coatings, 2016, Vol. 100.

28. **Keizo Makuuchi, Song Cheng.** *Radiation Processing of Polymer Materials and Its Industrial Applications.* s.l. : John Wiley & Sons, 2012.

29. **J.P Fouassier, J.F Rabek.** *Radiation curing in polymer science and technology.* s.l. : Kluwer Academic Publishers, 1993.

30. *The use of UV irradiation in polymerization.* **Decker, Christian.** s.l. : Polymer international, 1998, Vol. 45.

31. *Kinetic study and new applications of UV radiation curing. .* **C., Decker.** s.l. : Macromol. Rapid Comm, 2002, Vol. 23.

32. **Drobny, Jiri George.** *Radiation technology for polymers.* s.l. : CRC Press, 2010.

33. *Review of basic chemistry of UV curing technology. .* **Shukla, V, et al.** s.l. : R Pigment & Resin Technology, 2004, Vol. 33.

34. *Plasma Polymerization.* **Yasuda., H. K.** s.l. : Academic Press, 1985.

35. *Plasma-induced polymerization.* **Brosse, F. Epaillard and J. C.** s.l. : Journal of Applied Polymer Science, 1989, Vol. 38.

36. *Real-time FTIR–ATR spectroscopy to study the kinetics of ultrafast photopolymerization reactions induced by monochromatic UV light.* **T. Scherzer, U. Decker.** s.l. : Vibrational Spectroscopy, 1999, Vol. 19.

37. *Comparative Study of Electron-Beam- and Ultraviolet-Cured Films of Urethane Acrylate .* **M. AZAM All, MUBARAK A. KHAN, and K. M. IDRISS.** s.l. : Journal of Applied Polymer science, 1996, Vol. 60.

38. **Tracton, Arthur A.** *Coatings technology handbook.* s.l. : CRC Press, 2005.

39. *Hysteresis-Free Vacuum-Processed Acrylate-Pentacene Thin-Film Transistors. .* **Abbas, G., Ding, Z., Mallik, K., Assender, H., & Taylor, D. M.** s.l. : IEEE Electron Device Letters, 2013, Vol. 34.

40. **Mattox, Donald M.** *Handbook of Physical Vapor Deposition (PVD) Processing.* s.l. : Materials Science and Process Technology, 1988.

41. *A photo-curing study of a pigmented UV-curable alkyd.* **P. Chittavanich, K. Miller, M.D. Soucek.** s.l. : Progress in Organic Coatings, 2012, Vol. 73.

42. *A theory of large elastic deformation.* **Mooney, M.** s.l. : Journal of Applied Physics, 1940, Vol. 11.

43. *Calculation of crosslink density in short chain networks.* **Hill, Loren W.** s.l. : Progress in Organic Coatings, 1997, Vol. 31.

44. *Principles of polymer chemistry .* **PJ., Flory.** s.l. : Cornell University Press, 1953.

45. *Influence of the silanes on the crosslink density and crosslink structure of silica-filled solution styrene butadiene rubber compounds.* **Jong-Yeop Lee, Nam Park, Seokhwan Lim, Byeongkyu Ahn, Woong Kim,Hyunsung Moon, Hyun-jong Paik and Wonho Kim,.** s.l. : Composite Interfaces, 2016, Vol. 24.

46. *Designing of antibacterial plastics: thymol release from photocured thymol-doped acrylic resins.* **F. Pilati, M. Degli Esposti,M. Bondi • R. Iseppi,M. Toselli.** s.l. : J Mater Sci, 2013, Vol. 48.

47. *Mechanical Properties of Polymer/Liquid Crystal Films Elaborated by Electron Beam and UV Radiation.* **A. Berrayah, L. Zair , A. Olivier, U. Maschke.** s.l. : Molecular Crystals and Liquid Crystals, 2011, Vol. 54.

48. *Resin Composite Properties and Energy Density of Light Cure.* **A. Peutzfeld, E. Asmussen.** s.l. : J Dent Res, 2005, Vol. 84.

49. *Dynamic mechanical studies on epoxy resins cured by electron beam radiation.* **Gang Sui, Zuo-Guang Zhang, Zhi-Yong Liang, Chang-Qi Chen.** s.l. : Materials Science and Engineering , 2003, Vol. A342.

50. *Optical Surface Making by UV-Curing of Monomeric Compositions in the Near Field of a Coherent Light Source,,.* **Fokina, M. I.** s.l. : Molecular Crystals and Liquid Crystals, 2007, Vol. 468.

51. *Polymeric microlens array formed directly on glass plate.* **Zuowei Zhou, Hongwen Ren.** s.l. : Opt. Eng, 2017, Vol. 1.

52. **Subramanian, Muralisrinivasan.** *Polymer Testing : New Instrumental Methods.* s.l. : Momentum Press, 2012.

53. *Modern Fourier: Transform Infrared Spectroscopy. .* **A.A.Cristy, Y.Ozaki and V.G. Gregoriou.** s.l. : Comprehensive Analytical Chemistry, 2001, Vol. 35.

54. *UV-curable acrylated coating from epoxidized palm oil.* **Rahman, Nurliyana Abd.** s.l. : AIP Conference Proceedings, 2014, Vol. 1614.

55. **M.D. Luque de Castro, L.E. García Ayuso.** *Encyclopedia of Separation Science.* 2000.

56. *Effects of solvent properties on the Soxhlet extraction of diterpenoid lactones from Andrographis paniculata leaves.* **Andri Cahyo Kumoroa, Masitah Hasana,Harcharan Singh.** s.l. : ScienceAsia, 2009, Vol. 35.

57. **Bittrich, Eva, et al.** *Polymer Surface Characterization.* s.l. : De Gruyter, 2014.

58. *Characterization of Tribological Materials.* **Glaeser, William A.** s.l. : Momentum Press, 2012.

59. *Atomic Force Microscopy. .* **Peter Eaton, Paul West.** s.l. : Oxford University Press, 2010.

60. **Redouane Borsali, Robert Pecora.** *Soft Matter Characterization.* s.l. : Springer, 2008.

61. **Guo, Quipen.** *Polymer Morphology : Principles, Characterization, and Processing .* s.l. : John Wiley & Sons, 2016.

62. **Peter Haines, Peter G. Laye, S. B. Warrington, G. Roger Heal,Duncan M. Price,Richard Wilson.** *Principles of Thermal Analysis and Calorimetry.* s.l. : Royal Society of Chemistry, 2016.

63. **Menard, Kevin P. Menard Noah R.** *Dynamic Mechanical Analysis in the Analysis of Polymers and Rubbers.* s.l. : John Wiley & Sons, 2015.

64. *Ion-beam modification of polymeric materials – fundamental principles and applications.* **H.E.Lee.** s.l. : Nuclear Instruments and Methods in Physics Research Section B: Beam Interactions with Materials and Atoms, 1999, Vol. 151.

65. *Lithium ion penetration depth profiles and reversibility of electrochromic reaction for TiO2 thin films.* **Ueda, M., Tsukamoto, M., Sakai, A.** s.l. : Journal of Solid State Electrochemistry , 2014, Vol. 18.

66. **Cucinotta, Ianik Plante,Francis A.** Monte-Carlo Simulation of Ionizing Radiation Tracks. [book auth.] Charles J. Mode. *Applications of Monte Carlo Methods in Biology, Medicine and Other Fields of Science.* s.l. : IntechOpen, 2011.

67. *Rutherford Backscattering Spectrometry studies of 100 keV nitrogen ion implanted polypropylene polymer.* **Mahak Chawla, Sanjeev Aggarwal, Annu Sharma,.** s.l. : Nuclear Instruments and Methods in Physics Research Section B: Beam Interactions with Materials and Atoms, 2017, Vol. 407.

68. *Depth profiling of organic materials using improved ion beam conditions.* **H.-G. Cramer, T. Grehl, F. Kollmer, R. Moellers, E. Niehuis, D. Rading,.** s.l. : Applied Surface Science, 2008, Vol. 225.

69. *Computer simulations of surface analysis using ion beams.* **V. Ignatova, D. Karpuzov, I. Chakarov, I. Katardjiev.** s.l. : Progress in Surface Science, 2006, Vol. 81.

70. *The Stopping and Range of Ions in Solids.* **J.F. Ziegler, J.P. Biersack, U. Littmark.** s.l. : Pergamon Press, 1985.

71. *Radiation-induced change of polyimide properties under high-fluence and high ion current density implantation.* **al., POPOK et.** s.l. : Applied Physics A, 2004, Vol. 78.

72. *Influence of helium ion irradiation on the structure and strength of diamond.* **Ming Chen, James P. Best, Ivan Shorubalko, Johann Michler, Ralph Spolenak, Jeffrey M. Wheeler.** s.l. : Carbon, 2019.

73. *Polyurethane acrylate networks including cellulose nanocrystals: a comparison between UV and EB- curing.* **K. Furtak-Wrona, P. Kozik-Ostrówka, K. Jadwiszczak, J.E. Maigret, V. Aguié-Béghin, X. Coqueret.** s.l. : Radiation Physics and Chemistry, 2018, Vol. 142.

74. *An overview of polymer latex film formation and properties.* **Steward, P.A., Hearn, J., Wilkinson, M.C.** s.l. : Adv. Coll. Interf. Sci, 2000, Vol. 86.

75. *Real-time in-situ observation of vapor deposition polymerization of N-methylolacrylamide with IR-RAS .* **al., M Tamada et.** s.l. : Thin Solid Films, 1995, Vol. 260.

76. *A new method for vacuum deposition of polymer films.* **Affinito, John.** s.l. : Thin Solid Films, 2002, Vol. 420.

77. *Plasma-induced physicochemical effects on a poly(amide) thin-film composite membrane.* **Rackel Reis, Ludovic F. Dumée, Andrea Merenda, John D. Orbell, Jürg A. Schütz, Mikel C. Duke.** s.l. : Desalinitation, 2017, Vol. 403.

78. *Surface modification of cellulosic substrates via atmospheric pressure plasma polymerization of acrylic acid: Structure and properties.* **Jose Garcia-Torres, Dioulde Sylla, Laura Molina, Eulalia Crespo.** s.l. : Applied surface science, 2014, Vol. 305.

79. *Chain Extension and Branching of Poly(ethylene terephthalate) (PET) with di- and multifunctional epoxy or isocyanate additives: an Experimental and modelling study.* **P. Raffa, S. Coltelli, S. Stefania, S. Bianchi, V. Castelvetro.** s.l. : React Funct Polym, 2012, Vol. 72.

80. *Monitoring of thickness and conversion of thick pigmented UV-cured coatings by NIR hyperspectral imaging.* **Olesya Daikos, Katja Heymann, Tom Scherzer.** s.l. : Progress in Organic Coatings, 2018, Vol. 125.

81. *Shrinkage of UV Oligomers and Monomers* . **Andreas Moeck, Tongzhou Jiang,Chunguang Li,Wantai Yang,Jun Nie.** s.l. : Journal of Coatings Technology and Research , 2013, Vol. 10.

82. *Ion beam and laser-assisted micromachining of single-crystal diamond.* **J.D. Hunn, C.P. Christensen.** s.l. : Solid State Technology, 1994, Vol. 37.

83. **J.L. Magee, A. Chatterjee.** Chapter 1, 5, and 6 . [book auth.] Farhataziz and M.A.J. Rodgers. *Radiation Chemistry.* s.l. : VCH Publishers, 1987.

84. *Electron beam damage of epoxy resin films studied by scanning transmission X-ray spectromicroscopy.* **Weiwei Zhang, Lis G. de A. Melo, Adam P. Hitchcock, Nabil Bassim.** s.l. : Micron, 2019, Vol. 120.

85. *Depth variation of absorbed dose in materials irradiated by fast electrons.* **Chepel, L. V.** s.l. : Soviet Atomic Energy, 1971, Vol. 30.

86. *Interactions of Ionizing Radiation with Matter and Direct Energy Conversion.* **Prelas M., Boraas M., De La Torre Aguilar F., Seelig JD., Tchakoua Tchouaso M., Wisniewski D.** s.l. : Nuclear Batteries and Radioisotopes, 2016, Vol. 56.

87. *Interactions of Ionizing Radiation with Matter and Direct Energy Conversion.* . **Prelas M., Boraas M., De La Torre Aguilar F., Seelig JD., Tchakoua Tchouaso M., Wisniewski D.** s.l. : Nuclear Batteries and Radioisotopes, 2016, Vol. 56.

88. *Monte Carlo Simulation of Electron Interaction With a Thin Film.* **Starý, Vladimír.** s.l. : Thin Solid Films, 2003, Vol. 433.

89. *Low-energy electron beam cured tape placement for out-of-autoclave fabrication of advanced polymer composites.* **Dilmurat Abliz, Yugang Duan, Xinming Zhao, Dichen Li.** s.l. : Composites Part A: Applied Science and Manufacturing, 2014, Vol. 65.

90. *Influence of pulse-delay curing on softening of polymer structures.* **E. Asmussen, A. Peutzfeldt.** s.l. : Journal of Dental Research, 2001, Vol. 80.

91. *Influence of selected components on crosslink density in polymer structures.* **E. Asmussen, A. Peutzfeldt.** s.l. : European Journal of Oral Science, 2001, Vol. 108.

92. *Influence of curing modes on crosslink density in polymer structures.* **M.S. Soh, Adrian U.J. Yap.** s.l. : Journal of Dentistry, 2004, Vol. 32.

93. *Effect of high intensity vs. soft-start irradiation on light-cured resin-based composites.* **Hofmann N, Markert T, Hugo B, Klaiber B.** s.l. : Am J Dent., 2004, Vol. 17.

94. *Controlled Electron-Beam Synthesis of Transparent Hydrogels for Drug Delivery Applications.* **Sarah Glass, Mathias Kühnert,Bernd Abel andAgnes Schulze.** s.l. : Polymers, 2019, Vol. 11.

95. *Evolution of the free volume and glass transition temperature with the degree of cure of polybutadiene rubbers.* **M.A. Mansilla, A.L. Rodríguez Garraza, L. Silva, W. Salgueiro, C. Macchi, A.J. Marzocca, A. Somoza.** s.l. : Polymer Testing, 2013, Vol. 32.

96. *Effect of self and dual-curing on degree of conversion and crosslink density of dual-cure core build-up materials .* **Duygu Karakis, Arzu Zeynep Yıldırım-Bicer, Arife Dogan, Haluk Koralay, Sukru Cavdar.** s.l. : Journal of Prosthodontic Research, 2017, Vol. 61.

97. *Effects of Cross-Link Density and Distribution on Static and Dynamic Properties of Chemically Cross-Linked Polymers.* **Jianxiang Shen, Xiangsong Lin,Jun Liu,Xue Li.** s.l. : Macromolecules, 2019, Vol. 52.

98. *Effects of precursor topology on polymer networks simulated with molecular dynamics.* **Shimiao Zhang, Li Xi.** s.l. : Polymer, 2017, Vol. 116.

99. *Hybridization of the polymer multi-layer (PML) deposition process.* **Affinito, John D.** s.l. : Surface and Coatings Technology, 2000, Vols. 133-134.

100. *Etch Properties of 193nm Resists: Issues and Approaches.* **Munirathna Padmanaban, Eric L. Alemy,Ralph Dammel,Woo-Kyu Kim,Takanori Kudo,Dalil Rahman,.** s.l. : Journal of Photopolymer Science and Technology, 2002, Vol. 15.

101. *Characterization by Atomic Force Microscopy of the Nanoheterogeneities Produced by the Radiation-Induced Cross-Linking Polymerization of Aromatic Diacrylates.* **Mickael Krzeminski, Michael Molinari,Michel Troyon,Xavier Coqueret.** s.l. : Macromolecules, 2010, Vol. 43.

102. *Microstructure aspects of radiation-cured networks: Cationically polymerized aromatic epoxy resins.* **Christelle Kowandy, Guillaume Ranoux, Marta Walo, Bertrand Vissouvanadin, Gilbert Teyssedre, Christian Laurent, Alexandre**

Berquand, Michaël Molinari, Xavier Coqueret,. s.l. : Radiation Physics and Chemistry, 2018, Vol. 143.

103. *Surface modification of cellulosic substrates via atmospheric pressure plasma polymerization of acrylic acid: Structure and properties.* **Jose Garcia-Torres, Dioulde Sylla, Laura Molina, Eulalia Crespo, Jordi Mota, Llorenç Bautista.** s.l. : Applied Surface Science, 2014, Vol. 305.

104. *Rheological and Mechanical Properties of Recycled PET Modified by Reactive Extrusion.* **Supawee Makkam, Wanlop Harnnarongchai.** s.l. : Energy Procedia, 2014, Vol. 56.

105. *Surface Roughening of Polystyrene and Poly(methyl methacrylate) in Ar/O2 Plasma Etching.* **Yuk-Hong (Jeff) Ting, Chi-Chun Liu,Sang-Min Park,Jiang Hongquan.** s.l. : Polymers, 2010, Vol. 2.

106. *Benzyl alcohols as accelerators in the photoinitiated cationic polymerization of epoxide monomers* . **J.V. Crivello, R.A. Ortiz.** s.l. : J. Polym. Sci. Part A: Polym. Chem, 2002, Vol. 40.

107. *High Energy Electron Climatology that Supports Deep Charging Risk Assessment in GEO.* **Bodeau, M.** Orlando, Florida : The 48th AIAA Aerospace Sciences Meeting, 2010.

108. *The AE-8 Trapped Electron Model Environment.* **Vette, J. I.** Goddard, Maryland : NSSDC/WDC-A-R&S, 1991.

109. *Review of Quantitative Models of the 0 to 100 keV NearEarth Plasma.* **Garrett, H. B.** s.l. : Reviews of Geophysics and Space Physics, 1979, Vol. 17.

110. *Preparation of ion exchange membranes by radiation grafting of acrylic acid on FEP films.* **Bhuvanesh Gupta, Nusrat Muzyyan, Shalini Saxena, Navdeep Grover, Sarwar Alam.** s.l. : Radiation Physics and Chemistry, 2008, Vol. 77.

111. *Modification methods for poly(arylsulfone) membranes: A mini-review focusing on surface modification.* **Norhan Nady, Maurice C.R. Franssen, Han Zuilhof, Mohamed S. Mohy Eldin, Remko Boom, Karin Schroën.** s.l. : Desalinitation, 2011, Vol. 275.

112. *New strategy of grafting hydroxyethyl acrylate (HEA) via γ ray radiation to modify polyvinylidene fluoride (PVDF) membrane: Thermodynamic mechanisms of the improved antifouling performance,.* **Liguo Shen, Hongzhan Wang, Yicheng Zhang,**

Renjie Li, Bucyibaruta Fabien, Genying Yu, Hongjun Lin, Bao-Qiang Liao. s.l. : Separation and Purification Technology, 2018, Vol. 207.

113. *Morphology of polytetrafluoroethylene before and after irradiation.* **Sergei A. Khatipov, Sergei A. Serov, Nataliya V. Sadovskaya, Elena M. Konova.** s.l. : Radiation Physics and Chemistry, 2012, Vol. 81.

114. *Plasma treatment of polyolefins: Influence of material composition: 2. Lacquer adhesion and locus of failure.* **Anna Nihlstrand, Thomas Hjertberg, Kenth Johansson.** s.l. : Polymer, 1997, Vol. 38.

115. **van, der Heide, Paul.** *X-ray Photoelectron Spectroscopy : An introduction to Principles and Practices.* s.l. : Wiley, 2011.

116. *XPS Study of the Surface of UV Cured Acrylates.* **LUO Yan, WANG De-hai, CAI Yan-qing.** s.l. : Imaging Science and Photochemistry, 2006, Vol. 24.